1-1-2017

Effect of Exponential Correlation Model on Spectral and Energy Efficiency for Massive MIMO Systems

Saleh Albdran
University of Denver

EFFECT OF EXPONENTIAL CORRELATION MODEL ON SPECTRAL AND ENERGY EFFICIENCY FOR MASSIVE MIMO SYSTEMS

A Dissertation

Presented to

the Faculty of the Daniel Felix Ritchie School of Engineering and Computer Science

University of Denver

In Partial Fulfillment

of the Requirements for the Degree

Doctor of Philosophy

---

by

Saleh Albdran

November 2017

Advisor: Mohammad Matin

Author: Saleh Albdran
Title: EFFECT OF EXPONENTIAL CORRELATION MODEL ON SPECTRAL AND ENERGY EFFICIENCY FOR MASSIVE MIMO SYSTEMS
Advisor: Mohammad Matin
Degree Date: November 2017

Abstract

During the past few years, the number of wireless devices has been increasing rapidly. Wireless networks are serving and connecting billions of wireless devices where these devices are demanding higher data rate and lower latency to be able to support voice, video and gaming applications. Moreover, the consumed energy by the wireless systems will be increasing. Hence, the Fifth generation (5G) wireless networks needs to provide higher data rate, serve larger number of users simultaneously and be more energy efficient. One of the promising technologies that can meet the above requirements is Massive Multiple Input Multiple Output (MIMO). The main concept of this technology is to equip the base station with hundreds of antennas and serve tens of users simultaneously. The amount of research on massive MIMO increases rapidly, but there is little attention so far on the spatial correlation between the channels. Most of the published work are assuming that the antennas are uncorrelated which is not the case in real-world situations. In this dissertation, the effect of channel correlation model on the Massive MIMO performance is investigated.

First, the exponential correlation model is applied to the Massive MIMO system model. We used a pilot based linear minimum mean square error (LMMSE) channel estimator for the uplink data transmission. The impact of the channel correlation on the channel estimation accuracy is investigated. Due to having channel reciprocity, the channel

state information will be the same for uplink and downlink data transmission. It is assumed that there is block fading where there are static channels. It is shown that the channel estimation is more accurate with higher SNR values.

Second, the uplink and downlink spectral efficiency of the LMMSE estimators are investigated where spatial correlation models are applied to the system to generate the channel covariance matrix. The lower capacity of the uplink and downlink data transmissions are derived to see the effect of applying exponential correlation model. We study the lower capacity bound based on imperfect knowledge of the channel. In the first part, we are considering a one cell system model with one base station that is equipped with N antennas and serving single antenna user. In the second part, a Massive MIMO system of a single cell is considered. The system model is having a base station with multiple antennas that is serving user terminals equipped with multiple antennas. It is proved that the spectral efficiency is improved by increasing the number of base station antennas which shows the scalability of Massive MIMO systems.

Finally, the transmit power of Massive MIMO system is defined as the consumed energy by the amplifier divided by coherence time while energy efficiency of Massive MIMO system can be expressed as the ratio between the spectral efficiency and the emitted power. The influence of the channel spatial correlation on the energy efficiency is investigated where it is noticed that there is higher energy efficiency with higher number of base station antennas.

Acknowledgements

I would like to express my sincere thanks to my advisor Dr. Mohammad Matin for allowing me to join his research group. I am grateful for his guidance and continuous support throughout the years. This work would not have been accomplished without his limitless encouragement and supervision. Also, I would like to extend my deepest gratitude to my graduate committee members, Dr. Ronald DeLyser, Dr. Yun Bo-Yi and Dr. Vijaya Narapareddy, for their cooperation and valuable advice.

Special thanks go to my parents and to my brothers and sisters who supported me throughout my life. Also, I would like to express my gratitude and love towards my wife for joining me on my long journey. This work is dedicated to my two children, Abdulaziz and Ziad. Having you around me is giving me strength and patience and encouraging me to do my best.

Table of Contents

Abbreviations

AD “Analogue to Digital”

AWGN “Additive White Gaussian Noise”

BLAST “Bell Labs Layered Space Time”

BS “Base Station”

CSI “Channel State Information”

DA “Digital to Analogue”

FDD “Frequency-Division Duplexing”

GSM “Global System for Mobile communication”

HSPA “High Speed Packet Access”

ITU “International Communication Union”

LMMSE “Linear Minimum Mean Square Error”

LoS “Line of Sight”

LTE “Long Term Evolution”

MMSE “Minimum Mean Square Error”

MIMO “multiple input multiple output”

MISO “Multiple Input Single Outputs”

MSE “Mean Square Error”

M2M “machine-to-machine”

NSF “National Science Foundation”

RF “Radio Frequency”

SISO “Single Input Single Output”

SIMO “Single Input Multiple Outputs”

SINR “Signal-to-Interference-plus-Noise Ratio”

SNR “Signal to Noise Ratio”

TDD “Time-Division Duplexing”

ULA “Uniform Linear Array”

UE “User Equipment”

V-BLAST “Vertical Bell Labs Layered Space Time”

Wi-Fi “Wireless Fidelity”

WiMAX “Worldwide Interoperability for Microwave Access”

WCDMA “Wideband Code Division Multiple Access”

List of Figures

List of Tables

Chapter One: Introduction

1.1 Motivation and Background

During the past few years, the demand for wireless data traffic has been increasing rapidly while the available electromagnetic spectrum range is limited [1]. The wireless communication is different from the fiber communications in terms of meeting the future demands where more optical fiber can be made while there is no easy solution to increase wireless throughput [2]. This high demand will keep increasing in the future due to the exponential growth of the number of wireless devices [3].

By 2020, it is forecasted that the global mobile data traffic will exceed 30 Exabyte per month compared to 6.2 Exabyte per month in 2016 as Figure 1.1 shows. Also, it is expected that the number of global mobile devices and connections will increase from 7.9 billion in 2015 to 11.6 billion devices by 2020 as shown in Figure 1.2. To meet this growing demand, we need new technologies that are clever and efficient yet can be implemented in real life [4], [5].

To improve the wireless throughput, it is important to apply new technologies that can increase the bandwidth or the spectral efficiency. One of the proposed solutions is millimeter wave technology where it is possible to get the benefits of the unused spectrum. The second solution is having small cell where we keep having more access points each one of them covers smaller region. The third solution is the use of multiple antennas in the base station (BS) terminals and the user terminals. The first two solutions will not be discussed in this report while our focus will be on the third solution. By using transceivers with multiple antennas, we are increasing the spectral efficiency and that yields higher wireless throughput.

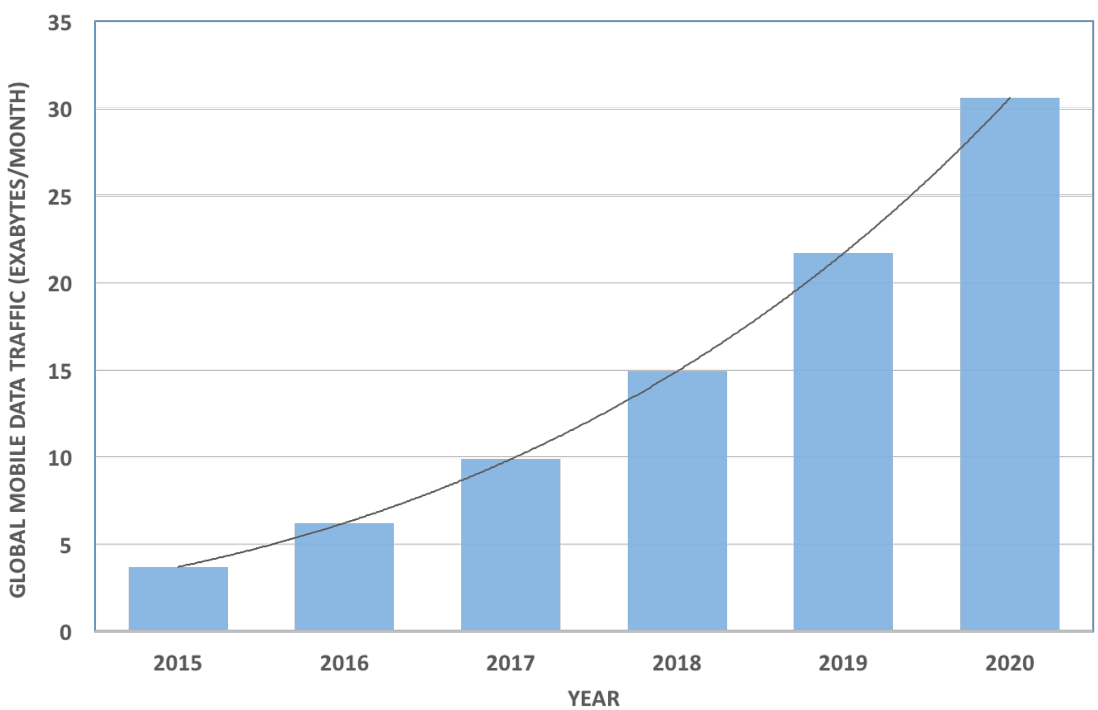

Figure 1.1: Global mobile data traffic [6].

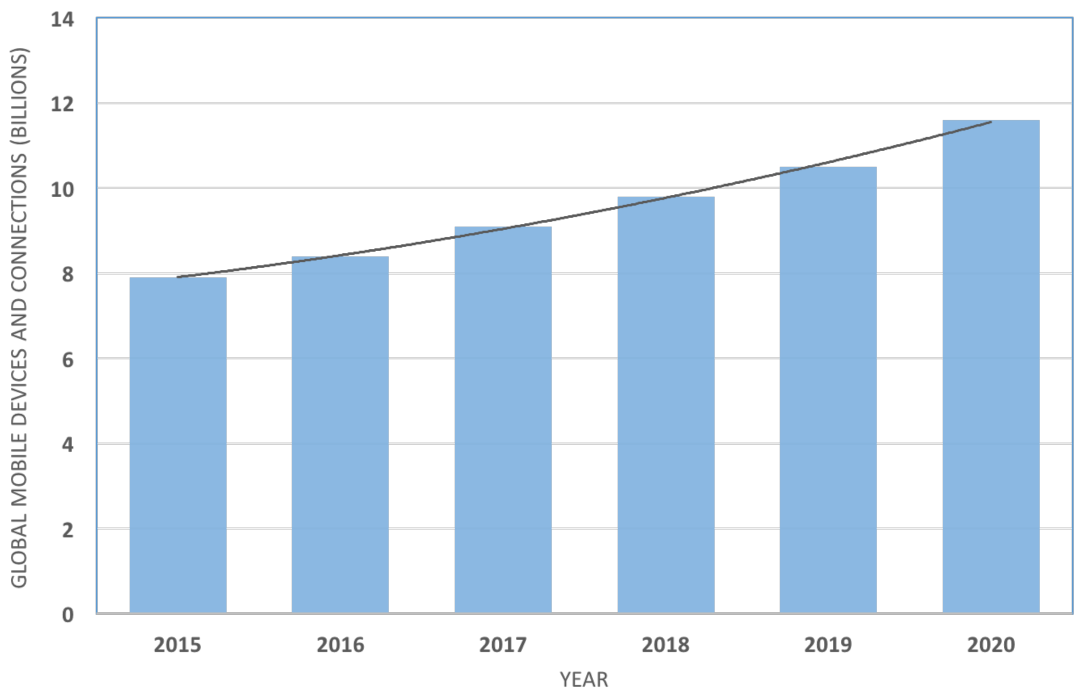

Figure 1.2: Global mobile devices and connections growth [6].

1.2 Problem Statement

Based on the discussion above, the main question is: How to provide enough wireless throughput that can increase rabidly and meet the rising demand in a certain area? Massive MIMO system is one of the promising candidates that could be implemented in the fifth generation (5G) by 2020. It has the abilities to meet the growing demand by improving the spectral efficiency by order of magnitude. This advantage of providing higher spectral efficiency cannot be achieved without having a good knowledge of the channel state information and without applying a good model to generate the channel covariance. In the research community, the technology of massive MIMO has grabbed significant attention during the last five years. There are several ongoing projects, one of them is in Bell Labs where they published several papers [2], [7].

Nowadays, most of the cellular systems are executed in frequency-division duplexing (FDD). By applying FDD mode in massive MIMO we would see several drawbacks such as feedback overhead when we use conventional channel estimator. On the other hand, if time-division duplexing (TDD) is used, it is easier to obtain the channel state information due to the channel reciprocity.

Motivated by the need of new technologies to meet the higher demand, in this research, we investigate the fundamental of massive MIMO including channel estimation using pilot based linear minimum mean square error (LMMSE) channel estimator. Also, we study the spectral and energy efficiencies and the impact of using exponential correlation model on them. Several scenarios are executed by using different number of base station antennas for high and low SNR values.

1.3 Methodology

The MATLAB simulation program is used where the communication system toolbox provides tools and functions that help us to analyze our model. Several codes are written to generate figures where the analysis are carried out first for the channel estimation. Also, spectral and energy efficiencies are analyzed for ideal and non-ideal case scenarios. The outcome results of this dissertation are validated by publishing several IEEE and SPIE conference papers.

1.4 Structure of the Report

The next chapters of the report are ordered as follows:

- Chapter 2 includes the history of MIMO and its use throughout the earlier decades. It contains the different stages of MIMO evolution: Single-user MIMO, Multiuser MIMO and Massive MIMO. The second part of chapter 2 is talking about the future of 5G wireless network where we went through the possible solutions that could be used to improve the spectral and energy efficiency of the future networks.
- Chapter 3 is including a definition of the system model where the uplink and downlink system models are stated. The main part of this chapter is studying the channel estimation accuracy of the Massive MIMO systems by applying spatial correlation model. Also the impact of the pilot length is shown and investigated by applying LMMSE pilot based estimator.
- Chapter 4 contains a study of the channel spectral efficiency using a system of one cell. The effect of the spatial correlation on the performance of the system is studied. The system parameters are expanded to include multiple user terminal where each one is equipped with multiple antennas.
- Chapter 5 shows the energy efficiency and the transmit power of a Massive MIMO system using exponential correlation model. The results include illustration of their performances by applying different scenarios.

- Chapter 6 contains the summary of the dissertation and the future work. Also, the publications are listed in this chapter.

Chapter Two: History and Future of Wireless Communications

2.1 What is MIMO?

MIMO stands for Multiple Input Multiple Output and refers to different signal processing methods that are used to improve the throughput and the reliability of the wireless systems [8]. The main idea of MIMO systems is to use multiple antennas at the receiver terminal or at the transmitter terminal or at both terminals where the performance is improved in which the multipath scattering is combated or exploited. There are different categories or techniques of MIMO, the first one is achieved by combating the multipath in the channel between the two terminals to generate spatial diversity. The second technique is spatial multiplexing which can be derived by exploiting multipath channel. The communication system reliability can be improved by space time coding method where fading is combated. On the other hand, the exploit fading approach is applied to increase system throughput where spatial demultiplexing method is used.

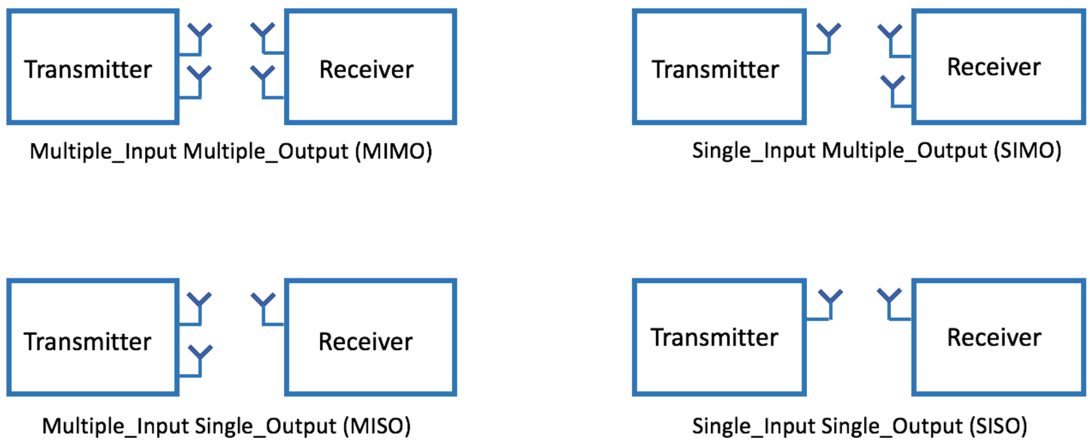

Figure 2.1: The possible combinations for the wireless system by using different antennas configurations [9].

In general, the term MIMO is used broadly to describe any communication system that has multiple antenna at one or both sides. To be more specific, the system with single antenna at the base station and multiple antenna at the user terminal is called MISO while when the opposite is true it is called SIMO. If there is a conventional wireless communication system with single antenna at the base station and single antenna at the user terminal it is called SISO system. To state the number of antennas it is starting normally with the number of antennas in the transmitter first, for instant, the 4×2 MIMO system has four antennas at the transmitter and two antennas at the receiver.

Historically, the term MIMO was used in the 1950s to describe the multiple input and the multiple output ports of the electric circuits. Four decades later, researchers of communication systems and information theory used the term “MIMO” to describe the new techniques which have multiple antennas at both ends of the communication system. In 1999, the term MIMO was used in the wireless communication field for the first time by Driessen and Foschini where they published their paper about the capacity formula of MIMO wireless channels [10].

The idea of using multiple antennas for the wireless communication is old and goes back to the beginning of the 20^{th} century. In 1905, Braun introduced his idea of multiple antennas to create phase array antennas to improve the radar performance [11]. Years later, the technology of phased arrays was implemented in the broadcast AM radio where the phase and the levels of the power are switched twice a day at sunrise and sunset. Instead of pointing the antennas mechanically to the ground wave propagation during the day time and then elevate their angles to the sky wave propagation at night, only switch the levels of phase and power. In addition, receive diversity was used widely to decrease the fading influence on the wireless communication systems. In 1931, Peterson and Beverage published their paper about the concept of diversity on the receivers for communication systems [12].

At the beginning of the 1990s, the number of publications about the technology of multiple antennas has been escalated quickly to implement transmit diversity. One of the first papers on this technology was published by Wittneben from ABB corporate research. He proposed a modulation diversity scheme for a base station [13]. In 1993, a group of researchers from the Signal Processing Research Department at AT&T Bell Laboratories published a paper about advanced modulation techniques for receive antenna diversity [14]. Few years later, Alamouti proposed his distinguished paper that introduced a simple way of transmit diversity for wireless communication systems [15]. In Alamouti's paper, he described the simplest space time coding method where it requires simple signal processing at the receiving side. Since then, Alamouti scheme became among the most important technique that is used until today by almost all wireless communication standards.

During the same period of time, another type of multiple antenna technique was proposed by Gerry Foschini. In 1996, Foschini and his team at the research lab of AT&T published his milestone paper about using multi-element antennas for layered space time in wireless communication in which he exploits fading to improve throughput capacity [16]. This paper described the main concept of the spatial multiplexing methods that was named BLAST which stands for Bell Labs Layered Space Time. Two years later, Foschini and his team from AT&T labs published their paper about the Vertical BLAST (V-BLAST) which a specific type of BLAST scheme [17].

After these extraordinary research papers during the 1990s about the spatial diversity, a lot of clever ideas was published where new methods of multiplexing and spatial diversity were used to propose MIMO techniques. MIMO technology was launched commercially for the first time in 2001 by Iospan Wireless Inc. [18]. Four years later, MIMO technology was integrated in the WiMAX standard where including MIMO technology in the WiMAX standard gave it a much higher spectral efficiency. Nowadays, MIMO is implemented commercially in several wireless standards for different antenna configuration as shown in Table 2.1.

Wireless Standard	Antenna Configuration
(WiFi) IEEE 802.11n	4×4
(WiMAX) IEEE 802.16e	4×4
(Enhanced HSPA) $HSPA^{+}$	2×2
LTE	4×4
LTE-Advanced	8×8
(Enhanced 802.11n)	8×8

Table 2.1: MIMO configurations that are used in the wireless standard commercially [9].

2.1.1 Single-User MIMO

The simplest and first form of multiple antennas is the point-to-point MIMO (or Single-user MIMO) system which was proposed at the end of the 20^{th} century [19], [20]. It is basically a base station that has number of antennas *N* that are serving a user terminal that has multiple antennas *M*. At the receiver, there is additive white Gaussian noise (AWGN) where at every channel there is sent and received vector. The spectral efficiency for point to point MIMO based on Shannon theory can be represented as follows

$$C^{UL} = \log_2 \left| I_N + \frac{SNR_{UL}}{M} KK^H \right|$$

$$C^{DL} = \log_2 \left| I_M + \frac{SNR_{DL}}{N} K^H K \right|$$

where K is $N \times M$ matrix which is the channel frequency response between the user terminal and the base station. The signal to noise ratio for uplink and downlink are proportional to the sum of powers. The normalizing by *N* and *M* shows that if the signal to noise ratios have constant values, the total power is independent of the number of *N* and *M*.

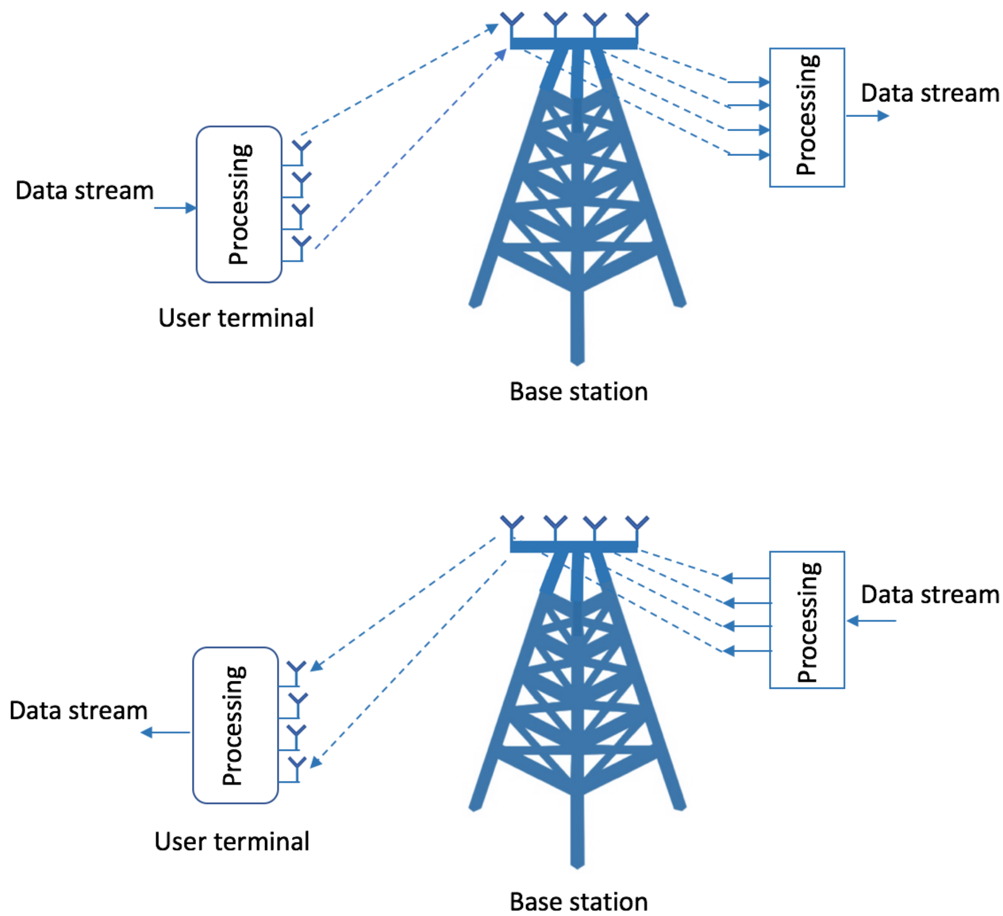

Figure 2.2: Uplink and downlink data transmission for Single-User MIMO.

Theoretically, spectral efficiency scale linearly with the number of antennas in the two terminals. In real life scenarios, however, there are several limitations that could affect the usefulness of point to point MIMO systems. First, since the line of sight conditions are stressing, the independent streams of min(N, M) are not supported by the propagation environment. Also, the equipment of the two terminals are complicated where each antenna needs distinct RF chains. Moreover, to split up the streams of data, advanced digital processors are needed. The last limitation, the scalability of channel spectral efficiency of the system with min(N, M) is getting slower at the edge of the cell where most of the users are found and where the signal to noise ratio is low due to the higher path loss.

2.1.2 Multiuser MIMO

The concept of Multiuser MIMO is based on a BS that is serving multiple user terminals and using the same frequency and time resources [21]. The idea of having a BS with antenna array serving multiple terminal simultaneously is not new [22], [23]. The model of Multiuser MIMO was derived from the concept of Single-user MIMO by splitting the multiple antennas in the Single-user terminal to multiple user terminals. The ultimate performance of Multiuser MIMO can be reached by Shannon theory.

Multiuser MIMO has some advantages over Single-user MIMO. The first advantage is the less sensitivity that the Multiuser MIMO has to propagation environment compared to Single-user MIMO. The LoS conditions is not stressing for the Multiuser MIMO while it is stressing for Single user MIMO. Another advantage, unlike Single-user MIMO that requires multi antenna in the user terminal, Multiuser MIMO needs user terminal with single antenna.

On the contrary, Multiuser MIMO has number of drawbacks that could affect the profit of using it. First, the spectral efficiency for uplink and downlink requires complicated signal processing to be archived. The second drawback is the need of knowing the channel matrix on the downlink for the base station and the user terminal. Also, the user scheduling is another challenge where multiple users are served using the same time and frequency resources. Implementing scheduling schemes would increase the cost of the system operation. Due to these disadvantages, Multiuser MIMO is not scalable with respect to the number of user terminal or to the number of antennas at the base station. Table 2.2 shows a comparison between Multiuser MIMO and Single user MIMO for different features.

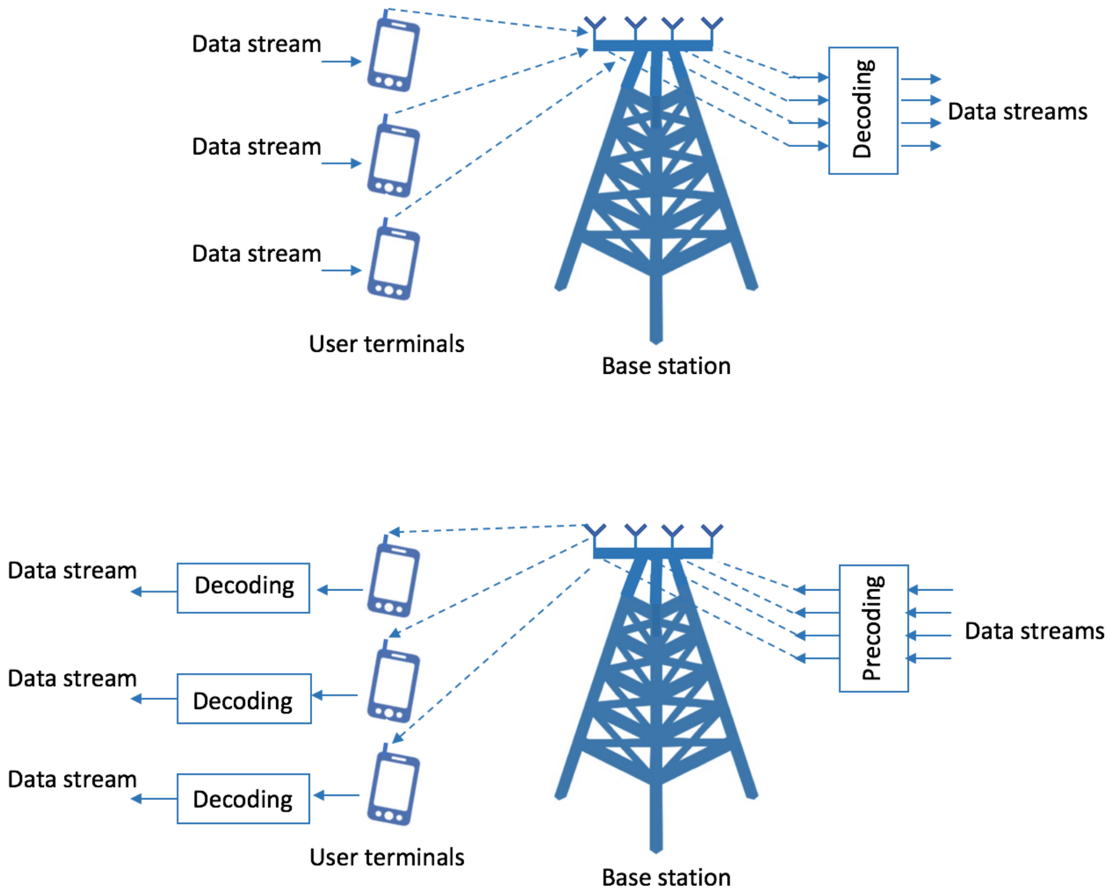

Figure 2.3: Uplink and downlink data transmission for Multiuser MIMO.

Table 2.2 shows a comparison between Multiuser MIMO and Single-user MIMO. The first feature is the main idea behind these schemes where the base station in the Single-user MIMO is communicating with single user terminal while there are several users that are connected with the base station for Multiuser MIMO system. To achieve higher spectral efficiency and to enhance the gain of multiplexing, Multiuser MIMO system needs perfect Channel State Information (CSI) [24]. The level of SNR plays a significant role in the system performance in which the Multiuser MIMO systems have higher throughput at higher SNR while Single user MIMO systems have higher throughput at lower SNR levels. One of the disadvantages of using Multiuser MIMO is the strong interference from the neighboring channels while there is no interference when Single user MIMO systems are used.

Feature	Single user MIMO	Multiuser MIMO
Main Aspect	Base station communicates with single user	Base station communicates with multiuser
Purpose	Having higher data rate	MIMO capacity gain
Channel State Information (CSI)	No need for CSI	It is required to have perfect CSI
Advantages	No interference	Multiplexing gain
Throughput	Higher throughput with lower SNR	Higher throughput with higher SNR

Table 2.2 : comparison between Multiuser MIMO and Single-User MIMO systems for different features [25], [26]

2.2 The Future of 5G

The possible standard of the upcoming Fifth Generation (5G) cellular network needs to meet several requirements so it can be integrated smoothly with the LTE and WiFi standards to provide perfect experience for the users [27]–[38]. One of the most important requirements for the 5G is the data rate that needs to meet the increasing demand. The data rate can be measured in different methods as follows:

- Area Capacity is the data that network can provide for the consumers and can be measured by bit/s/unit. The area capacity for the 5G system should be increased by a factor of 1000 compared to 4G system.
- Edge rate is the worst case scenario for the data rate that the user is receiving. For the current 4G cellular network systems, the edge rate is around 1 Mbps. The edge of 5G system should be ranged from 100 Mbps to 1 Gbps [5].
- Peak rate is the ideal case scenario where the user is getting the highest possible data rate. The peak rate the number that is used in the marketing commercials of the companies.

The second requirement that needs to be achieved is the network latency. The current 4G network has a latency of 15 ms. The latency for the current networks is more than enough for existing applications. On the other hand, the new applications that will be available when 5G comes to fruition need much lower latency. These applications include 2-way gaming, virtual reality glasses, cloud-based computing and other technologies. Consequently, the latency for the 5G network needs to be at least 1 ms, which is much lower latency compared to the existing 4G network or the previous networks as Table 2.3 shows.

Cost and energy consumption are one of many challenges that 5G should overcome. The consumed energy must be decreased significantly since the data rate will be increased by a factor of 100 per link so that the system become more efficient. Also, the operation cost in 5G should be much cheaper than the 3G and LTE networks. Nowadays, macrocells that are used in the 3G and 4G networks are more expensive than the expected small cells in 5G networks because of its simple signal processing. In the near future, 5G networks will be supporting a higher number of devices with different types, so it is a necessity to be able to support this large number of devices efficiently. Each cell might need to serve more than 10,000 devices that need low data rate besides supporting mobile devices that needs high date rate. The new cellular network will need a paradigm shift in terms of network management and control plan compared to 4G networks where the number of devices are much smaller.

In the near future, 5G networks could support several applications from gaming and entertainment to more critical application such as remote surgery. The patient in this type of operations can have a surgery in one country while a surgeon in another country is controlling a robot remotely. This critical situation is requiring much lower latency and much high bandwidth to reap the benefits of this type of applications and to assure flawless operations [39].

Another application that could be achieved when 5G networks come to fruition is Connected Cars technology. By equipping the vehicle with internet access, it will be able to communicate with outside environment or even with network that can manage the road traffic [40]. This application could increase the road safety and prevent traffic jams. To be applicable in the future, the idea of driverless cars requires a 100% coverage in every street to be applied in the future. This application needs a latency of 1 ms which can be achieved according to the specifications of the 5G networks.

Cloud-based offices, which needs high bandwidth and low latency, is another possible technology in the 5G era [41]. This type of systems could be achieved in the near future due to the expected high cloud data storage when 5G network is implemented. Videoconference for multiple people from different countries is a key element for the cloud-based offices technology which requires much lower latency and a 100% geographical coverage.

The machine-to-machine (M2M) applications such as connected home systems, healthcare monitoring and smart thermostat are used today but not widely. By 2020, it is forecasted that the number of M2M devices could exceeds 1 billion [42]. With much higher data rate and very low latency in 5G networks, M2M systems could be enhanced largely and creatively to cover more critical areas such as disaster response systems and automated traffic lights.

	2G GSM	3G WCDMA	LTE	5G (Expected)
Bandwidth	200 KHz	5 MHz	20 MHz	Hundreds of MHz
Type of Modulation	GMSK	QPSK, 16QAM	QPSK, 16QAM and 64QAM	256QAM
Maximum Data rate	14.4 Kbps	3.1 Mbps	100 Mbps	20 Gbps for downlink
Latency	700 ms	Less than 200 ms	Less than 30 ms	Much lower latency

Table 2.3 : comparison between mobile phone generations [43].

There are several technologies that might be used to achieve the 5G requirements especially achieving much higher data rate. These technologies can be classified into three categories:

- **Small cells** could be used to increase the spectral efficiency where the throughput is improved with higher cell density. Shrinking the cell size will provide several advantages yet it has its drawbacks.
- Using **mm-Waves** is another conventional solution to increase the bandwidth. It has potential where the available frequencies have wide range.
- **Massive MIMO** as a promising technology proposes a solution that could meet the requirements for the 5G networks. It may lead to major changes of the design of the base station itself.

2.2.1 Small Cells

One of the simplest yet effective way to enhance the capacity of cellular network is to increase the number of cells and making them smaller where this concept has been deployed in different generations of cellular networks [44], [45]. In the 1980s, the 1G wireless telephone technology, which had analog standard, used to have huge cell radius that could reach up to 30 km [46]. Few years later, the size of the cell is getting smaller for 2G and 3G networks where the cell could have a radius of 3 km. in today wireless networks, the base station can be serving users within a radius of 200 meters especially in dense metro areas.

The networks are shrinking in terms of size to picocells with a range of 100 meters and to femtocells with a range of 10 meters which is the same range of WiFi networks [47], [48]. The reduction of cell size as shown in Figure 2.4 has a number of advantages, electromagnetic spectrum reuse throughout a specific area is the most important benefit [5]. With smaller cell size, the number of users that need to be served is reduced and there will be more radio-frequency resources at each base station. By reducing the cell size, the base stations will be smaller and will require lower operation power and eventually the cost will be much cheaper [47].

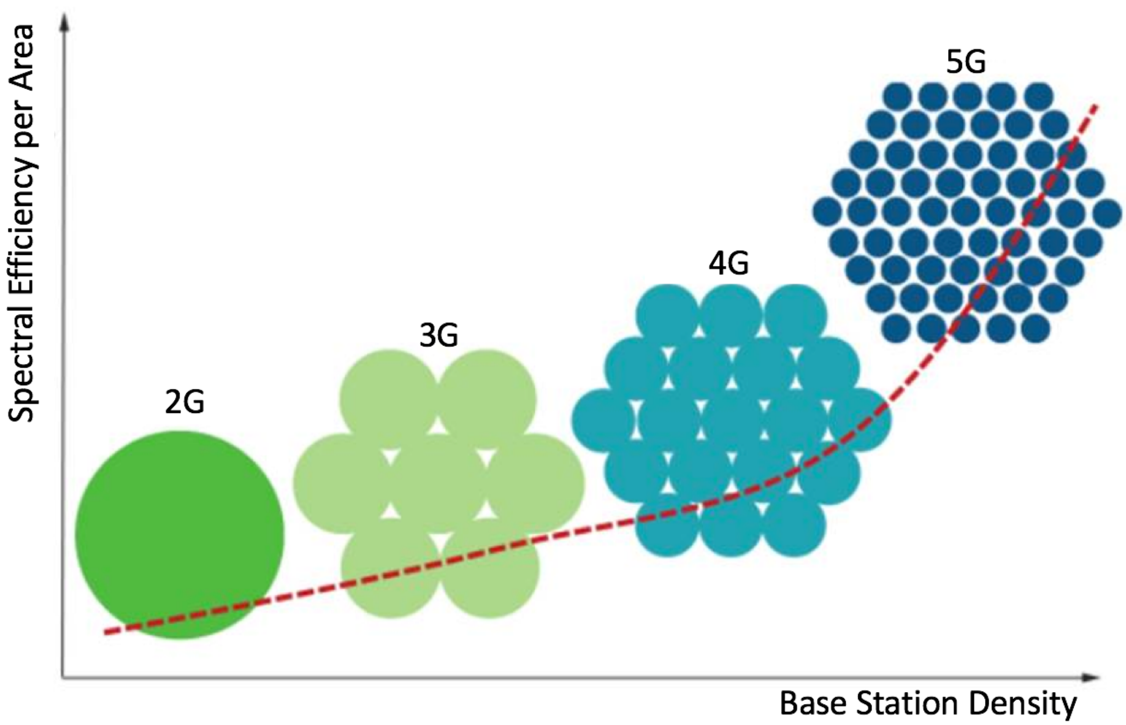

Figure 2.4: Base station density is getting higher by having smaller cells [49].

Even though the cost of the base stations equipment of small cells will be cheaper compared to larger base stations, the cost of the backhaul will increase. Fiber connection might be used for backhaul which is more expensive than the typical microwave systems. Another drawback of deploying small cells is the interference where it is getting worse. Also, the cellular and WiFi networks are already very dense.

2.2.2 Millimwter-Waves

The microwave spectrum that is used today by mobile systems is limited and it is ranged from 300 MHz to 3 GHz [50]. To double the bandwidth for the microwave spectrum there are two ways. One is to *refarm* spectrum, for example, refarming the television spectrum into smaller bands to be used at urban broadband access [4]. Unfortunately, refarming has its own drawbacks, such as, the limited spectrum and the higher cost. The other way to increase the bandwidth is to share microwave spectrum by applying cognitive radio technology [51] which has some issues in terms of spectrum efficiency [4].

Other than using the limited electromagnetic spectrum at microwave frequencies, it is possible to use the huge amount of spectrum that is ranged from 3 GHz to 300 GHz which is called millimeter-Waves [50]. The International Communication Union (ITU) proposed a list of frequencies above 24 GHz that can meet the commercial needs [52]. In December 2016 and after the proposal of ITU, the Federal Communication Commission (FCC) adopted rules for mmWave bands above 24 GHz [53].

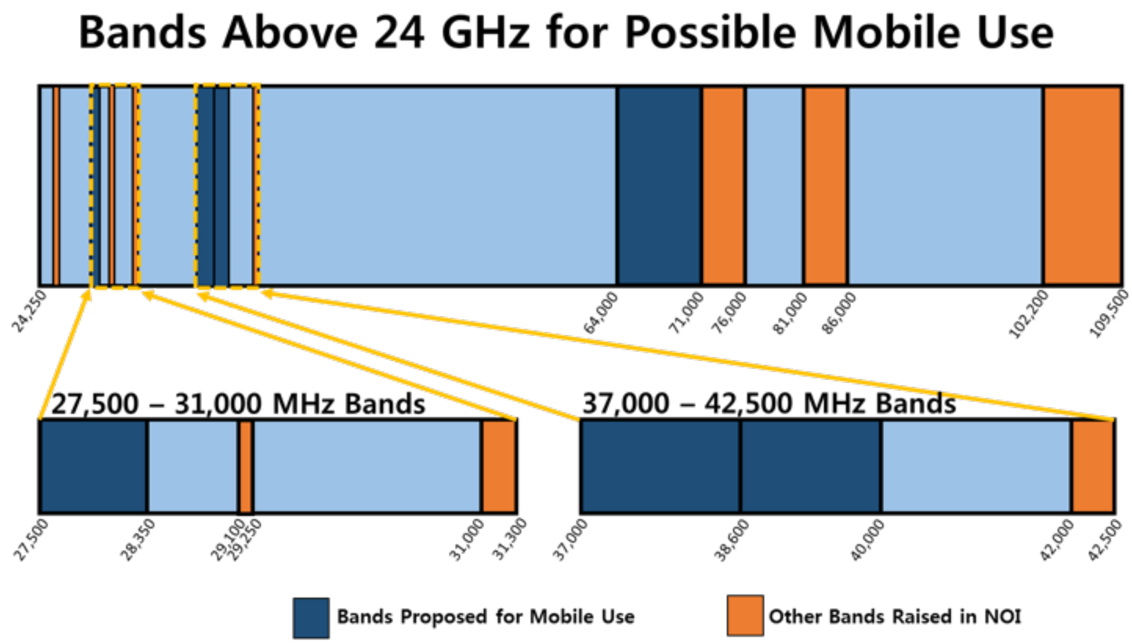

Figure 2.5 : Frequency bands proposed by FCC for mobile applications [54], [53].

Mm-Waves can provide enough frequency for the demand by mobile application in upcoming decades. The mm-Waves have a wavelength ranging from 1 mm to 10 mm and it has a spatial resolution higher than what microwaves have. Since the bandwidth is broader, the size of the antennas and the equipment will be smaller and the cost will be cheaper. Also, mmWaves require lower power supply voltage.

Still, the mmWaves has several challenges to be tackled such as pathloss since the transmitter and the receiver require line of sight connection. Moreover, the absorption due to rain and atmosphere condition such as air would play a negative role in the signal propagation. Also, with such a high frequency, the range of transmitted signal will be much shorter and it will be more difficult to penetrate through buildings. Even though the antenna size will be smaller and cheaper, some of the hardware components such as digital to analog converters will be pricy.

2.2.3 Massive MIMO

In wireless communication, the transmitted signal is exposed to harsh environment where it could be attenuated by fading because of the multipath propagation or attenuated by shadowing due to having large obstacles between the base station and the user terminal. The use of multiple antennas in the transceivers is known as multiple input multiple output (MIMO). In the past decade, MIMO systems has grabbed the attention and engaged into several wireless standards such as long term evolution LTE-Advanced [55], [56]. One of the developed form of this technology is the Multi-User MIMO where several users are connected to the multi-antennas BS and served simultaneously [55]. This technology has its own advantages yet there are several drawbacks such as multiuser interference, channel state information acquisition and user scheduling. The ultimate form of Multiuser MIMO is the promising technology that is called Massive MIMO (it is also known as large-scale MIMO) [5], [57].

Massive MIMO concept was proposed for the first time by Thomas Marzetta from Bell Labs in 2010 [58], [7]. It is a scalable form of Multiuser MIMO where there are several essential differences between Massive MIMO and Multiuser MIMO [59]–[68]. First of all, Massive MIMO has much larger number of antennas in the base station compared to the number of users. Second, in the Massive MIMO, only the base station needs to learn the frequency response matrix between the BS array and the user terminals array. Third, the uplink and downlink signal processing is simple for the Massive MIMO.

The proposed concept of massive MIMO is to equip the base station with hundreds of antennas which is much larger than the number of users as shown in Figure 1.3. The antenna array receives data signal from the user terminals and selectively sends data streams sharing the same time and frequency resources. On downlink, each user should receive only the data stream that is intended to him [69], [70]. On uplink, the BS receives and recovers the data signals that was sent by the user terminals. Due to line of sight conditions, the BS has an individual beam for each user terminal as shown in Figure 2.6. By increasing the number of antennas in the base station, the beams that are directed to the user terminal will be narrower and the power will be more focused.

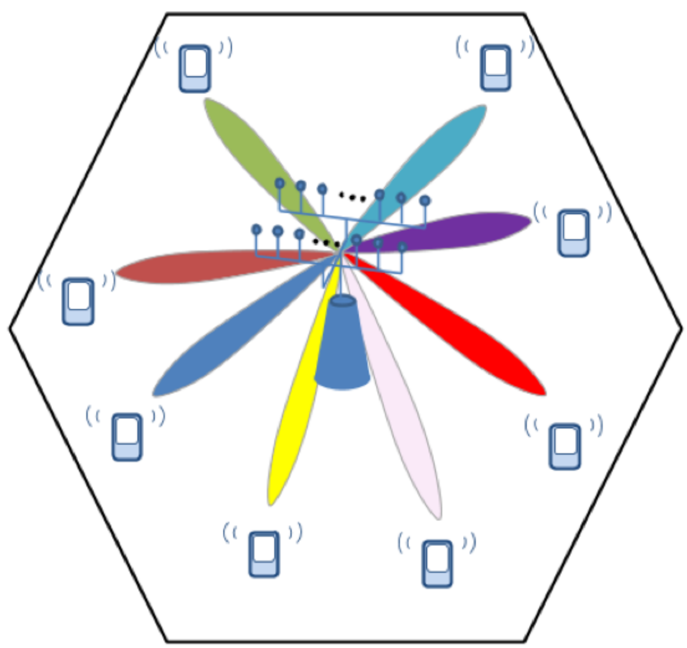

Figure 2.6: Beamforming transmission in a massive MIMO system [71].

Massive MIMO depends on measuring the channel frequency response where either the BS terminal or the user terminal sends known training signals and the receiver can estimate frequency response [72], [73]. The environment of the channels spatial correlation would affect the accuracy of the estimated channel [74]. There are several methods to estimate the channel and get accurate CSI where the most popular method is the pilot based estimator. After conducting the channel estimation, CSI should be established promptly to avoid any change in the state of the channel. To get accurate CSI, time division duplexing (TDD) should be used as operation mode to get the advantages of reciprocity where the CSI is the same for the uplink and the downlink transmission [75].

The frequency division duplexing (FDD) has a different operation form where the base station sends pilots to the user terminal to get the downlink channel, and send back the estimated channel state information to the base station which is called CSI feedback. By using FDD, resources are consumed since there must be a unique pilot for each antenna in the transmitter and these pilots are required to be orthogonal. The amount of consumed resources by the different forms of MIMO is shown in Table 2.4. The number of antennas in the base station is denoted by N and the number of user terminal is denoted by M. It is shown in Table 2.4 that when TDD is used as operation mode in Massive MIMO systems, the system scalability is not limited to the number of antennas in the base station N.

MIMO Variants	FDD UL	FDD DL	TDD UL	TDD DL
Single-user MIMO	M pilots (no CSI feedback)	N pilots	M pilots	N pilots
Multiuser MIMO	M pilots + N CSI feedback	N pilots	M pilots	N pilots
Massive MIMO	M pilots + N CSI feedback	N pilots	M pilots	none

Table 2.4: Possible resources that are consumed by MIMO variants [76].

By using TDD protocol, the pilot signal and the data signal are sharing the same time slot where the coherence time is divided into different stages for uplink and downlink transmission as shown in Figure 2.7. In this protocol the estimation accuracy is independent of the number of BS antennas N so it is possible to increase N to any desired number [74]. One of the advantages of using TDD is that the knowledge of the uplink channel need to be obtain only by the base station to operate coherently [77].

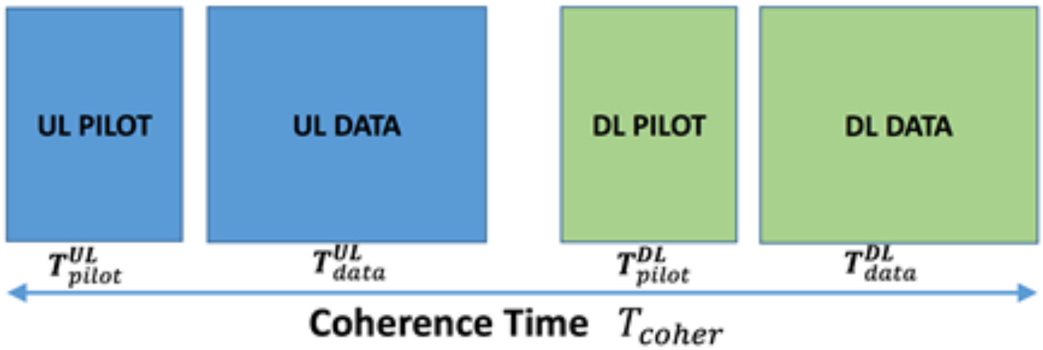

Figure 2.7: Uplink and downlink stages for TDD system [9].

2.2.3.1 Potentials of Massive MIMO

Massive MIMO has several benefits include:

- providing higher spectral efficiency where it can be increased 10 times or even more without increasing the number of base stations[78]. This improvement comes with a possibility of having lower transmit power [77]. Besides the improved capacity, the large number of BS antennas would improve the energy efficiency since the energy is sharply focused into small area. Thus, each user should only get the signal that is intended for him with the lowest amount of interference from other channels [75]. The channel response for Massive MIMO systems would become smoother due to the massive spatial diversity [5], [79].
- The structures of the transceivers and their signal processing are going to be much simpler compared to the multiuser MIMO because of the nature of the channels between the base station and the user terminal where the active users are sharing the same signaling resources [80]. In Massive

MIMO, instead of using 50 W amplifiers that are expensive, a low cost amplifiers are going to be used where these amplifiers have a power in the range of mW [81]. Coaxial cables, which are used in today BS and have a diameter of 4 centimeters, are another expensive item that can be eliminated.

- In wireless communications, the performance of the system can be affected badly by fading. The destructive multipath interference would make it difficult to create links with low latency. In Massive MIMO systems, the latency can be reduced since fading can be avoided due to the beamforming and the large number of antennas.
- The man-made interference that is intentionally made against the wireless system networks is a real threat and a serious concern. the jamming components are not expensive and would cost a couple of hundreds of dollars. Since Massive MIMO is multiple antenna technology, the robustness against jamming is high.

2.2.3.2 Limitations of Massive MIMO

Massive MIMO has several limitations include:

- Most of the published works on Massive MIMO systems are assuming that the channels are orthogonal and uncorrelated which is not the case in real life situation [74], [82]. The effect of correlation models on Massive MIMO systems need to be analyzed to see the performance of spectral efficiency and energy efficiency.
- Nowadays, the transmission mode that is used in most of the wireless communication systems is based on Frequency Division Duplexing (FDD). On the other hand, most of the proposed Massive MIMO models are based on Time Division Duplexing (TDD) due to its simple channel estimation. To have Massive MIMO based on FDD mode, it is important to reduce the overhead feedback. One way of reducing the feedback is to calculate the CSI of some antennas selectively instead of calculating CSI for each base station antenna.
- One of the challenges is to reduce the cost of the hardware components in Massive MIMO systems. There will be hundreds of elements in the BSs such as RF chains, AD converters, DA converters and so on. So, it is necessary to develop new algorithms to reduce the cost by getting rid of receiver quantization.
- Pilot contamination is one of the most serious challenges in Massive MIMO systems. Assume that there is two cells A and B. The effect of pilot

contamination could appear in two different stages where the BS in cell A may overhears the transmitted pilot from cell B during training phase. Then, the vectors that are transmitted form cell A will be partiality transmitted to users in cell B. To overcome this issue, estimation techniques need to be created. Also, the structure of the pilots need to be designed carefully to avoid overhead blast.

- Another issue that could decrease the accuracy of channel estimation and affect the capacity of Massive MIMO system is the hardware impairment. This problem need to be taking into consideration when designing a system of Massive MIMO. Several studies investigated the effect of the hardware impairments on the Massive MIMO systems performance [80], [69]. Studies show that hardware impairment has a limited effect on the BS terminal, while on the user terminal end it has higher effect on the system performance [80].

2.2.3.3 Massive MIMO Projects

Over the past few years, Massive MIMO has grabbed the attention of research community. There are several live projects on Massive MIMO in the United states, Europe and Asia. Most of these projects are still ongoing while some of them are completed where they released part of their research outcome and products. Some of the live project on Massive MIMO are listed below in details:

Figure 2.8: Massive MIMO Prototype used by Lund and Bristol Universities research [83].

One of the ongoing projects on Massive MIMO is conducted by **Lund University** and **Bristol University** where they used **National Instrument Testbed** [83]. A team of researchers from the two universities achieved a new record of spectrum efficiency. At their test in May 2016, they had a Massive MIMO system with 128 antenna array operated at 3.5 GHz radio channel. The results revealed much higher spectrum efficiency with 22-fold increase compared to the current standard LTE [84]. Figure 2.8 shows the Massive MIMO prototyping testbed with 128 antenna array at the base station.

MAMMOET is another project that was funded by European Union with an investment of $5 million [85]. This project is about making Massive MIMO more efficient and attractive technology for future networks. There were several objectives for this project need to be accomplished to achieve the overall goal. The first stage is to investigate the nature of the channel and exploring the possible configurations of antenna and analyzing its potentials and limitations. Another objective is providing scalable processing algorithms that can be implemented easily with the hardware components. The last stage of this project is to provide a solution to the standardization bodies.

Excellence Center at **Linköping** had a collaboration with **Lund University** on **ELLIIT** project for Massive MIMO antenna array [86]. They produced a fixable testbed with 100 antenna array as shown in Figure 2.9 [87]. The project investigates the use of Massive MIMO with more than 30 antenna arrays in the base station experimentally using the Lund testbed. They developed algorithms for antenna selection also they quantified the tradeoff relation between the energy and spectral efficiencies.

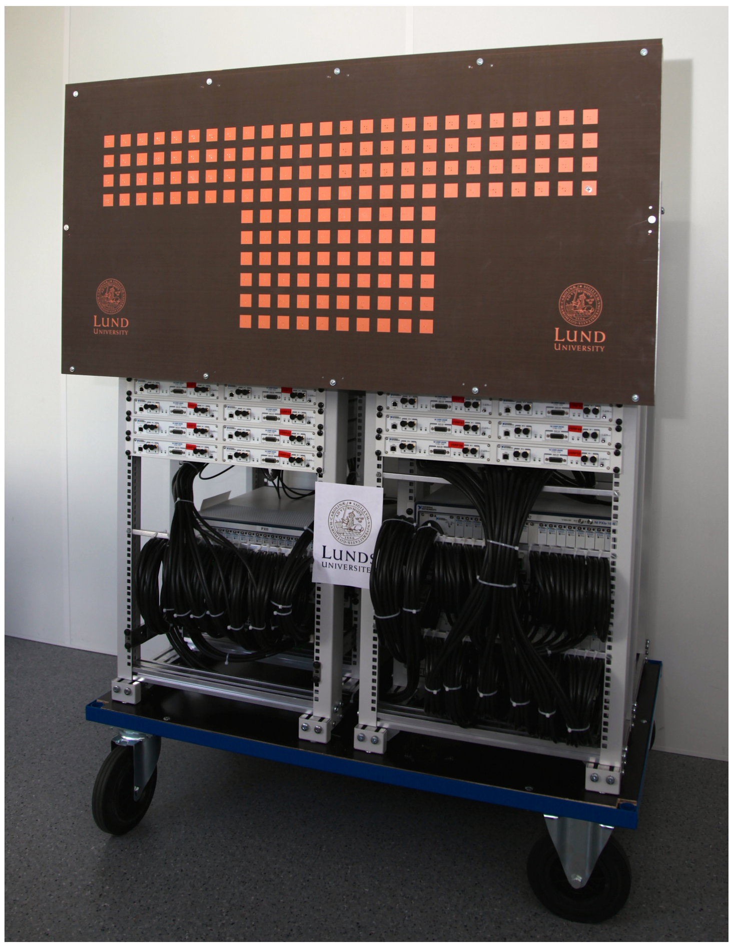

Figure 2.9: Massive MIMO testbed in Lund University [87].

Chalmers University of Technology and VINN Excellence Center CHASE worked together on a project to build a Massive MIMO testbed (**MATE**) [88]. In this project they had a partnership with different companies such Ericsson, Saab, National Instrument and others. The first goal for this project was to build the testbed and then investigate the advantages and drawbacks of Massive MIMO system with different interfaces for analog and digital components. One of the goals also is to create new techniques for Massive MIMO transmission synchronization.

National Science Foundation (NSF) has funded the **University of California-Berkeley** for a 3 years project to study the energy and cost efficiency of Massive MIMO systems [89]. The overall goal of this project is to address and overcome the critical challenges for the implementation of Massive MIMO systems. Specifically, the goals of this project are: creating a low cost Massive MIMO array architecture that can be deployed effectively in terms of power efficiency. Also, developing new techniques for medium access control (MAC) that are appropriate with synchronization and low latency.

Nokia and **Sprint U.S.** have been working on adaptive antenna for Massive MIMO systems [90]. At Mobile World Conference 2017 in Barcelona, the two companies demonstrated a showcase of Massive MIMO system where the system capacity was increased eight times compared to LTE systems. Their Massive MIMO is equipped with 64 antennas at the transmitting side with TDD operating mode. This project revealed the scalability of Massive MIMO in which it could be a key technology for 5G networks.

According to Günther Ottendorfer the Sprint technology chief operating officer, "Massive MIMO is a critical part of our strategy to increase the capacity of our LTE Plus network today, and in the future, it will be a key element of our 5G network. Working with Nokia to deliver massive MIMO is a competitive advantage for Sprint because it is more easily deployed on 2.5 GHz spectrum due to the smaller form factor of the radios, and it's an important innovation that will take advantage of our deep spectrum holdings" [90].

Chapter Three: Spatial Correlation Effect on Channel Estimation

The channel estimation accuracy is analyzed where channel spatial correlation is affecting its performance. In this chapter, the system model consists of single base station that is equipped with big number of antennas where it is serving a single user terminal. Base station terminal receives and sends data from a user terminal as shown in Figure 2.1. in this system, The Time Division Duplexing (TDD) protocol is used where its coherence time is divided into different stages for uplink and downlink data transmission. We are able to increase the number of base station antennas to any desired number since the channel estimation accuracy is independent of the number of antennas at the base station [69]. Due to having channel reciprocity, the channel state information will be the same for uplink and downlink data transmission. It is assumed that there is stochastic block fading channel between the base station and the user terminal. The realizations of the channels are produced randomly using Monte Carlo method of generating random numbers. It is assumed that there are synchronized and identical coherence period of time.

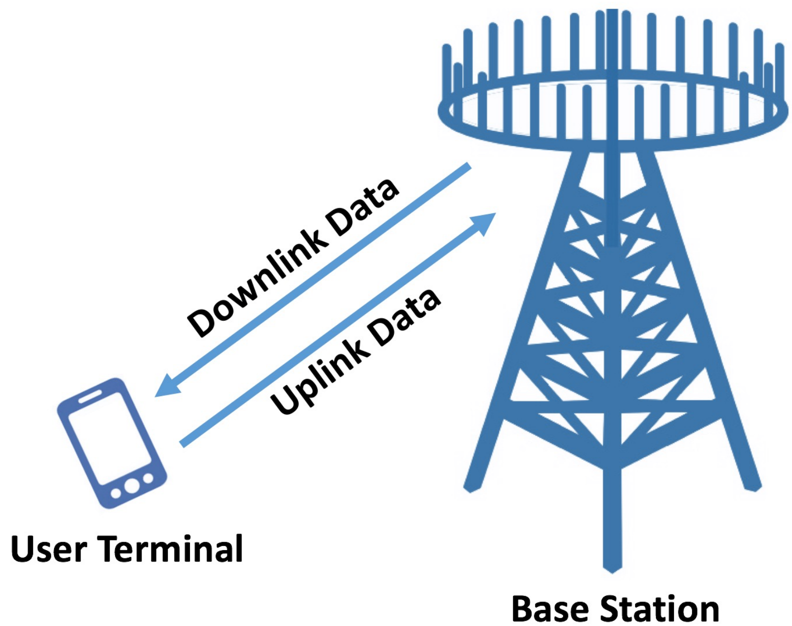

Figure 3.1: Uplink and downlink dtat transmission between user terminal and base station [9].

3.1 System Model and Assumptions

It is possible to maintain continues channel state information to detect uplink data information due to having channel reciprocity [91], [7]. Assume that the base station has a large number of antennas N and a single user terminal. There is Rayleigh block fading $\mathbf{h} \sim \mathcal{CN}\ (\mathbf{0}, \mathbf{R})$ between the two terminals. The block fading channel between the terminals is represented as $\mathbf{h} \in \mathbb{C}^{\mathrm{N}x1}$ while channel covariance matrix $\mathbf{R}$ can be represented as

$$\mathbf{R} = \mathbb{E}\{\mathbf{h}\mathbf{h}^{\mathbf{H}}\} \tag{3.1}$$

3.1.1 Uplink System Model

It is assumed that the channel statistical distribution is known by the base station while we have pilot based channel estimator in this system model. Equation (3.2) shows the received signal $\mathbf{y}$ at the BS as follows

$$\mathbf{y} = \mathbf{h}d + \boldsymbol{n} \tag{3.2}$$

$$p = \mathbb{E}\{|d|^{2}\} \tag{3.3}$$

In equation (3.2) the received signal $d \in \mathbb{C}$ could be either data signal or pilot signal while the average power is presented in (3.3). The following equation represents the additive noise $\boldsymbol{n}$ which consists of two terms

$$\boldsymbol{n} = \boldsymbol{n}_{\text{noise}} + \boldsymbol{n}_{\text{if}} \tag{3.4}$$

where $\boldsymbol{n}_{\text{if}}$ denotes interference noise from other transmissions and $\boldsymbol{n}_{\text{noise}}$ represents the noise of the independent receiver that has $(\sigma_{BS}^{2}\mathbf{I})$ covariance and zero mean. For the interference noise $\boldsymbol{n}_{\text{if}}$, it is assumed that it has covariance denoted as $\mathbb{E}\{\boldsymbol{n}_{\text{if}}\boldsymbol{n}_{\text{if}}^{\text{H}}\}$ with zero mean. The conditional covariance matrix that has a channel realization of $\boldsymbol{\mathcal{H}}$ can be characterized as

$$\boldsymbol{Q}_{\boldsymbol{\mathcal{H}}} = \mathbb{E}\{\boldsymbol{n}_{\text{if}}\boldsymbol{n}_{\text{if}}^{\text{H}}|\boldsymbol{\mathcal{H}}\} \tag{3.5}$$

In this system model analysis, it is assumed that for channel covariance matrix **R,** the spectral norm is uniformly bounded independent of the number of BS antennas.

3.1.1.1 Exponential Correlation Model

The exponential correlation model is used in this system to create the channel covariance matrix [92]. We are assuming that **R** consists of two elements (i, j) and can be expressed as

$$[\mathbf{R}] = \begin{cases} \delta r^{j-i}, & i \leq j \\ \delta (r^{j-i})^{*}, & i > j \end{cases} \tag{3.6}$$

where δ represents the scaling factor and r denotes the correlation factor of the neighboring subchannels. The value of correlation factor r is limited between 0 and 1 while the angle of departure and arrival is denoted by $\angle r$. The exponential correlation model is easy to be implemented and it might not be the most accurate model for creating the channel covariance matrix [93]. The value of correlation factor $|r|$ denotes eigenvalue spread of **R** while $\angle r$ represents the eigenvectors for **R**. Since the angle of r has no effect on the mean square error, it is assumed that r is a real value. By increasing the correlation factor the spectral efficiency will be affected in a similar way of decreasing the value of signal to noise ratio.

3.1.1.2 One Ring Model

The one ring model is another way to create the channel covariance matrix [26]. In this model, it is assumed that the user terminal is bounded by a ring of scattering with a radius of r. Figure 3.2 shows a base station with N antennas where it is not affected by local scattering since it is elevated. The distance between the base station and the user terminal is denoted as d and the azimuth angle is denoted as θ. The multipath components have angular spread of Δ. The channel covariance matrix for any two antennas n and p cane be expressed as

$$[\mathbf{R}]_{n,p} = \frac{\mathbf{1}}{\mathbf{2}\Delta} \int_{-\Delta}^{\Delta} e^{jk^{T}(\alpha+\theta)(u_n - u_p)}\, d\alpha, \qquad 1 \leq n, p \leq N \tag{3.7}$$

where

$$k(\alpha) = -\frac{2\pi}{\lambda}(\cos(\alpha), \sin(\alpha))^{\mathrm{T}} \tag{3.8}$$

The position vectors of the base station are denoted as u_n, u_p. It is assumed that the spacing between antennas is half wavelength with uniform linear array (ULA). The Toeplitz form of the channel covariance can be represented as

$$[\mathbf{R}]_{n,p} = \frac{\mathbf{1}}{\mathbf{2}\Delta} \int_{-\Delta+\theta}^{\Delta+\theta} e^{-j2\pi D(n-p)sin(\alpha)}\, d\alpha \tag{3.9}$$

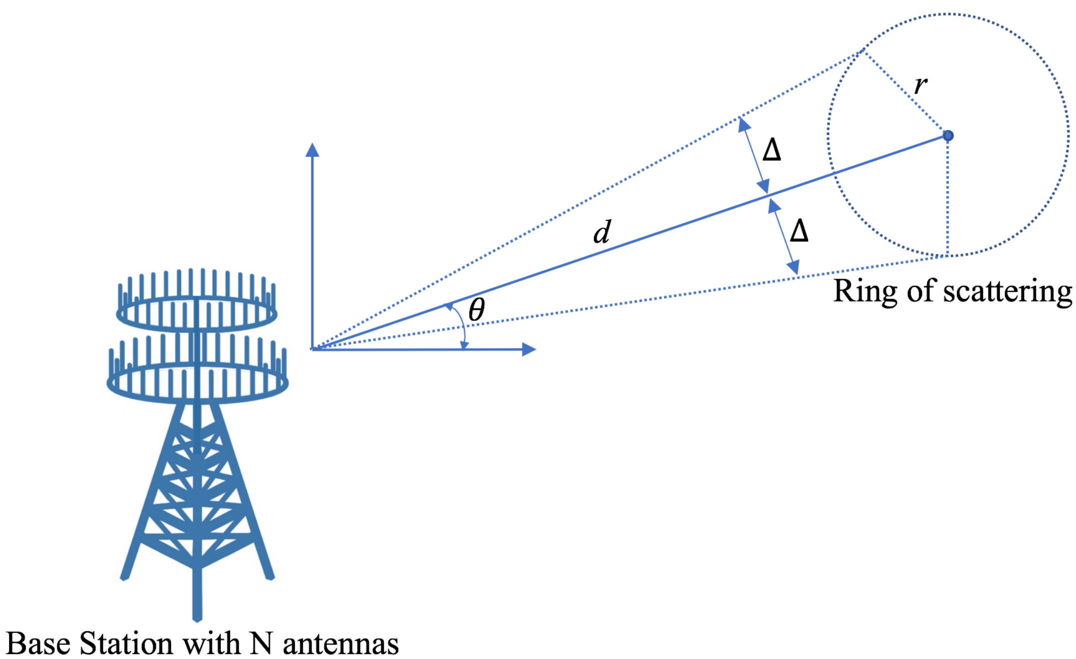

Figure 3.2: One ring model for a base station with N antennas.

3.1.2 Downlink System Model

The downlink system model is shown in Figure 2.1. The received downlink signal is flat fading and can be signified as follows

$$\mathbf{z} = \mathbf{h}^{\mathrm{T}}\mathbf{s} + \boldsymbol{v} \tag{3.10}$$

where $\mathbf{s} \in \mathbb{C}^{\mathrm{N}x1}$ and it could be pilot signal or stochastic data signal that has zero mean. The covariance matrix of the signal $\mathbf{s}$ can be represented as $\mathbf{W} = \mathbb{E}\{\mathbf{s}\mathbf{s}^{\boldsymbol{H}}\}$ where its average power is trace($\mathbf{W}$). On the other hand, the term $\boldsymbol{v}$ is the additive noise where it consists of two terms as follows

$$\boldsymbol{v} = \boldsymbol{v}_{\mathrm{noise}} + \boldsymbol{v}_{\mathrm{if}} \tag{3.11}$$

where $\boldsymbol{v}_{\mathrm{if}}$ denotes the interference noise and $\boldsymbol{v}_{\mathrm{noise}}$ represents the independent receiver noise.

3.1.3 LMMSE Uplink Channel Estimation

In this chapter, linear minimum mean square error (LMMSE) estimator is used where the received signal is compared with the identified uplink pilot signal [94]. The following equation shows the LMMSE estimator of the channel realization

$$\hat{\mathbf{h}} = d^{*}\mathbf{R}\overline{\mathbf{Y}}^{-1}\boldsymbol{y} \tag{3.12}$$

where d represnts the identified pilot signal. The value of user equipment power (p^{UE}) equals to $|d|^{\mathbf{2}}$. The covariance matrix of the received signal $\mathbf{y}$ consists of a combination of different terms that includes average power of user equipment, channel covariance matrix and additive noise as follows

$$\overline{\mathbf{Y}} = \mathbb{E}\{\, \mathbf{y}\mathbf{y}^{\mathrm{H}}\} = p^{UE}\mathbf{R} + \mathbf{S} + \sigma_{BS}^{2}\mathbf{I} \tag{3.14}$$

$$\mathbf{C} = \mathbb{E}\left\{\left(\,\hat{\mathbf{h}} - \mathbf{h}\right)\left(\,\hat{\mathbf{h}} - \mathbf{h}\right)^{\boldsymbol{H}}\right\} = \mathbf{R} - p^{UE}\mathbf{R}\overline{\mathbf{Y}}^{-1}\mathbf{R} \tag{3.15}$$

The total value of MSE can be derived based on the value of **C** that is generated in (3.15) as follows

$$\mathbf{MSE} = \mathbb{E}\left\{\,\left\|\hat{\mathbf{h}} - \mathbf{h}\right\|_{\mathbf{2}}^{2}\right\} = \mathbf{tr}(\mathbf{C}) \tag{3.16}$$

Based on (3.16) the stochatic channel can be represented as a combination of two terms includes the unknown estimate error $\boldsymbol{\epsilon}$ and $\hat{\mathbf{h}}$ which is the LMMSE estimate value as follows

$$\mathbf{h} = \hat{\mathbf{h}} + \boldsymbol{\epsilon} \tag{3.17}$$

3.2 Numerical illustrations and analysis

This section shows the performance of the channel estimation accuracy using different types of spatial correlation models. One ring model and exponential correlation models are used to state a comparison between these two methods. Also, the effect of the pilot length on the channel estimation accuracy is investigated.

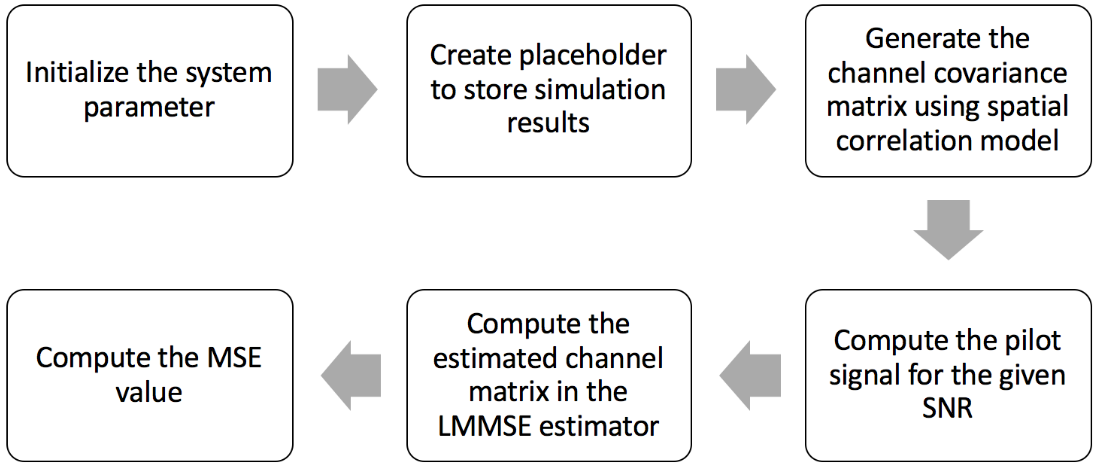

Figure 3.3: Block diagram for the simulation process.

3.2.1 Channel Estimation Accuracy

Figure 3.4 demonstrates the channel estimation accuracy using pilot-based LMMSE estimator with 100 antennas in the base station and single user terminal. The relative estimation error can be represented as a relationship between the mean square error and the trace of **R** as follows

$$\mathrm{MSE}_{relative} = \frac{\mathrm{MSE}}{\mathrm{tr}(\mathbf{R})} \tag{3.18}$$

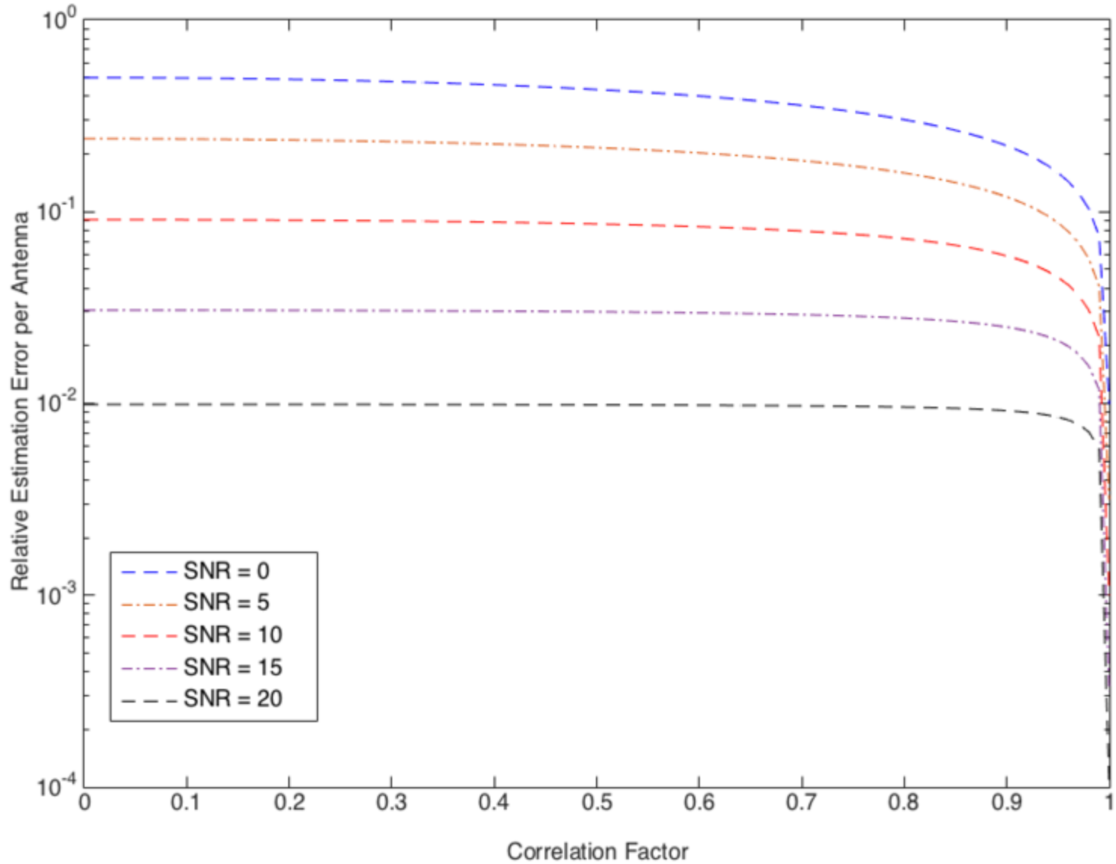

Figure 3.4: Relative estimation error as a function of exponential correlation factor for LMMSE. The SNR values increased from 0 to 20 dB with an increment of 5 [95].

The channel covariance matrix is generated using exponential correlation model where the values of correlation factor are within 0 to 1with an increment of 0.01. the relative estimation error is demonstrated as a function of correlation factor. Figure 3.4 shows that with higher SNR values the estimator is more accurate. Also it is clear that there is a slight development in the accuracy of the estimator when we have greater correlation factor.

Figure 3.5 shows the relative estimation error versus correlation factor with ($N = 2$, 4, 8, 64, 128). It is clear that there is improvement in the estimator performance by increasing the correlation factor and getting closer to 1. We can see that until reaching correlation factor of 0.3 there is no enhancement and after that the channel estimation is getting more accurate. By increasing the number of antennas in the base station, we can see clear improvement at the beginning until we reach large number of antennas where there is no more improvement.

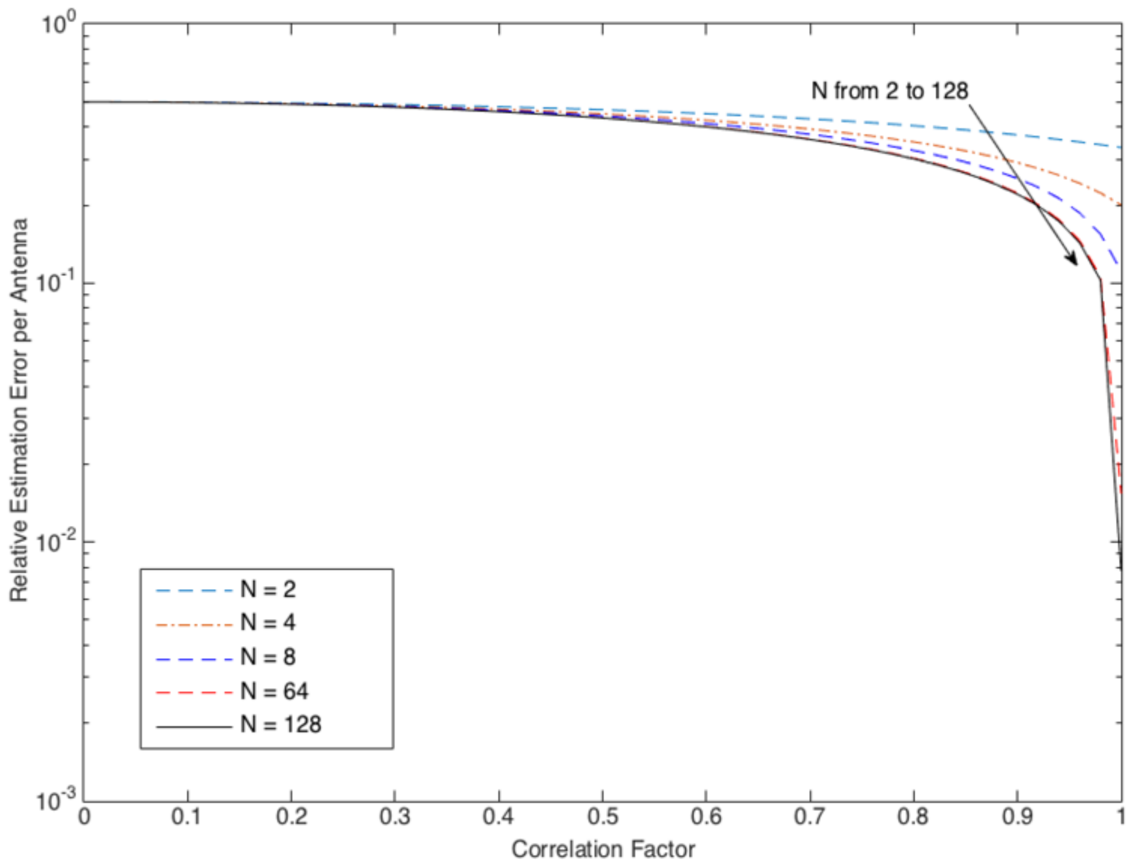

Figure 3.5: Relative estimation error as a function of exponential correlation factor for LMMSE with different values of N [95].

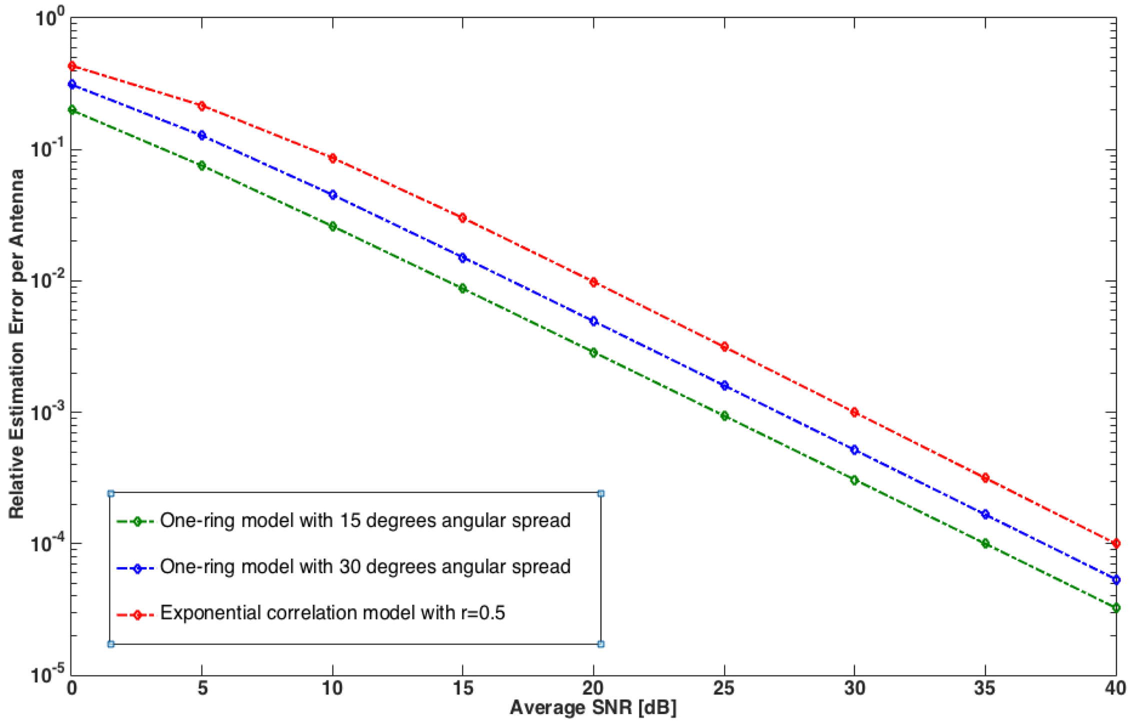

Figure 3.6: Relative estimation error as a function of SNR for *N*=50.

The channel estimation accuracy is shown in Figure 3.6 where the relative estimation error per antenna is presented as a function of signal to noise ratio. The number of antennas in the base station is 50. The estimation error is decreasing at higher signal to noise ratio. The figure shows that the worst channel estimation accuracy is happening when exponential correlation model is used with 0.5 coefficient factor. By using one ring model to generate the channel covariance matrix, the channel estimation is getting more accurate especially when the angular spread is getting smaller.

3.2.2 Impact of the Pilot Length

Using pilot signal d is needed to decrease the total mean square error. By making assumption that the length of the pilot is B and we would like to calculate the value of $\hat{\mathbf{h}}_i = \mathbf{h} + \boldsymbol{\epsilon}$ for $i = 1, .., B$, after taking the average we have

$$\widehat{\hat{\mathbf{h}}} = \frac{1}{B}\sum_{i=1}^{B} \hat{\mathbf{h}}_i = \mathbf{h} - \frac{1}{B}\sum_{i=1}^{B} \boldsymbol{\epsilon}$$

The total value of MSE for the estimate $\widehat{\hat{\mathbf{h}}}$ when having uncorrelated noise is achieved as

$$\mathbb{E}\left\{\left(\frac{1}{B}\sum_{i=1}^{B} \boldsymbol{\epsilon_i}\right)^H \left(\frac{1}{B}\sum_{j=1}^{B} \boldsymbol{\epsilon_j}\right)\right\} = \frac{\mathrm{tr}(\mathbf{C})}{B}$$

From prevouse equation we can observe for the ideal case that by increasing the length of the pilot B, the total value of MSE for the estimate $\widehat{\hat{\mathbf{h}}}$ becomes zero eventually.

The effect of pilot length on the estimator is presented in Figure 3.7. The relative estimation error is displayed as a function of pilot length with 50 antennas in the base station. The noticeable observation is that we can see the advantages of having higher pilot length where the estimation is improving. The matrix of the channel covariance **R** is generated using exponential correlation model. We begin studying the influence of pilot length by having signal to noise ratio equals to 0 dB. The values of correlation factor are 0, 0.7, and 0.9 where we can see that the coefficient factor has a large impact on the accuracy of the channel estimator where the performance is improving with higher correlation factor.

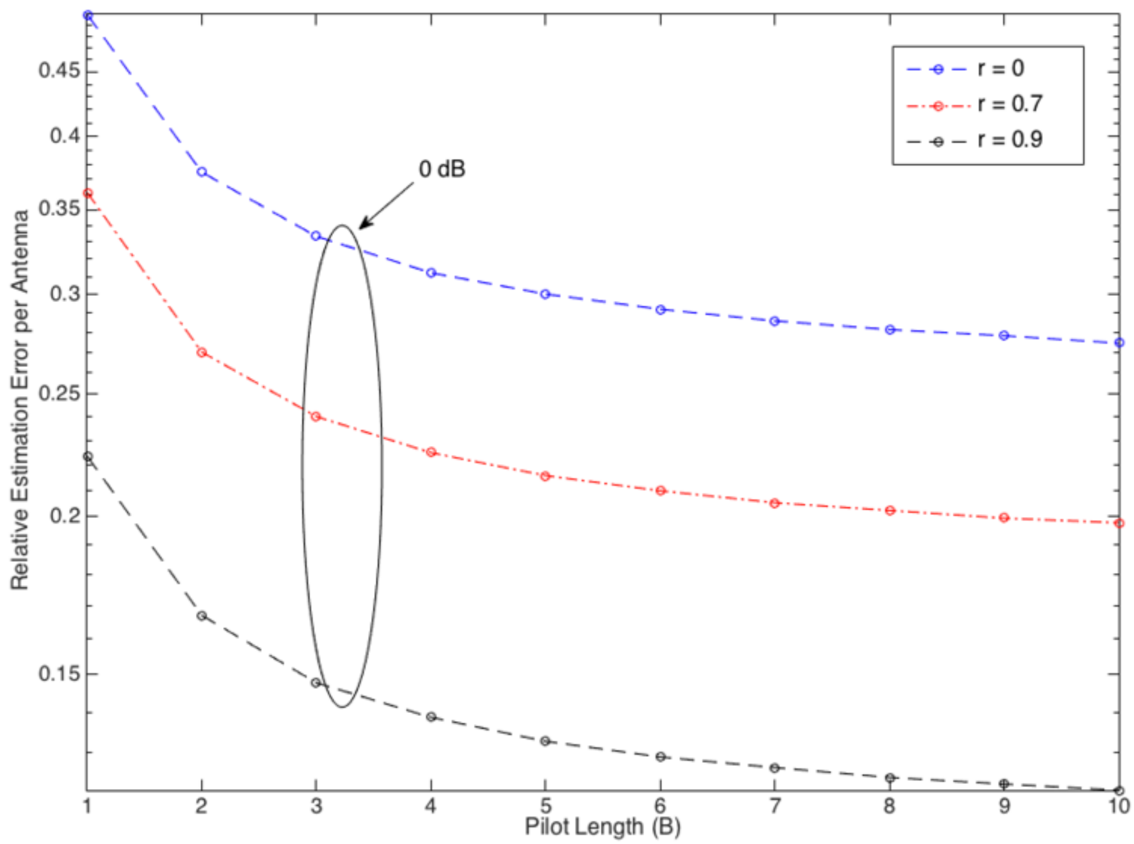

Figure 3.7: Relative estimation error as a function of pilot length. The signal to noise ratio is 0 dB [95].

Figure 3.8 is basically a similar scenario to Figure 3.7 but with SNR equals to 15 dB where the relative estimation error per antenna is shown versus pilot length *B* with 50 antennas in the base station. We can see in Figure 3.8 that the influence of increasing the correlation factor is reduced compared to Figure 3.7 because of having higher signal to noise ratio. Yet, the higher the coefficient of correlation factor we have the more accurate estimation we get.

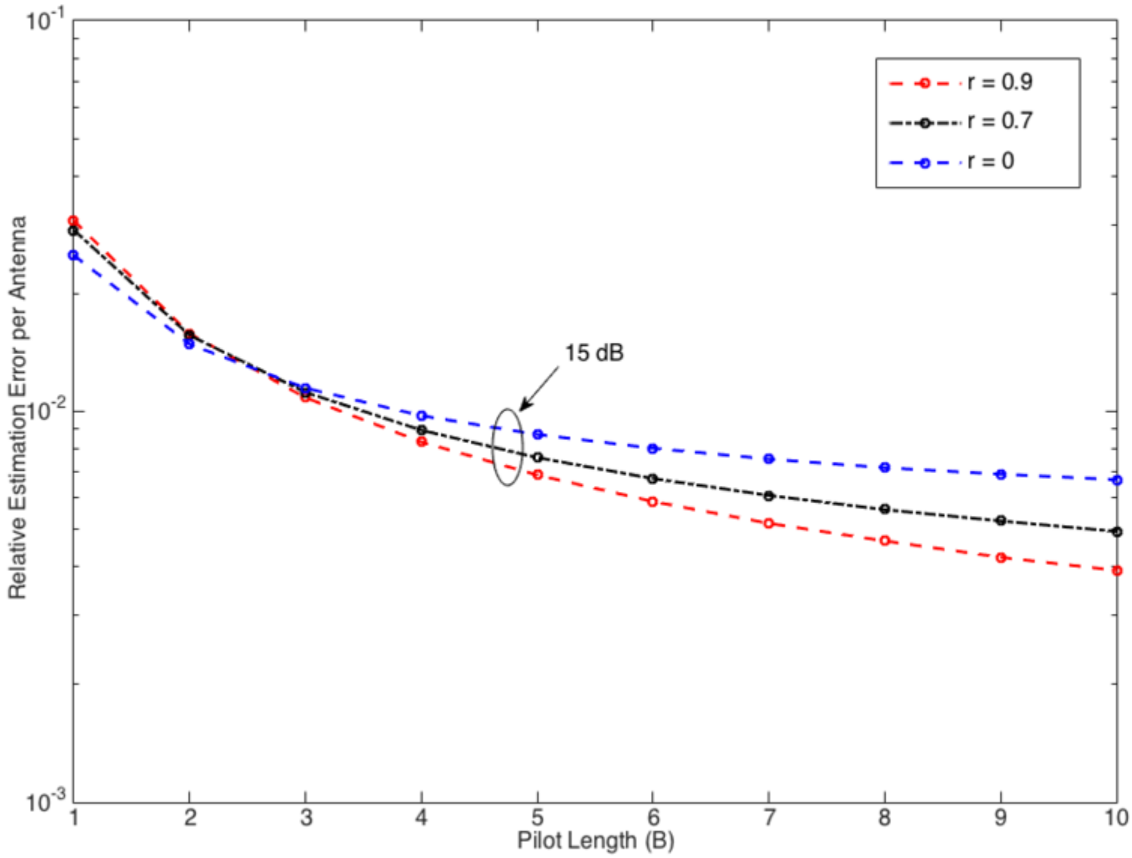

Figure 3.8: Relative estimation error as a function of exponential correlation factor for LMMSE. The signal to noise ratio is 15 dB [95].

A comparison between two different channel spatial correlation models is shown in Figure 3.9. One-ring model and exponential correlation model are compared for one cell system with 50 antennas in the base station. The plot shows relative estimation error as a function of pilot length. It is shown that the accuracy of the channel estimation is much better at higher pilot length. The one-ring model with angular spread of 20 degrees outperforms the exponential correlation model with coefficient value of 0.8 where the channel estimation is more accurate.

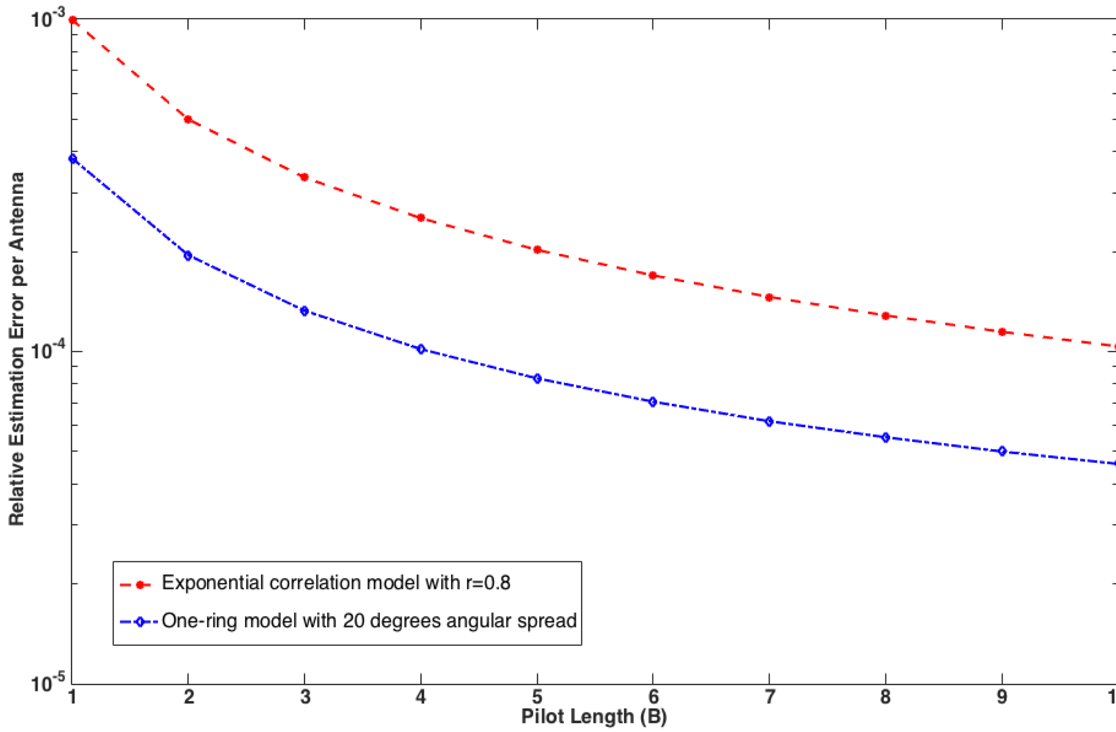

Figure 3.9 : Relative estimation error as a function of pilot length for N=50.

Chapter Four: Impact of channel spatial correlation on Spectral Efficiency

4.1 Spectral Efficiency for Single Antenna User

The first scenario is considering a one cell system model with one base station that and single user terminal. The impact of exponential correlation model on the spectral efficiency performance is investigated. Also, a comparison between one-ring model and exponential correlation model is stated by changing the number of base station antennas. The system model that is used in this chapter is the same model that is used in Chapter 3. It is assumed that the base station is equipped with *N* antennas and the number of antennas in user terminal is denoted by *M*. The Time Division duplexing protocol is used and the received signal at the base station is the represented as is $\mathbf{y} = \mathbf{h}d + \boldsymbol{n}$ where it is combination of the receiver noise $\boldsymbol{n}$ and block-fading channel $\mathbf{h}$. The channel covariance matrix $\mathbf{R}$ is generated using different spatial correlation models, exponential correlation model (3.6) and the one-ring model (3.9). The received downlink signal is flat fading channel and can be represented as $\mathbf{z} = \mathbf{h}^{\mathrm{T}}\mathbf{s} + \boldsymbol{v}$, where $\boldsymbol{v}$ represents the noise. The pilot based estimator LMMSE is used for uplink channel estimation and represented as $\hat{\mathbf{h}} = d^{*}\mathbf{R}\bar{\mathbf{Y}}^{-1}\boldsymbol{y}$.

4.1.1 Uplink and Downlink Data Transmission

In this chapter, the channel capacity using TDD protocol is studied. The lower capacity of the uplink and downlink data transmission are derived to see the impact of the channel spatial correlation models. The lower capacity bound is examined based on imperfect knowledge of stochastic block fading channel **h** where we used pilot based estimator. The imperfect knowledge of CSI in the base station and user equipment (UE) terminals are denoted as $\mathcal{H}^{\mathrm{BS}}$ and $\mathcal{H}^{\mathrm{UE}}$ respectively, while $\mathcal{H}$ is the channel actual state. The downlink capacity can be stated as

$$\mathrm{C}^{\mathrm{DL}} = \frac{T_{\mathrm{data}}^{\mathrm{DL}}}{\mathrm{T}_{cohr}} \mathbb{E}\left\{ \max_{f\left(\mathbf{s}\middle|\mathcal{H}^{\mathrm{BS}}\right):\mathbb{E}\{\|\mathbf{s}\|_2^2\} \leq p^{BS}} \mathcal{I}\left(\mathbf{s};\mathbf{z}\middle|\mathcal{H},\mathcal{H}^{\mathrm{BS}},\mathcal{H}^{\mathrm{UE}}\right) \right\} \tag{4.1}$$

where the mutual information for the received signal, $\mathbf{z}$, and the data signal, $\mathbf{s}$, for $\mathcal{H},\mathcal{H}^{\mathrm{BS}}$ and $\mathcal{H}^{\mathrm{UE}}$ is denoted as $\mathcal{I}\left(\mathbf{s};\mathbf{z}\middle|\mathcal{H},\mathcal{H}^{\mathrm{BS}},\mathcal{H}^{\mathrm{UE}}\right)$. On the other hand, the capacity for uplink data transmission can be expressed as follows

$$\mathrm{C}^{\mathrm{UL}} = \frac{T_{\mathrm{data}}^{\mathrm{UL}}}{\mathrm{T}_{cohr}} \mathbb{E}\left\{ \max_{f\left(d\middle|\mathcal{H}^{\mathrm{UE}}\right):\mathbb{E}\{\|d\|_2^2\} \leq p^{UE}} \mathcal{I}\left(d;\mathbf{y}\middle|\mathcal{H},\mathcal{H}^{\mathrm{BS}},\mathcal{H}^{\mathrm{UE}}\right) \right\} \tag{4.2}$$

The main part of this chapter is studying the behavior of the capacity bounds when the correlation factor goes from 0 to 1 which gives an idea of how the exponential correlation model would affect the capacity performance.

For the lower bound capacity, it is assumed that there is Gaussian noise in the interference and for the downlink it is assumed that a single stream is used. Furthermore, pilot based estimator is used and due to maximizing Gaussian distribution we have uncertain channel state information for downlink and uplink data transmission. Based on (4.1) and (4.2) and by applying (4.5) and (4.6), downlink and uplink capacities are denoted as

$$\mathrm{C}^{\mathrm{DL}} \geq \mathrm{C}_{lower}^{DL} = \frac{T_{\mathrm{data}}^{\mathrm{DL}}}{\mathrm{T}_{cohr}} \mathbb{E}\{\log_2(1 + \mathrm{SINR}_{lower}^{DL}(\mathbf{v}^{DL}))\} \tag{4.3}$$

$$\mathrm{C}^{\mathrm{UL}} \geq \mathrm{C}_{lower}^{UL} = \frac{T_{\mathrm{data}}^{\mathrm{UL}}}{\mathrm{T}_{cohr}} \mathbb{E}\{\log_2(1 + \mathrm{SINR}_{lower}^{UL}(\mathbf{v}^{UL}))\} \tag{4.4}$$

where the vectors $\mathbf{v}^{UL}$ and $\mathbf{v}^{DL}$ represent receive combining and beamforming respectively. Each vector has a unit norm and they are functions of $\hat{\mathbf{h}}$.

$$\mathrm{SINR}_{low}^{\mathrm{DL}}(\mathrm{v}^{\mathrm{DL}}) = \frac{\left|\mathbb{E}\{\mathrm{h}^{H}\mathrm{v}^{\mathrm{DL}}|\widetilde{\mathcal{H}}^{\mathrm{UE}}\}\right|^2}{\left\{\left|\mathrm{h}^{H}\mathrm{v}^{\mathrm{DL}}\right|^2|\widetilde{\mathcal{H}}^{\mathrm{UE}}\right\} - \left|\mathbb{E}\{\mathrm{h}^{H}\mathrm{v}^{\mathrm{DL}}|\widetilde{\mathcal{H}}^{\mathrm{UE}}\}\right|^2 + \frac{\mathbb{E}\left\{I_{\mathcal{H}}^{UE}|\widetilde{\mathcal{H}}^{\mathrm{UE}}\right\} + \sigma_{\mathrm{UE}}^2}{p^{BS}}} \tag{4.5}$$

$$\mathrm{SINR}_{low}^{\mathrm{UL}}(\mathrm{v}^{\mathrm{UL}}) = \frac{\left|\mathbb{E}\{\mathrm{h}^{H}\mathrm{v}^{\mathrm{UL}}|\widetilde{\mathcal{H}}^{\mathrm{BS}}\}\right|^2}{\left\{\left|\mathrm{h}^{H}\mathrm{v}^{\mathrm{UL}}\right|^2|\widetilde{\mathcal{H}}^{\mathrm{BS}}\right\} - \left|\mathbb{E}\{\mathrm{h}^{H}\mathrm{v}^{\mathrm{UL}}|\widetilde{\mathcal{H}}^{\mathrm{BS}}\}\right|^2 + \frac{\mathbb{E}\{(\mathrm{v}^{\mathrm{UL}})^{H}(\mathrm{Q}_{\mathcal{H}} + \sigma_{\mathrm{BS}}^2\mathrm{I})\mathrm{v}^{\mathrm{UL}}|\widetilde{\mathcal{H}}^{\mathrm{BS}}\}}{p^{UE}}} \tag{4.6}$$

4.1.2 Numerical Illustrations

Our numerical illustrations in this section are conducted to see the performance of the spectral efficiency based on different spatial correlation models . The average signal to noise ratio for downlink and uplink channel are $p^{\mathrm{BS}} \frac{\mathrm{tr}(\mathbf{R})}{N\sigma_{\mathrm{UE}}^2}$ and $p^{\mathrm{UE}} \frac{\mathrm{tr}(\mathbf{R})}{N\sigma_{\mathrm{BS}}^2}$, respectively. We take into consideration the value of SNR where we use high and low SNR values. We assume that the values of downlink and uplink data percentage are identecal and equal to 0.45. By making this assumption we get identical capacities for uplink and downlink.

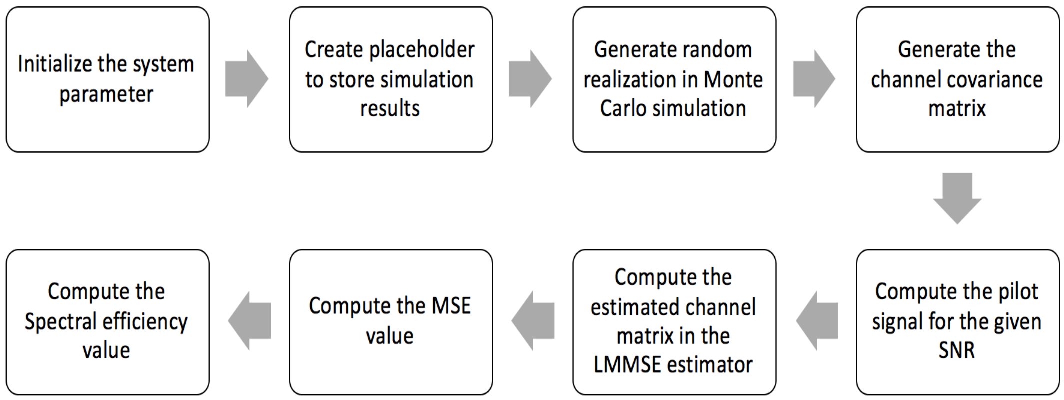

Figure 4.1: Block diagram for the simulation process.

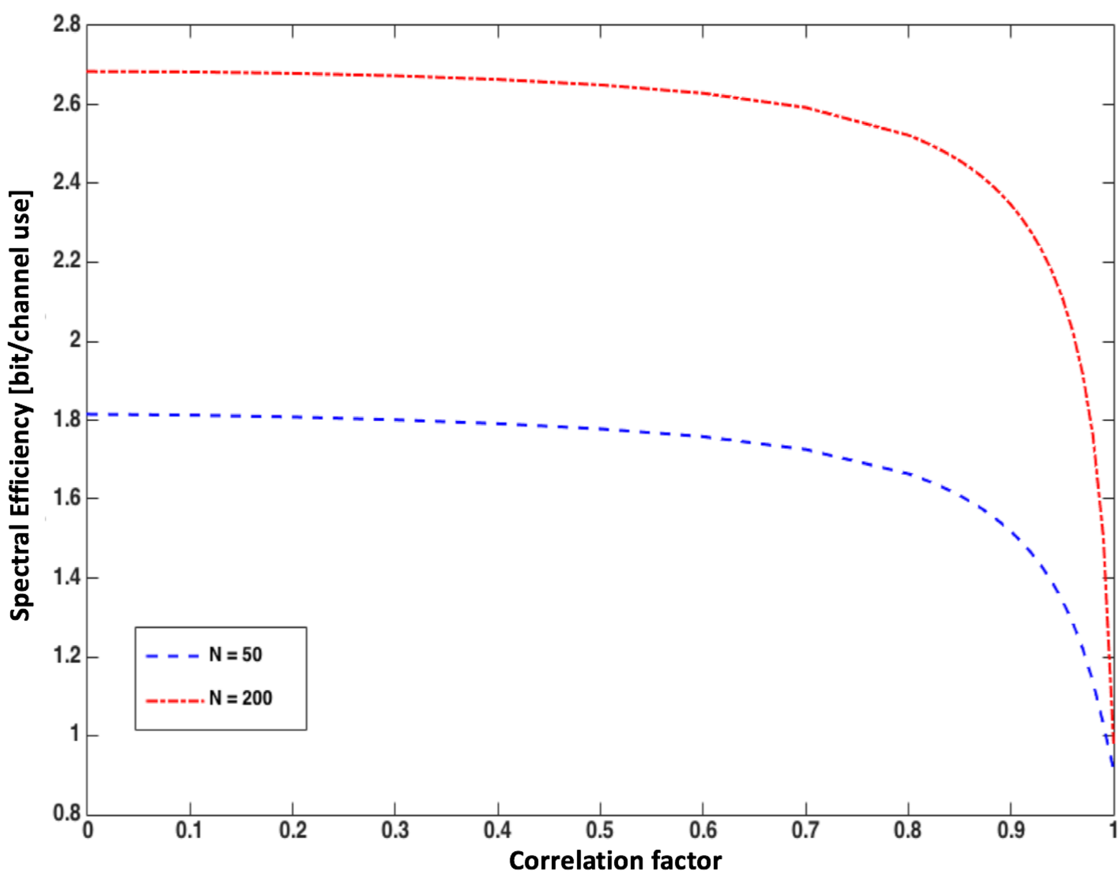

Figure 4.2: Spectral efficiency as a function of correlation factor with 0 dB SNR [9].

The spectral efficiency is shown in Figure 4.2 as a function of the exponential correlation factor. We considers a scenario with SNR equals to 0 dB and number of antennas N equals to 50 and 200 in the base station terminal. The maximum value of the spectral efficiency is achieved when there is zero correlation, which means having completely independent subchannels. The value of spectral efficiency is decreasing when the correlation factor is increasing until we get to correlation factor of 1 where we have the worst channel capacity. Also, it is shown that at larger number of base station antennas, there is higher channel capacity.

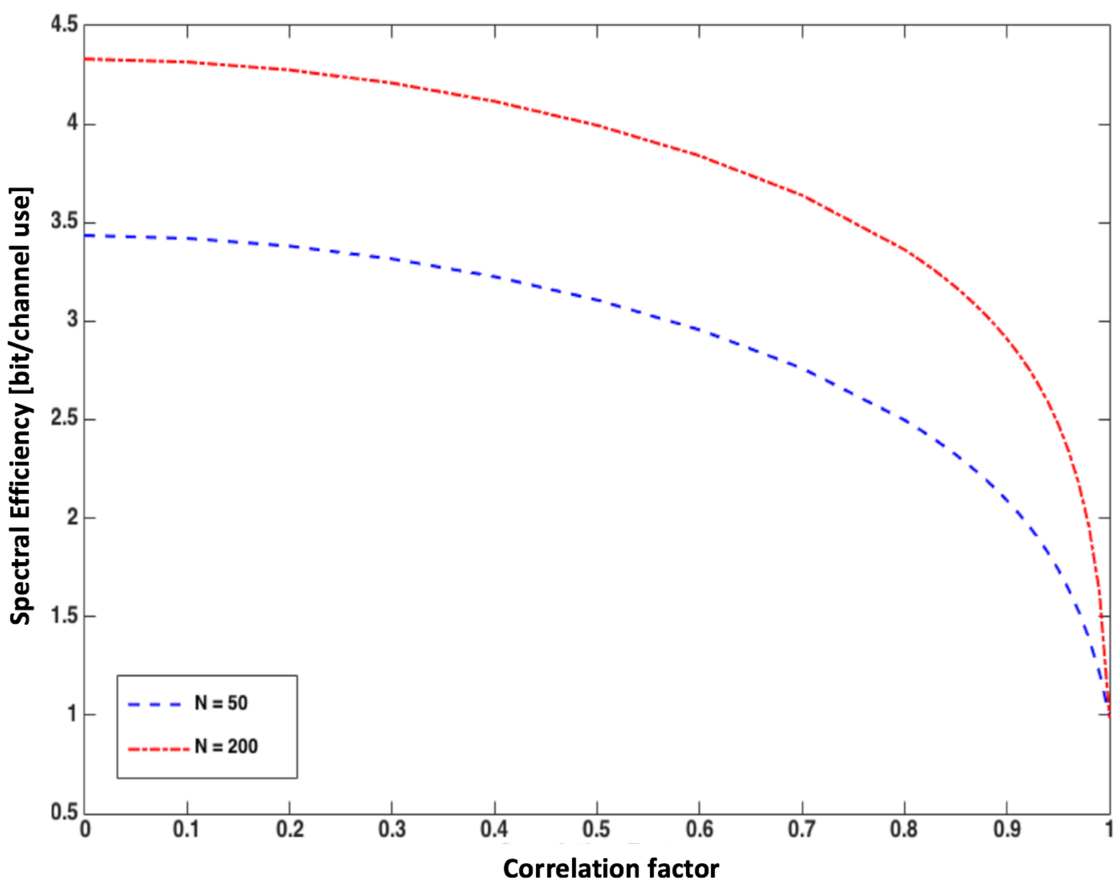

Figure 4.3: Spectral efficiency versus correlation factor with 30 dB SNR [9].

By increasing the value of SNR to 30 dB in Figure 4.3, the capacity is getting much higher compared to the capacity in Figure 4.2. Also, it is observed that the capacity behavior has better performance when we have larger number of antennas in the base station terminal. It is clear that the spectral efficiency is more sensitive to the change of exponential correlation factor where the spectral effeicincy declines much faster compared to the one with 0 dB SNR.

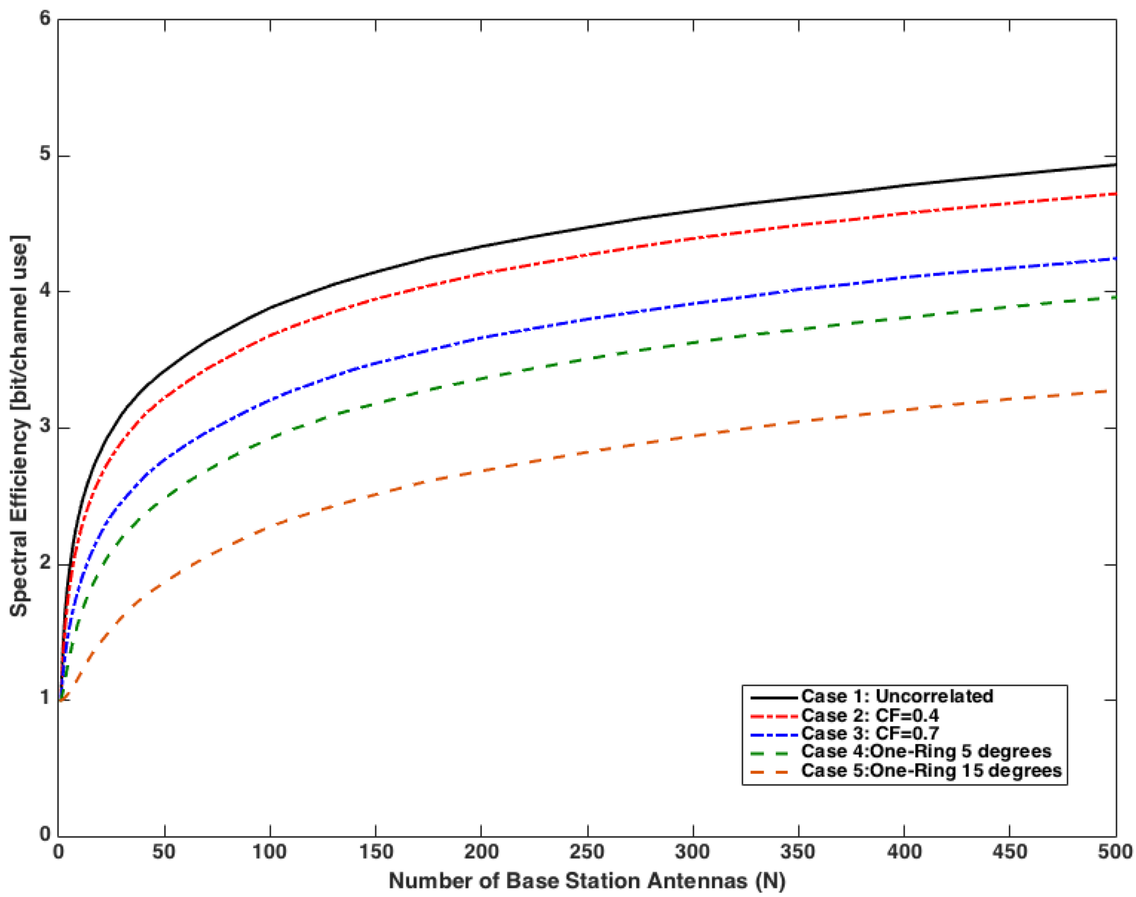

Figure 4.4: Spectral efficiency versus number of base station antennas using different spatial correlation models.

Figure 4.4 shows a comparison between different channel models. The figure includes 5 curves where each one represents a covariance model for the channel. Spectral efficiency is shown as a function of number of antennas at the base station. Figure 4.4 shows that the spectral efficiency is improving by increasing the number of antennas in the base station. The main observation is that the spectral efficiency is the lowest by using one-ring model with 15 degrees of angular spread while when there is no correlation the spectral efficiency is the highest.

4.2 Spectral Efficiency for Multi Antenna User

Similar to the previous scenario, the operation mode is TDD and a system of a single cell is considered. The system model is having a base station with *N* antennas that is serving *T* user terminals where each terminal is equipped with *M* antennas. It is assumed that the channel response from the user *t* to the base station is denoted by $\mathbf{K}_t \in \mathbb{C}^{N\times M}$. The spatial correlation is described using Kronecker model [96]:

$$\mathbf{K}_t = \mathbf{R}_{re,t}^{\frac{1}{2}} \, \mathbf{K}_{w,t} \, \mathbf{R}_{tr,t}^{\frac{1}{2}} \tag{4.7}$$

where the entries elements of $\mathbf{K}_{w,t} \in \mathbb{C}^{N\times M}$ are independent and identically distributed i.i.d. $\mathbf{R}_{re,t} \in \mathbb{C}^{N\times N}$ represents the base station spatial correlation to user *t* and $\mathbf{R}_{tr,t} \in \mathbb{C}^{N\times N}$ denotes the user *t* spatial correlation. $\mathbf{R}_{re,t}$ is including the parameters of the large scale fading and can be expressed as $\frac{1}{\mathrm{N}}\mathrm{tr}(\mathbf{R}_{re,t})$. Let the decomposition of the eigenvalues of spatial correlation $\mathbf{R}_{tr,t}$ is denoted as

$$\mathbf{R}_{tr,t} = \mathbf{U}_t\ \mathbf{\Lambda}_t\ \mathbf{U}_t^H \tag{4.8}$$

where the eigenvalues are contained in $\mathbf{\Lambda}_t = \mathrm{diag}\{\lambda_{t,1}, \dots, \lambda_{t,M}\}$ and unitary matrix is denoted as $\mathbf{U}_t \in \mathbb{C}^{M\times M}$.

For the uplink channel estimation, it is desired to have sequence of orthogonal pilot signals as $S = M\ T$ where the pilot matrix at the base station for the user *t* is denoted as $\mathbf{F}_t \in \mathbb{C}^{M\times S}$. If each user knows only its own statistical channel state information, then the energy of the pilot signal can be denoted as $\mathrm{tr}\ (\mathbf{B}_t\ \mathbf{B}_t^H) \leq S\ P_t$, where P_t represents the maximum transmit power for the user *t*. To minimize the channel estimation MSE, the following pilot matrix can be used $\mathbf{B}_t = \mathbf{U}_t\ \mathbf{G}_t^{\frac{1}{2}}\ \mathbf{V}_t^T$, where $\mathbf{G}_t$ is the diagonal distribution of the transmit power P_t among the channel dimensions of *M*. $\mathbf{V}_t \in \mathbb{C}^{S\times M}$ is satisfying $\mathbf{V}_t^H\mathbf{V}_t = S\mathbf{I}_M$ and if $t \neq k$ then $\mathbf{V}_t^H\mathbf{V}_k = 0$. The uplink received signal at the base station can be represented as

$$\mathbf{Y} = \sum_{t=1}^{T} \mathbf{K}_t\mathbf{B}_t + \mathbf{N} = \sum_{t=1}^{T} \mathbf{H}_t\mathbf{D}_t^{\frac{1}{2}}\ \mathbf{V}_t^T + \mathbf{N} \tag{4.9}$$

where $\mathbf{D}_t = \mathbf{\Lambda}_t\ \ \mathbf{G}_t$ and its *i*th diagonal element is denoted as $d_{t,i}$, while $\mathbf{H}_t = \mathbf{R}_{re,t}^{\frac{1}{2}}\ \mathbf{K}_{w,t}\ \ \mathbf{U}_t^H$. The independent noise of the receiver is denoted by **N** and it has zero mean and a covariance of $(\sigma^{\mathbf{2}}\ \mathbf{I}_{SN})$. It is assumed that the base station has a knowledge of $\mathbf{D}_t$ statistical information,so based on [97] the MMSE estimator for $\hat{\mathbf{h}}_t$ can be represented using Kronecker product ⊗ as

$$\hat{\mathbf{h}}_t = \left(\mathbf{D}_t^{\frac{1}{2}} \otimes \mathbf{R}_{re,t}\right)\left((\mathbf{D}_t \otimes \mathbf{R}_{re,t}) + \frac{\sigma^2}{S}\ \mathbf{I}_{NM}\right)^{-1} \mathbf{c}_t \tag{4.10}$$

where we define $\mathbf{c}_t = \text{vec}(\frac{1}{S}\mathbf{Y}_t\ \mathbf{V}_t^*)$. Assume $\hat{\mathbf{h}}_{t,i}$ is the ith column of the matrix $\widehat{\mathbf{H}}_t$, so the expected value of $\hat{\mathbf{h}}_{t,i}$ could be

$$\mathbb{E}\{\hat{\mathbf{h}}_{t,i}\ \hat{\mathbf{h}}_{t,j}^H\} = \begin{cases} d_{t,i}\ \mathbf{R}_{re,t}\left(\ d_{t,i}\ \mathbf{R}_{re,t} + \dfrac{\sigma^2}{S}\ \mathbf{I}_{NM}\right)^{-1} \mathbf{R}_{re,t}, & i = j \\ 0, & i \neq j \end{cases}$$

4.2.1 Uplink Data Transmission

For the uplink data transmission, the base station as a receiver knows the exact channel state information for each user. On the other hand, every user in the transmitting side has a knowledge of its own statistical channel state information only. Assume that the precoding matrix for user *t* is denoted by $\overline{\mathbf{B}}_t \in \mathbb{C}^{M\times M}$ and can be represented as

$$\overline{\mathbf{B}}_t = \mathbf{U}_t\ \mathbf{P}_t^{\frac{1}{2}} \tag{4.11}$$

where $\mathbf{P}_t$ represents the power matrix as $\mathbf{P}_t = \{P_{t,1}, \dots, P_{t,M}\}$ and $\mathbf{tr}(\mathbf{P}_t) \leq P_t$. On the base station side, the received signal can be represented as

$$\mathbf{y} = \textstyle\sum_{t=1}^{T} \mathbf{K}_t\overline{\mathbf{B}}_t\ x_t + \mathbf{n} \tag{4.12}$$

where the transmitted data is denoted by x_t with zero mean and $\mathbf{I}_M$ covariance while the additive noise of the receiver is denoted by $\mathbf{n}$ with zero mean and $(\sigma^2\ \mathbf{I}_N)$ covariance. The LMMSE estimator can be used to estimate the data stream individually based on [98], the estimated ith data stream for the user *t* can be expressed as

$$\mathbf{b}_{t,i} = \sqrt{\lambda_{t,1}\ P_{t,i}}\ \Sigma\ \hat{\mathbf{h}}_{t,i} \tag{4.13}$$

The uplink spectral efficiency for the user t can be represented by applying the value of the linear MMSE detector in (4.13) to the received signal in (4.12) as

$$\mathrm{C}_t^{\mathrm{UL}} = \sum_{i=1}^{M} \mathbb{E}\left\{\log_2\left(1 + \mathrm{SINR}_t^{\mathrm{UL}}\right)\right\} \tag{4.14}$$

The value of the SINR for the ith stream of the user t can be expressed as

$$\mathrm{SINR}_{t,i}^{\mathrm{UL}} = \frac{\lambda_{t,1}\, P_{t,i}\, \left|\mathbf{b}_{t,i}^{H}\, \hat{\mathbf{h}}_{t,i}\right|^2}{\mathbb{E}\{\mathbf{b}_{t,i}^{H}(\mathbf{y}\mathbf{y}^{\boldsymbol{H}} - \lambda_{t,1}\, P_{t,i}\ \hat{\mathbf{h}}_{t,i}\ \hat{\mathbf{h}}_{t,i}^{H})\mathbf{b}_{t,i}|\hat{\mathbf{H}}\}} \tag{4.15}$$

4.2.1 Downlink Data Transmission

For the downlink data transmission, it is assumed that there is no pilot signal or channel state information from the base station to the user terminal. The precoding matrix in the downlink for the user t is assumed to be $\mathbf{W}_t \in \mathbb{C}^{N\times M}$ and the total transmit power is allocated in $\Omega_t = \mathrm{diag}\{w_{t,1}, \dots, w_{t,M}\}$. For the user t, the downlink recived signal is

$$\mathbf{y}_{\boldsymbol{t}} = \mathbf{K}_t^H \sum_{l=1}^{T} \mathbf{W}_l\ \Omega_l^{\frac{1}{2}}\, \mathrm{x}_l + \mathbf{n}_{\boldsymbol{t}} \ \in \mathbb{C}^{M\times 1} \tag{4.16}$$

where the receiver noise is denoted by $\mathbf{n}_{\boldsymbol{t}}$ and it has zero mean and $(\sigma^{\mathbf{2}}\, \mathbf{I}_M)$ covariance while the downlink signal that is sent to the user l is denoted by x_l with zero mean and $\mathbf{I}_M$ covariance. Assume that the user t has a matrix of eigenvector for its own correlation as $\mathbf{U}_t^H$. Then the received signal after detector process is

$$\mathbf{z}_{\boldsymbol{t}} = \mathbf{U}_t^H \mathbf{y}_{\boldsymbol{t}} = \boldsymbol{\Lambda}_t^{\frac{1}{2}}\, \mathbf{U}_t^H \sum_{l=1}^{T} \mathbf{W}_l\ \Omega_l^{\frac{1}{2}}\, \mathrm{x}_l + \mathbf{U}_t^H \mathbf{n}_{\boldsymbol{t}} \tag{4.17}$$

The linear MMSE can be used to setect the received symbol where the ith column of the matrix $\overline{\mathbf{H}}_t$ is denoted by $\bar{\mathbf{h}}_t$. The downlink spectral efficiency for the user t can be represented by applying the value of the linear MMSE detector to the received signal as

$$C_t^{\mathrm{DL}} = \sum_{i=1}^{M} \mathbb{E}\left\{\log_2\left(1 + \mathrm{SINR}_t^{\mathrm{DL}}\right)\right\} \tag{4.18}$$

The value of the SINR for the *i*th stream of the user t can be expressed as

$$\mathrm{SINR}_{t,i}^{\mathrm{UL}} = \frac{\left|\mathbf{r}_{t,i}^{H}\, \bar{\mathbf{h}}_{t,i}\right|^2}{\mathbf{r}_{t,i}^{r}\mathbb{E}\{\mathbf{z}_t\mathbf{z}_t^{H}\}\, \mathbf{r}_{t,i} - \left|\mathbf{r}_{t,i}^{H}\, \bar{\mathbf{h}}_{t,i}\right|^2} \tag{4.19}$$

4.2.1 Numerical Illustrations

The results in this section are carried out to see the effect the exponential correlation factor on the spectral efficiency based on different number of base station antennas and SNR values. The scalability of Massive MIMO systems by encreasing the number of user terminals is investigated.

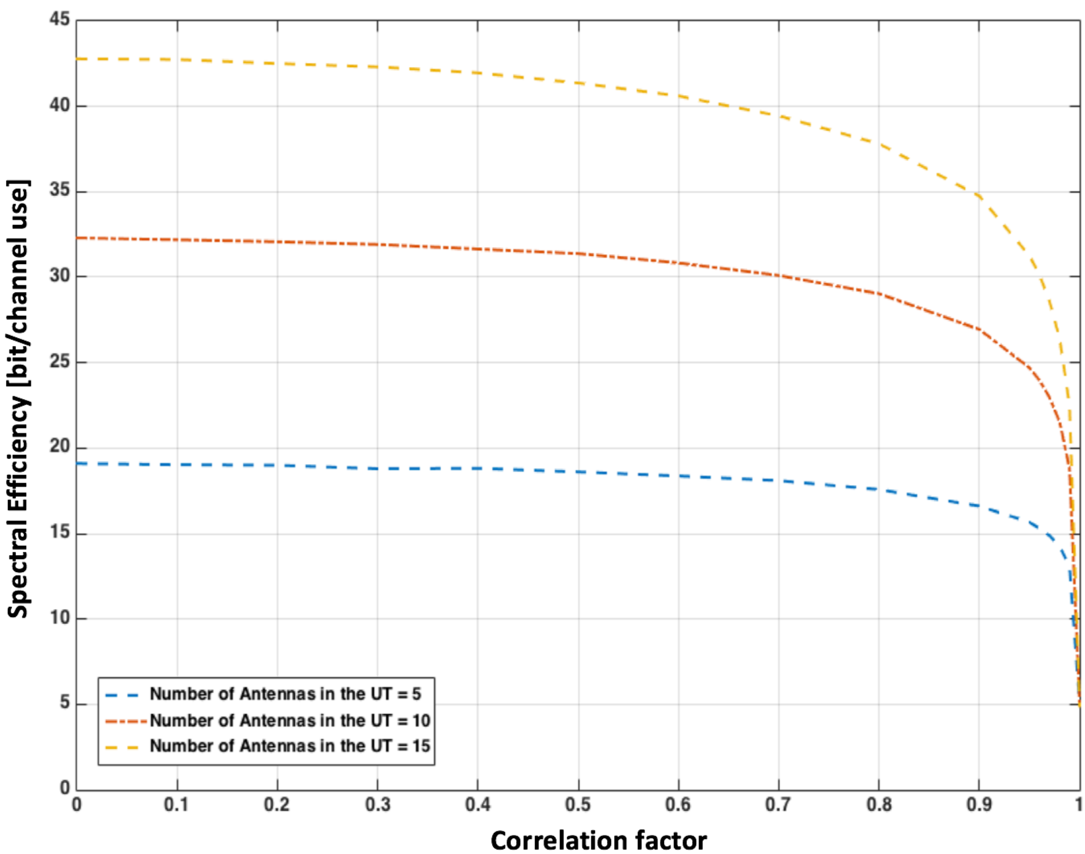

Figure 4.5: Spectral efficiency versus exponential correlation factor with signal to noise ratio equals to 30 dB and *N* equals to 50 antennas.

A different scenario is considered in Figure 4.5 with SNR equals to 30 dB and number of antennas N equals to 50. In this figure the number of antennas in the user terminal M is changed several times to investigate the effect of increasing the number of antennas in the user terminal. Figure 4.5 shows that the maximum value of the spectral efficiency is reached when we have uncorrelated antennas when the correlation factor equals to 0. By increase the correlation factor, the bounds of spectral efficiency keep decreasing until we get to correlation factor of 1. Also we can realize that at larger number of UT antennas, we have higher channel spectral efficiency.

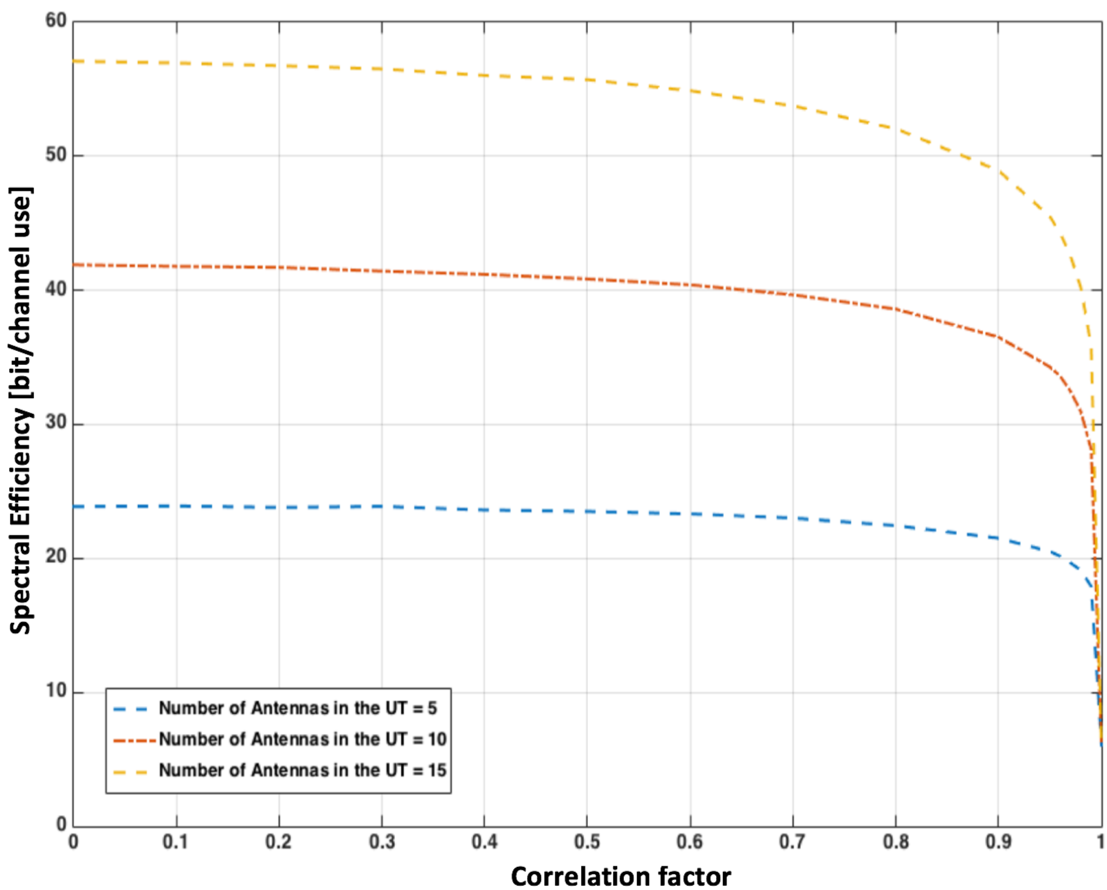

Figure 4.6: Spectral efficiency versus exponential correlation factor with signal to noise ratio equals to 30 dB and N equals to 200 antennas.

Figure 4.6 shows similar scenario to Figure 4.5 with signal to noise ratio equals to 30 dB and number of antennas N equals to 200 at the base station terminal. In this figure the number of antennas in the user terminal is changed several times to investigate the effect of increasing the number of antennas M. Figure 4.6 displays that the higher value of the spectral efficiency is achieved when we have zero correlation, which means having completely independent subchannels. Also, we can realize that at larger number of antennas in the user terminal we have higher spectral efficiency.

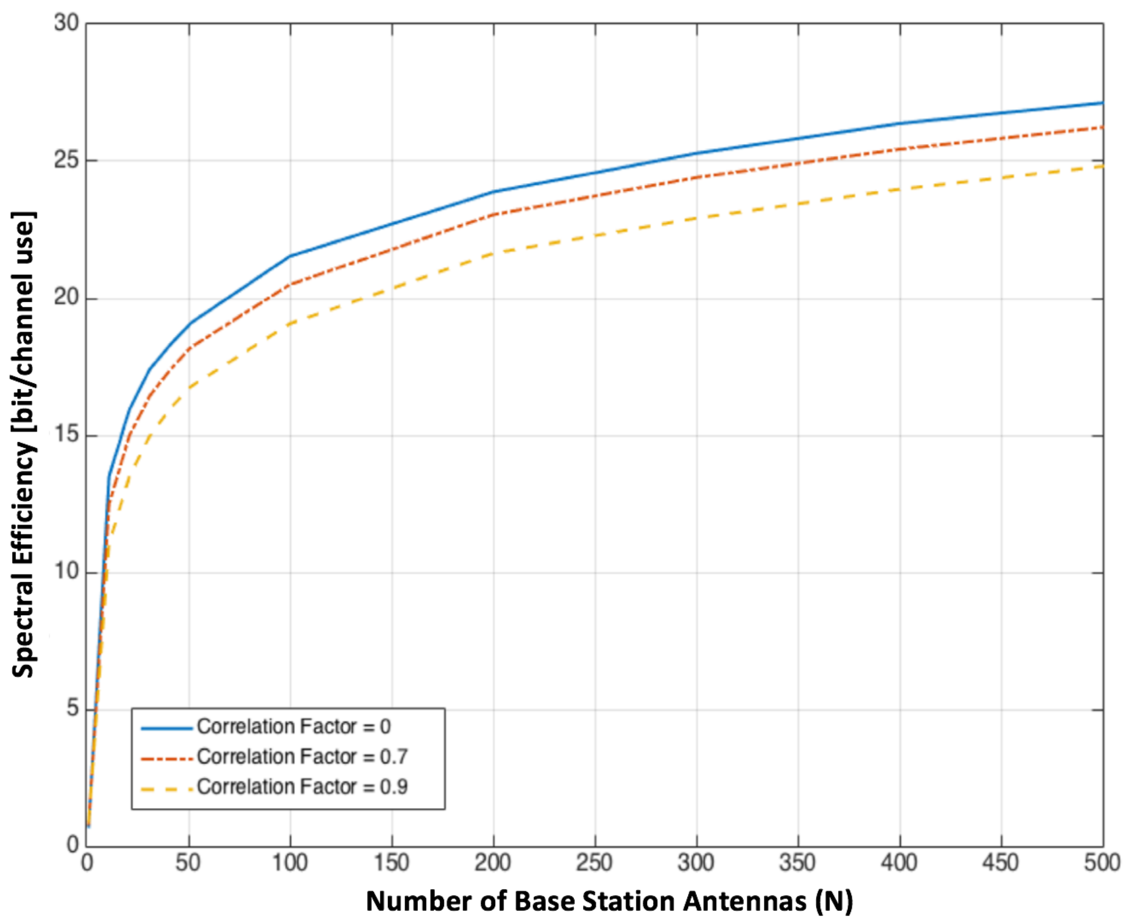

Figure 4.7 : Spectral efficiency as a function of the number of BS antennas for 1 user with 5 antennas.

A comparison between different values of correlation factors using exponential correlation model is shown in Figure 4.7. Spectrla efficiency is plotted versus number of antennas at the base station. Figure 4.7 shows that the spectral efficiency is improving by increasing the number of antennas in the base station. the main obsevation from this figure is that the spectral efficiency is higher when the correlation factor is lower. The highest spectral efficiency is occuring when the antennas are uncorrelated which is represented by the blue curve.

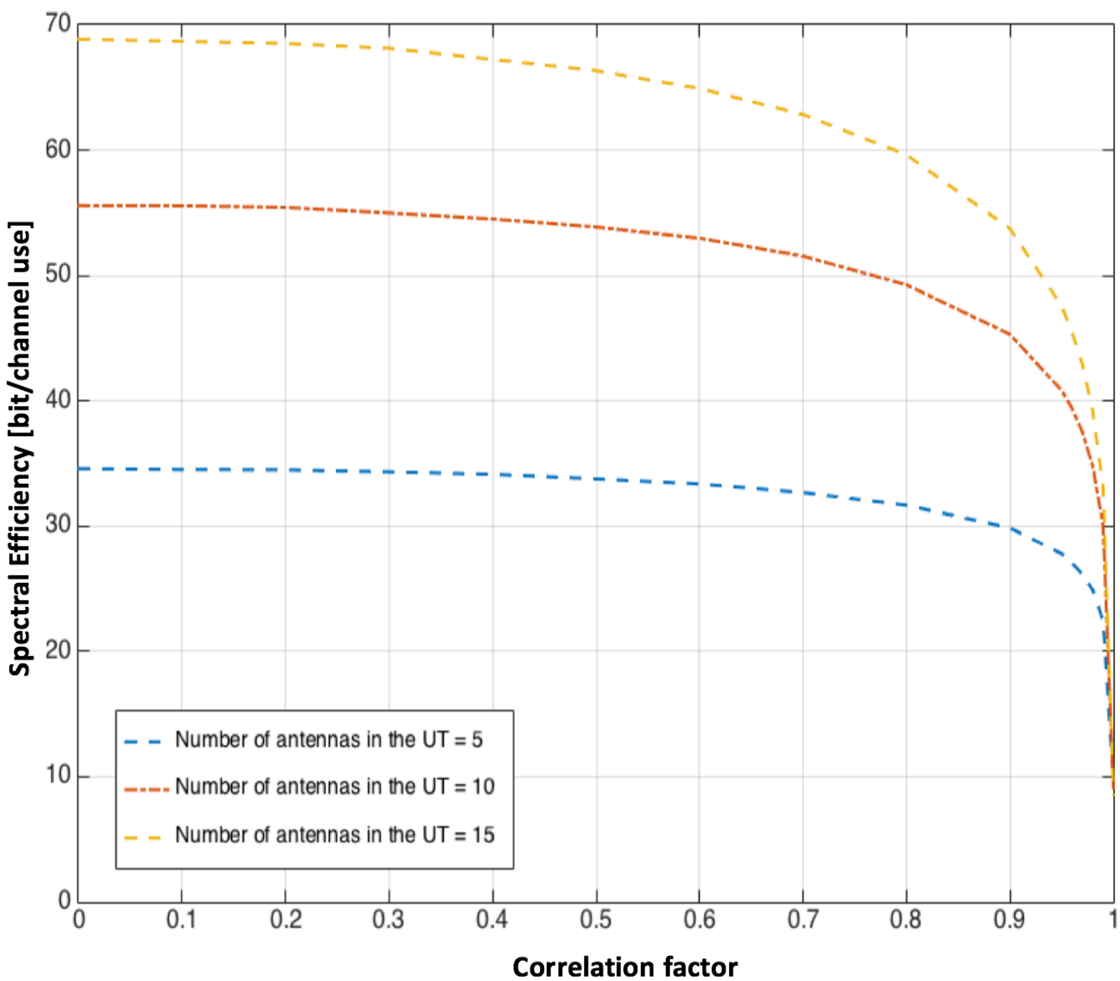

Figure 4.8: Spectral efficiency versus exponential correlation factor with signal to noise ratio equals to 30 dB and N equals to 50 antennas with 2 users [99].

Figure 4.8 considers a scenario with signal to noise ratio equals to 30 dB and number of antennas N equals to 50 at the base station terminal where we have two user terminals. In this figure the number of antennas in the user terminal M is changed three times to investigate the effect of increasing the number of antennas in the user terminal. Figure 4.7 displays that the highest value of the spectral efficiency is occurring when we have uncorrelated subchannels at 0 correlation factor. By increase the value of correlation factor, the bounds of spectral efficiency keep going down until we get to correlation factor of 1. Compared to Figure 4.4, the spectral efficiency in Figure 4.7 is almost doubled after increasing the number of user terminal from 1 to 2.

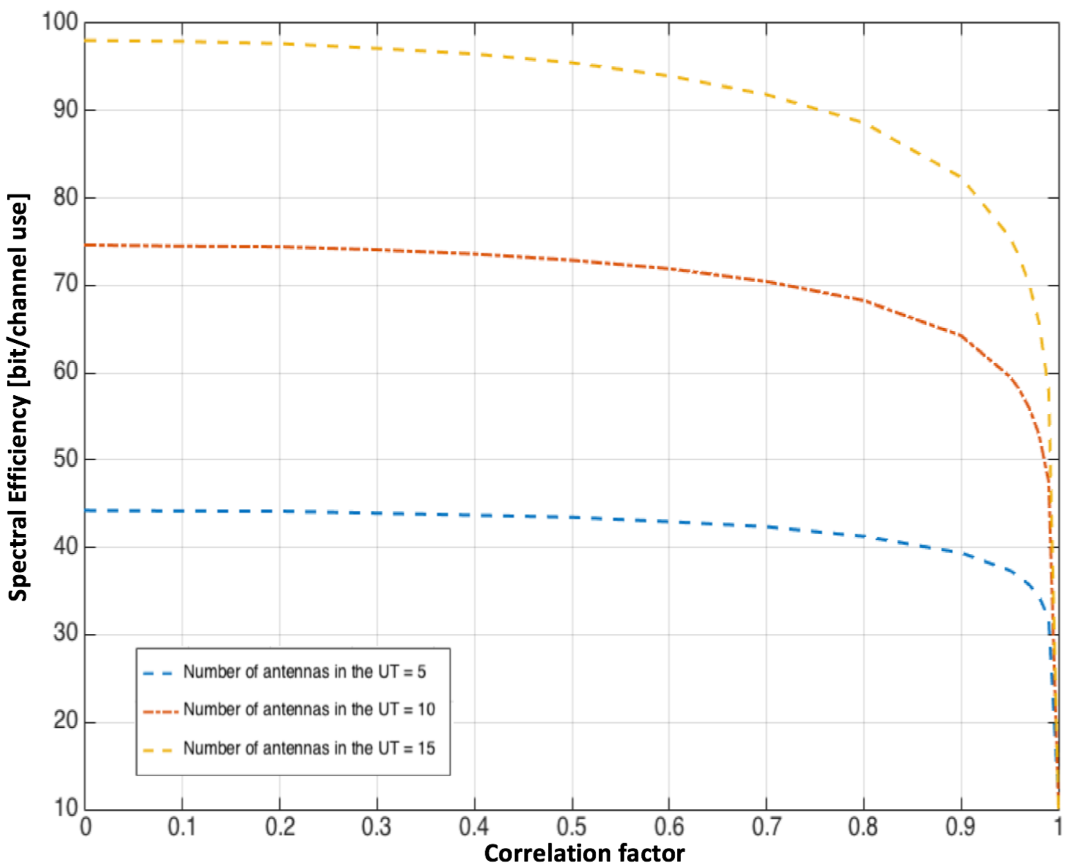

Figure 4.9: Spectral efficiency versus exponential correlation factor with signal to noise ratio equals to 30 dB and N equals to 200 antennas with 2 users [99].

Figure 4.9 demonstrates similar situation to Figure 4.8 with signal to noise ratio equals to 30 dB but with number of antennas N equals to 200 at the base station where there are 2 user terminals. In this figure the number of antennas in the user terminal is increased several times to investigate the effect of having different number of antennas at the user terminal. Figure 4.8 shows that the higher value of the spectral efficiency is reached when there is 0 correlation, which means having completely independent subchannels. Also, we can realize that at larger number of antennas in the user terminal we have higher spectral efficiency. By comparing this figure with Figure 4.5, we can see that the spectral efficiency almost doubled due to having 2 user terminals instead of 1.

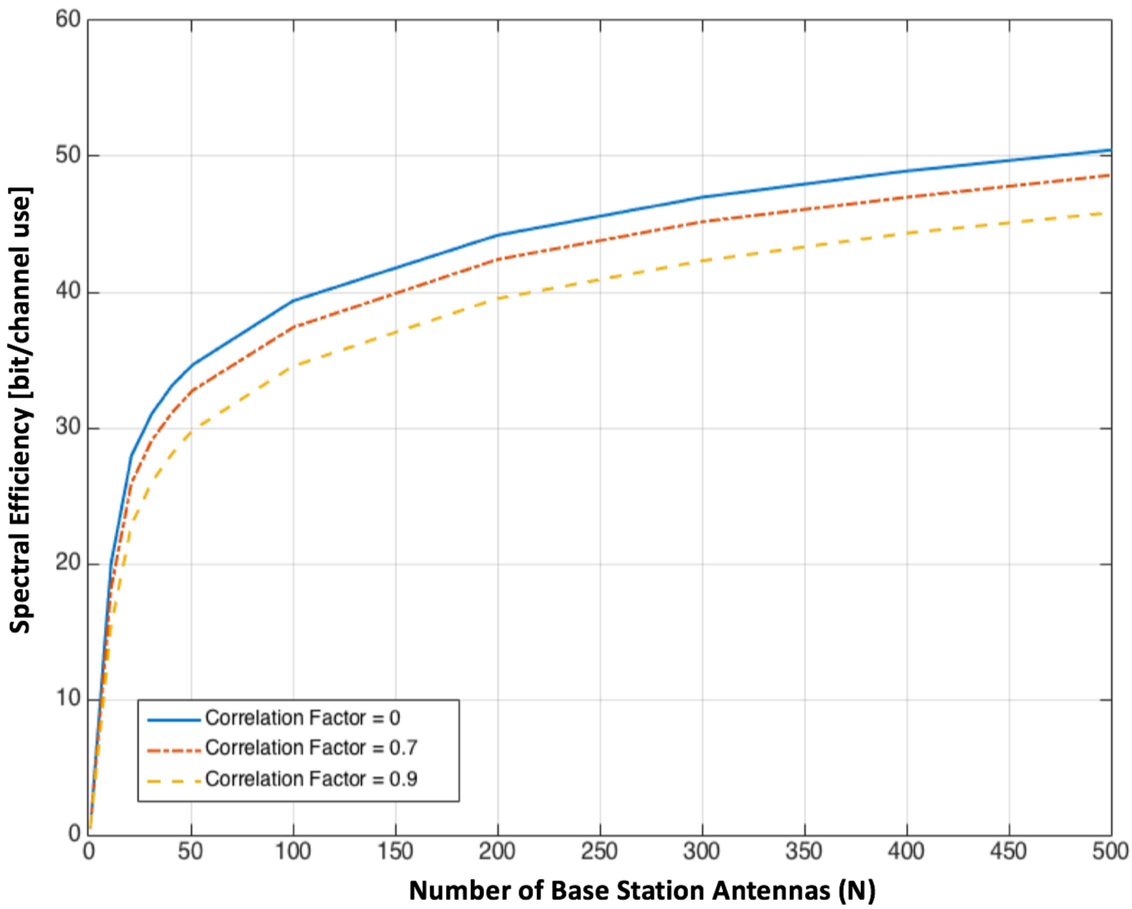

Figure 4.10: Spectral efficiency as a function of the number of BS antennas for 2 users.

There are three curves are plotted in Figure 4.10 where each one represents a values of correlation factors using exponential correlation model. Spectral efficiency is shown as a function of the number of base station antennas. Figure 4.10 shows that the spectral efficiency is increasing by having larger number of antennas in the base station. It is observed that the spectral efficiency is larger when the correlation factor is lower. Moreover, the highest spectral efficiency is achieved when the antennas are uncorrelated at correlation factor equals to zero.

Chapter Five: Energy Efficiency and Transmit Power

Massive MIMO systems can be used to improve the energy efficiency by reducing the emitted power. Energy efficiency can be expressed as the ratio between spectral efficiency and emitted power and it is measured in (bit/Joule). The transmit power, in (Joule/channel use), is represented as the energy consumed by the amplifier divided by the coherence time [100]. In this chapter, the influence of the channel spatial correlation on the energy efficiency and transmit power is investigated where the exponential correlation model is applied to the Massive MIMO system model.

5.1 System Model and Assumptions

It is assumed that there is a single cell with one base station that is equipped with N antennas and a user terminal. The operation mode that is used is TDD and the received signal at the base station is a combination of the block-fading channel $\mathbf{h}$ and the receive noise $\mathbf{n}$ and can be represented as $\mathbf{y} = \mathbf{h}d + \boldsymbol{n}$. The exponential correlation model is used to generate the channel covariance matrix $\mathbf{R}$. The received downlink signal is flat fading channel and can be represented as $\mathbf{z} = \mathbf{h}^{\mathrm{T}}\mathbf{s} + \boldsymbol{v}$, where $\boldsymbol{v}$ represents the noise. The uplink channel estimation is LMMSE and denoted as $\hat{\mathbf{h}} = d^{*}\mathbf{R}\overline{\mathbf{Y}}^{-1}\boldsymbol{y}$.

5.1.1 Energy Efficiency and Transmit Power

The transmit power can be generated by finding the consumed energy of the amplifier divide it by the coherence time T_{cohr} [100]. The following equations (5.1) and (5.2) represent uplink and downlink transmit power respectively

$$\left(\frac{\mathrm{E}_{amp}}{\mathrm{T}_{cohr}}\right)_{UL} = \alpha_{UL}\left(\frac{T_{\text{pilot}}^{\text{DL}}}{\mathrm{T}_{cohr}}\ \frac{p^{BS}}{\omega^{BS}} + \frac{T_{\text{pilot}}^{\text{UL}}}{\mathrm{T}_{cohr}}\ \frac{p^{UE}}{\omega^{UE}}\right) + \frac{T_{\text{pilot}}^{\text{UL}}}{\mathrm{T}_{cohr}}\ \frac{p^{UE}}{\omega^{UE}} \tag{5.1}$$

$$\left(\frac{\mathrm{E}_{amp}}{\mathrm{T}_{cohr}}\right)_{DL} = \alpha_{DL}\left(\frac{T_{\text{pilot}}^{\text{DL}}}{\mathrm{T}_{cohr}}\ \frac{p^{BS}}{\omega^{BS}} + \frac{T_{\text{pilot}}^{\text{UL}}}{\mathrm{T}_{cohr}}\ \frac{p^{UE}}{\omega^{UE}}\right) + \frac{T_{\text{pilot}}^{\text{DL}}}{\mathrm{T}_{cohr}}\ \frac{p^{BS}}{\omega^{BS}} \tag{5.2}$$

where ω^{BS} and ω^{UE} are the power efficiency of the amplifiers at the two terminals where they are bounded from 0 to 1. The uplink and downlink ratios that are used in the previous equations can be interpreted as follows

$$\alpha_{UL} = \frac{T_{\text{data}}^{\text{UL}}}{T_{\text{data}}^{\text{DL}} + T_{\text{data}}^{\text{UL}}} \tag{5.3}$$

$$\alpha_{DL} = \frac{T_{\text{data}}^{\text{DL}}}{T_{\text{data}}^{\text{DL}} + T_{\text{data}}^{\text{UL}}} \tag{5.4}$$

Energy efficiency of the Massive MIMO system is measured in (bit/Joule) and can be represented as the ratio between capacity limits that are derived in (4.3) for downlink capacity and (4.4) for uplink and consumed power that are shown in (5.1) and (5.2) as the following equations show

$$EE^{UL} = \frac{\mathrm{C}^{UL}}{\left(\frac{T_{\mathrm{pilot}}^{\mathrm{DL}}}{\mathrm{T}_{cohr}}\frac{p^{BS}}{\omega^{BS}}+\frac{T_{\mathrm{pilot}}^{\mathrm{UL}}}{\mathrm{T}_{cohr}}\frac{p^{UE}}{\omega^{UE}}+N\rho+\zeta\right)+\frac{T_{\mathrm{pilot}}^{\mathrm{UL}}}{\mathrm{T}_{cohr}}\frac{p^{UE}}{\omega^{UE}}} \tag{5.5}$$

$$EE^{DL} = \frac{\mathrm{C}^{DL}}{\left(\frac{T_{\mathrm{pilot}}^{\mathrm{DL}}}{\mathrm{T}_{cohr}}\frac{p^{BS}}{\omega^{BS}}+\frac{T_{\mathrm{pilot}}^{\mathrm{UL}}}{\mathrm{T}_{cohr}}\frac{p^{UE}}{\omega^{UE}}+N\rho+\zeta\right)+\frac{T_{\mathrm{pilot}}^{\mathrm{DL}}}{\mathrm{T}_{cohr}}\frac{p^{BS}}{\omega^{BS}}} \tag{5.6}$$

The previous equations represent the uplink and downlink energy efficiency respectively where ρ is the circuit power and ζ is the static circuit power.

5.2 Numerical Illustrations

Our numerical illustrations show how the exponential correlation factor would affect the energy efficiency behavior [9]. We choose to have 0 splitting between ρ and ζ, also we set the value of ρ+ζ equals to 0.02×10^{-6} (Joule/channel use). In the simulation part, to have identical uplink and downlink energy efficiency we let $\alpha_{UL} = \alpha_{DL} = 0.5$.

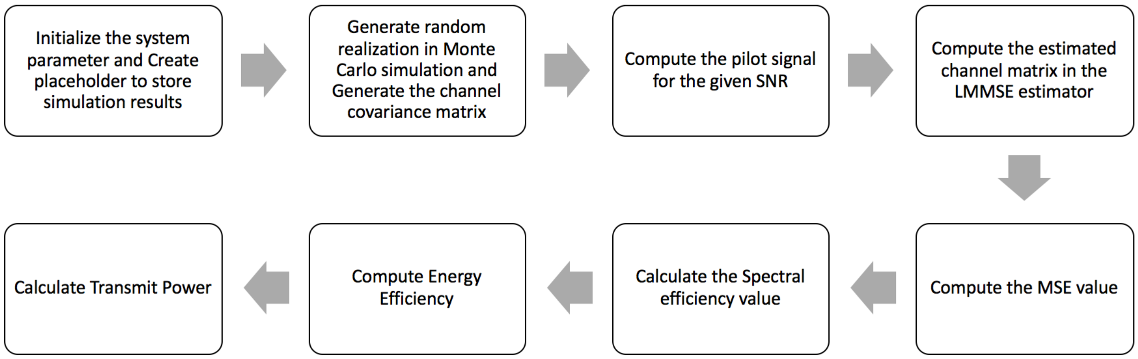

Figure 5.1: Block diagram for the simulation process.

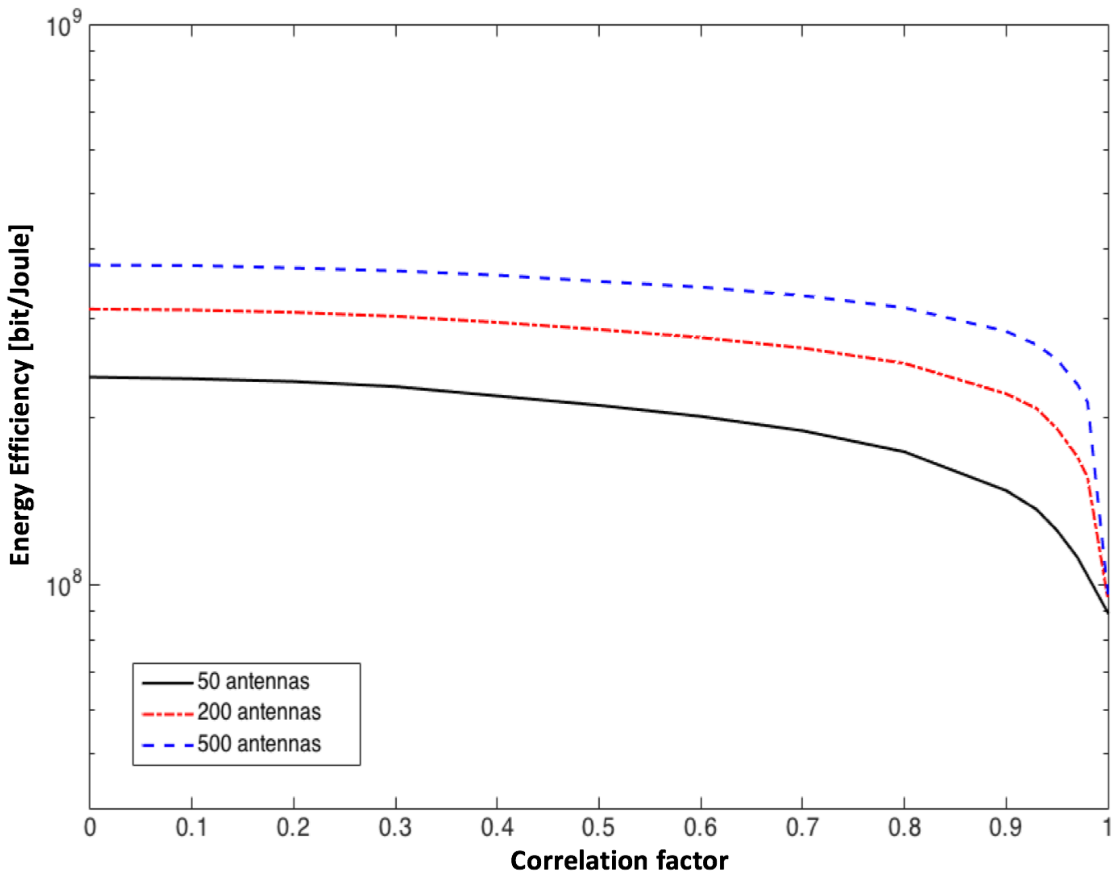

Figure 5.2: Energy efficiency as a function of exponential correlation factor with signal to noise ratio equals to 20 dB [9].

Figure 5.2 shows the energy efficiency of the Massive MIMO (in bit/Joule) with signal to noise ratio equals to 20 dB. We can see number of curves where each curve indicates different number of base station antenna where the scenario of having 500 antennas gives us the highest energy efficiency while we have the lowest energy efficiency by having 50 antennas. Also, it is shown that the highest energy efficiency is occurring when the correlation factor is 0 and it decreases gradually until we get the lowest energy efficiency at 1 correlation factor.

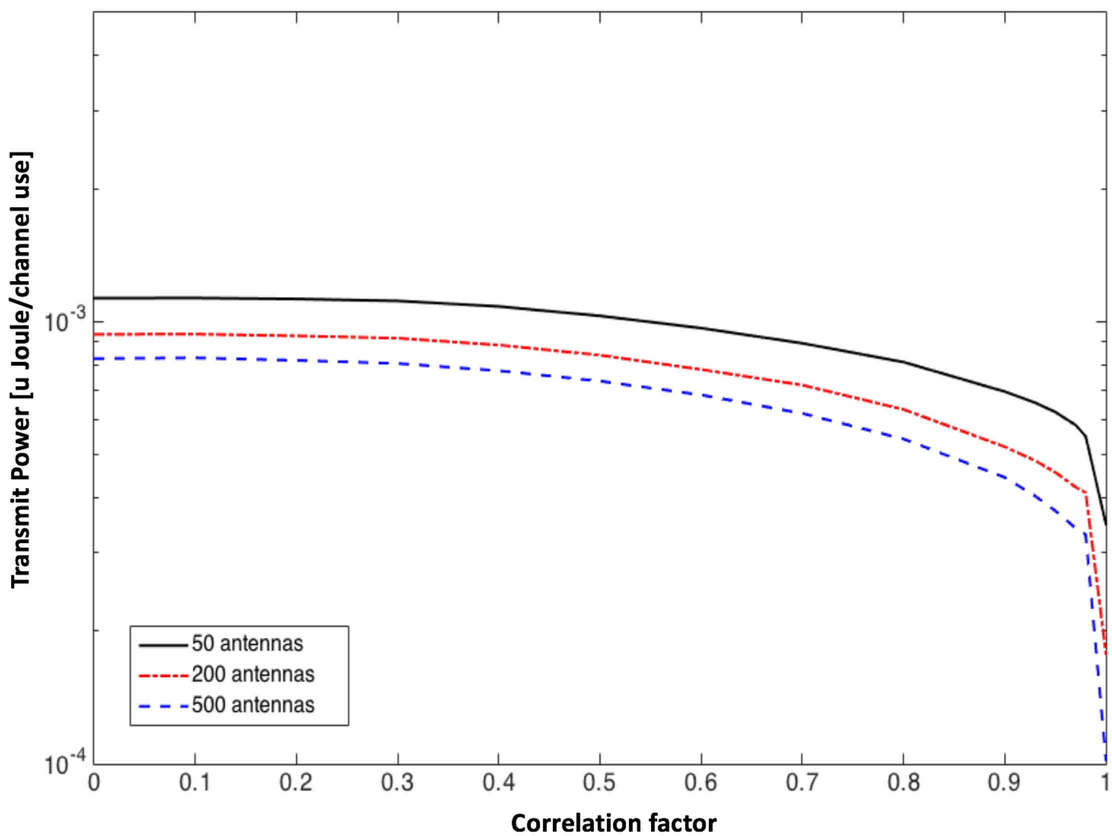

Figure 5.3: Transmit power as a function of exponential correlation factor with signal to noise ratio equals to 20 dB [9].

Figure 5.3 demonstrates the Massive MIMO transmit power (in *u* Joule/channel use) with SNR equals to 20 dB. We can see three curves each curve represents different number of base station antennas. We can see that the highest transmit power is occurring when the number of base station antennas is 50 while the lowest transmit power is happening when we have 500 antennas in the base station. Also, it is noticeable that the highest transmit power occurred when the correlation factor is 0 and it decreases regularly until we get the lowest transmit power at correlation factor of 1.

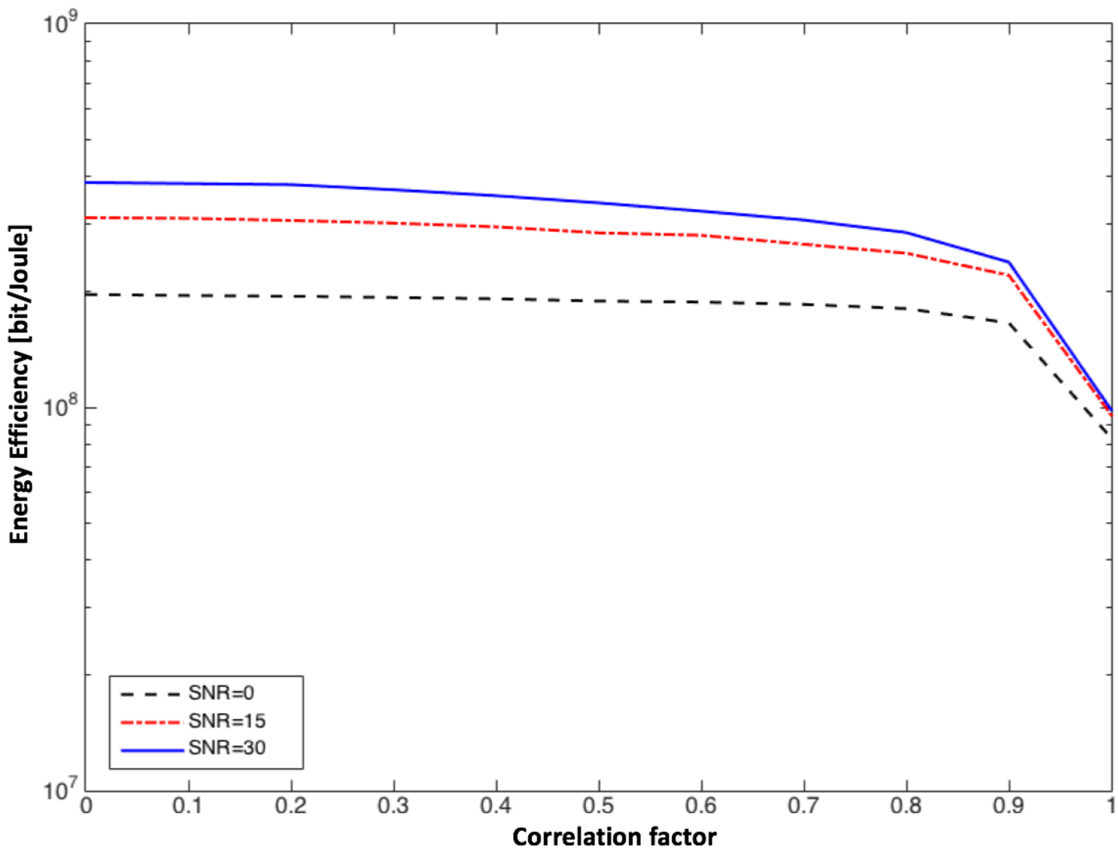

Figure 5.4: Energy efficiency versus correlation factor with different SNR values.

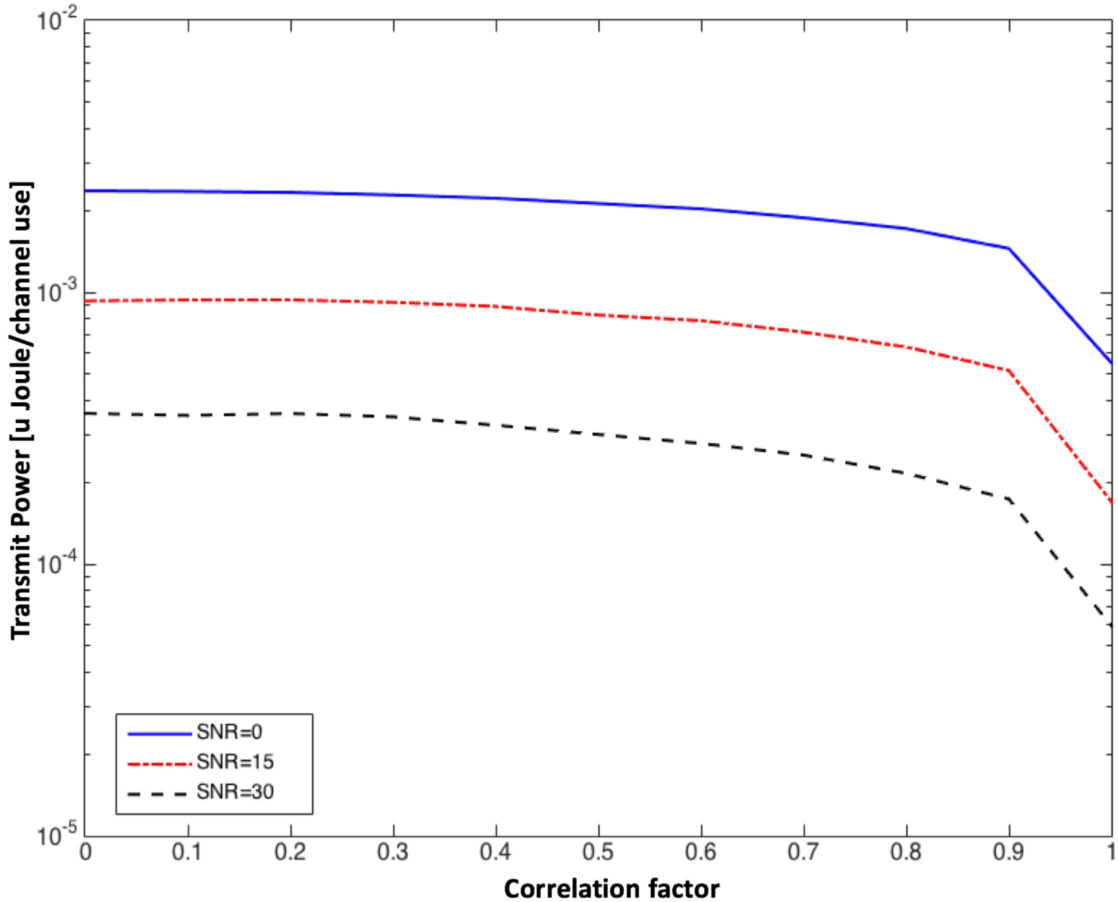

Figure 5.5: transmit power versus correlation factor with different values of SNR.

Figure 5.4 shows energy efficiency as a function of correlation factor with 50 antennas at the base station. We can see three curves each one indicates different SNR value where the highest energy efficiency is occurring when SNR equals to 30 dB while we have the lowest energy efficiency by having 0 dB. Also, it is shown that the highest energy efficiency occurred when the correlation factor is 0 and it decreases slowly until we get the lowest energy efficiency at fully correlated antennas with correlation factor equals to 1. Figure 5.5 shows transmit with 50 antennas at the base station. Also, there are three curves each one represents different number of SNR values. We can realize that the highest transmit power is occurring when the value of SNR is 30 dB while the lowest transmit power is occurring when we 0 dB. Also, it is clear that the highest transmit power occurred when the correlation factor is 0 and it decreases regularly until we get the lowest transmit power at 1 correlation factor.

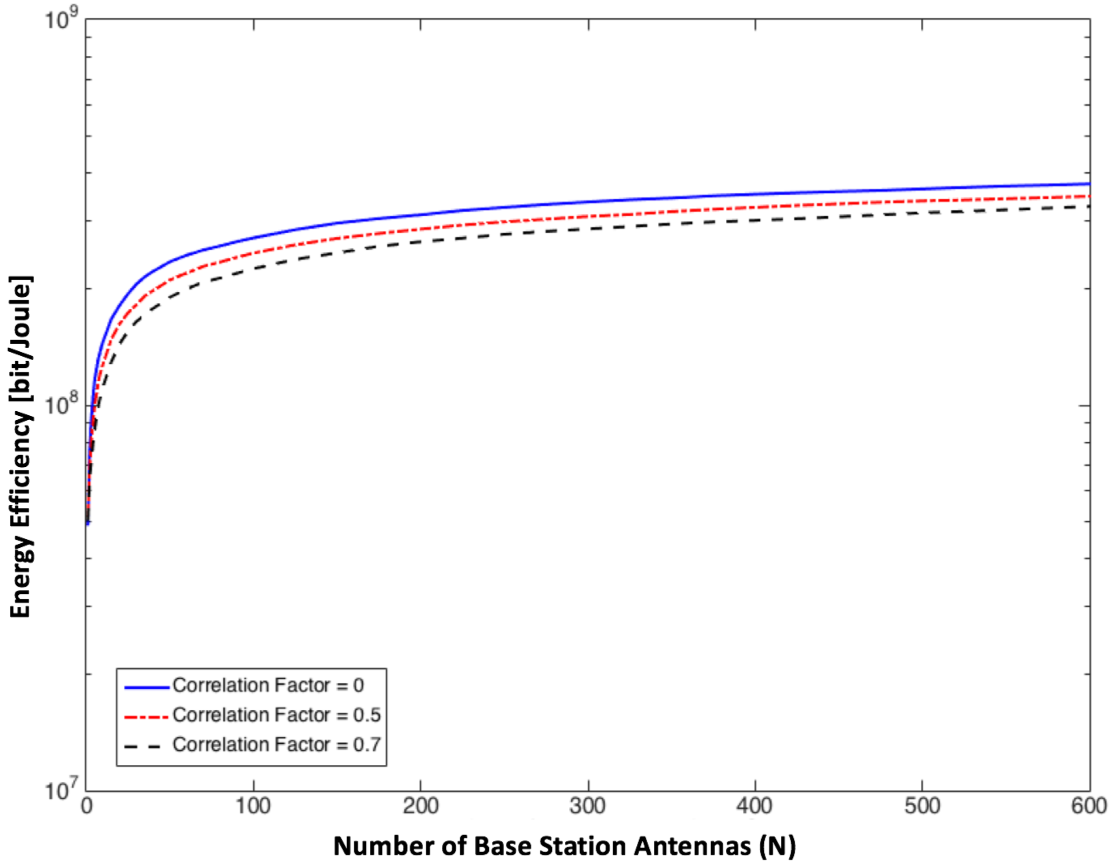

Figure 5.6: Energy Efficiency as a function of the number of antennas at the base station [99].

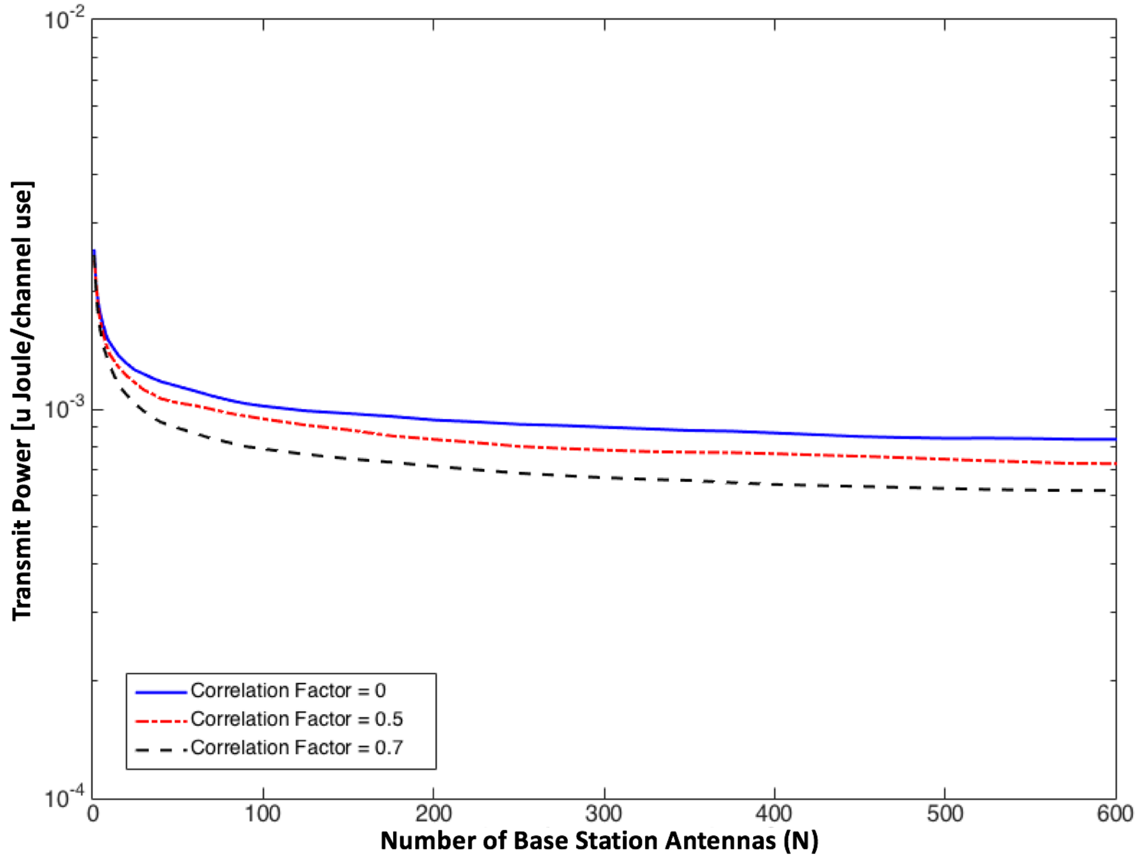

Figure 5.7 : Transmit Power as a function of the number of antennas at the base station [99].

Energy efficiency is shown as a function of the number base station antennas. Figure 5.6 shows a comparison between different correlation factors of exponential correlation model. It is shown that the energy efficiency is improving by increasing the number of antennas in the base station. the main observation from this figure is that the energy efficiency is getting higher when the correlation factor value is getting lower. Transmit power is shown in Figure 5.7 as a function of number of antennas at the base station. Figure 5.7 shows three curves where each one represents different correlation factors for exponential correlation model. It is shown that the transmit power is decreasing by increasing the number of antennas in the base station. It is observed that the energy efficiency has different behavior compared with the transmit power where by increasing the number of antennas in the base station, the energy is increasing while the transmit power in decreasing.

Chapter Six: Conclusion and Future Work

6.1 Conclusion

in the previous two decades, the demand for wireless data traffic has been increasing rapidly while the available electromagnetic spectrum range is limited. Wireless networks are connecting billions of smartphones, tablets and wireless devices where these devices are demanding higher throughput and much lower latency to their applications. Moreover, the wireless systems will keep consuming more energy. Thus, the Fifth generation (5G) wireless networks have several requirements such as providing higher data rate, serving larger number of users simultaneously and being more energy efficient. One of the promising technology that can meet the above requirements is Massive Multiple Input Multiple Output (MIMO). The proposed concept of massive MIMO is to equip the base station with hundreds of antennas which is larger than the number of users and to serve them using the same time-frequency resources.

In the first part of this dissertation, the exponential correlation model is used and implemented to the Massive MIMO system model. linear minimum mean square error (LMMSE) is used as a pilot based channel estimator for the uplink channel. The effect of the spatial correlation on the accuracy of the channel estimation is investigate. We compared different spatial correlation models for ideal and non-ideal case scenarios.

Because of the channel reciprocity, the CSI will be the same for uplink and downlink data transmission. It is proved that there is more accurate channel estimation when having higher SNR values.

In the second part, the spectral efficiency for uplink and downlink of the LMMSE estimators are studied where spatial correlation models are applied to the system to generate the channel covariance matrix. The lower capacity of the uplink and downlink data transmission are derived to investigate the impact of using exponential correlation model. The lower capacity bound is calculated based on imperfect knowledge of the channel where pilot based estimator is used. In the first section of Chapter 4, there is one cell system model with one base station that is equipped with N antennas and serving single user terminal. In the second part, we have a single cell system. The system model consists of a base station with multiple antennas that is serving multiple antenna user where. It is shown that the spectral efficiency is enhanced by having larger number of base station antennas which proves the scalability of Massive MIMO systems.

In the last part of this dissertation, The transmit power and energy efficiency of the Massive MIMO system are investigated. The transmit power is represented as the energy consumed by the amplifier divided by the coherence time while the energy efficiency can be expressed as the ratio between spectral efficiency and emitted power. The impact of the channel spatial correlation on the energy efficiency is studied where it is shown that we have higher energy efficiency when we use higher number of base station antennas while the transmit power is decreasing when the number of base antennas are increasing.

6.2 Future Work

As mentioned in section 2.2.3.2, there are several limitations in Massive MIMO systems need to be studied. There are several possible directions that could be a good research topic in Massive MIMO in the future:

- Pilot contamination is one of the challenges that need to be tackled and investigated. This issue would affect the performance of the Massive MIMO badly. One solution is to increase the cell size to eliminate the contamination but in that case there will be power interference came from neighboring cells. The other solution is to change the factor of frequency-reuse. Though, this solution will affect the Massive MIMO performance and reduce the spectral efficiency. There must be an appropriate system design that balance between the cell size and the factor of frequency- reuse to reduce the effect of pilot contamination.
- One of the important issues is designing Massive MIMO system architecture that could be combined easily with current practical systems such as 3G, 4G and LTE. The new thoughts and the promising technologies that could be used in the upcoming 5G networks such as Massive MIMO or millimeter wave need to be combined smoothly with the wireless standard that are used today.
- In our work that is published in 7th *IEEE CCWC*, using pilot-based LMMSE estimator we could improve it by using different types of estimators such as Zero Forcing (ZF) and Maximal Ratio Combining (MRC).

- In our work that is published in 19th *IEEE ICCIT*, it is assumed that there is ideal hardware. We could improve this work by investigating the impact of having non-ideal hardware and see how would this limit the performance of the Massive MIMO system.

List of Publications

Journal Papers

1. **S. Albdran**, A. Alshammari and M. Matin, "Spatial Correlation Influence on the Channel Estimation and Spectral Efficiency for Massive MIMO Systems" – International Journal of Computer Science and Information Security, 2017.
2. A. Alshammari, **S. Albdran** and M. Matin, "Impact of Spatial Correlation and Users Allocation on The Performance of Massive MIMO Systems" – International Journal of Computer Science and Information Security, 2017.
3. **S. Albdran** and M. Matin, "Spectral and Energy Efficiency for Single Cell Massive MIMO Systems for Correlated Antennas" – To be submitted.

Conference Papers

4. **S. Albdran**, A. Alshammari and M. Matin, "Spectral and Energy Efficiency for Massive MIMO Systems Using Exponential Correlation Model," in *The 7th IEEE annual Computing and Communication Workshop and Conference,* In Press, 2017.
5. **S. Albdran**, A. Alshammari, M. A. R. Ahad, and M. Matin, "Effect of Exponential Correlation Model on Channel Estimation of Massive MIMO," in *The 19th IEEE International Conference on Computer and Information Technology (ICCIT)*, In Press, 2016.

6. **Saleh Albdran**, Ahmad Alshammari, Mohammad Matin, "Uplink channel estimation error for large scale MIMO system", *in SPIE 9970, Optics and Photonics for Information Processing X*, 99701J (September 14, 2016), doi:10.1117/12.2238004.

7. A. Alshammari, **S. Albdran** and M. Matin, "The Effect of Channel Spatial Correlation on Capacity and Energy Efficiency of Massive MIMO Systems," in *The 7th IEEE annual Computing and Communication Workshop and Conference*, In Press, 2017.

8. A. Alshammari, **S. Albdran**, M. A. R. Ahad, and M. Matin, "Impact of Angular Spread on Massive MIMO Channel Estimation," in *The 19th IEEE International Conference on Computer and Information Technology (ICCIT)*, In Press, 2016.

9. A. Alshammari, **S. Albdran** and M. Matin, "Channel Capacity of Next Generation Large Scale MIMO Systems," *in SPIE 9970, Optics and Photonics for Information Processing X*, 99701J (September 14, 2016), doi:10.1117/12.2238004.

References

[1] J. Hoydis, S. ten Brink, and M. Debbah, "Massive MIMO in the UL / DL of cellular networks : How many antennas do we need ?," *IEEE J. Sel. Areas Commun.*, vol. 31, no. 2, pp. 160–171, 2013.

[2] T. L. Marzetta, "Massive MIMO: An introduction," *Bell Labs Tech. J.*, vol. 20, pp. 11–22, 2015.

[3] T. J. Barnett, A. Sumits, S. Jain, and U. Andra, "Cisco Visual Networking Index (VNI) Update Global Mobile Data Traffic Forecast," 2016.

[4] F. Boccardi and T. L. Marzetta, "Five disruptive technology directions for 5G," *IEEE Commun. Mag.*, vol. 52, no. 2, pp. 74–80, 2014.

[5] J. Andrews, S. Buzzi, W. Choi, S. Hanly, A. Lozano, A. Soong, and J. C. Zhang, "What will 5G be?," *IEEE J. Sel. Areas Commun.*, vol. 32, no. 6, pp. 1065–1082, 2014.

[6] "Cisco Visual Networking Index: Global Mobile Data Traffic Forecast Update, 2016–2021 White Paper," *Cisco*, 2017. [Online]. Available: http://www.cisco.com/c/en/us/solutions/collateral/service-provider/visual-networking-index-vni/mobile-white-paper-c11-520862.html. [Accessed: 01-Feb-2017].

[7] T. L. Marzetta, “Noncooperative cellular wireless with unlimited numbers of base station antennas,” *IEEE Trans. Wirel. Commun.*, vol. 9, no. 11, pp. 3590–3600, 2010.

[8] H. Jerry, "*Introduction to MIMO Communication"*. 2014.

[9] S. Albdran, A. Alshammari, and M. Matin, “Spectral and Energy Efficiency for Massive MIMO Systems Using Exponential Correlation Model,” in *The 7th IEEE annual Comuting and Communication Workshop and Conferernce*, 2017.

[10] P. F. Driessen, “On the capacity formula for multiple input-multiple output wireless channels: a geometric interpretation,” *IEEE Trans. Commun.*, vol. 47, no. 2, pp. 173–176, 1999.

[11] K. F. Braun, “Electrical oscillations and wireless telegraphy,” *Nobel Lect. December*, vol. 11, no. 1909, pp. 226–245, 1909.

[12] H. H. Beverage and H. O. Peterson, “Diversity Receiving System of R.C.A. Communications, Inc., for Radiotelegraphy,” *Proceeding Inst. Radio Eng.*, vol. 19, no. 4, pp. 529–561, 1931.

[13] A. Wittneben, “Basestation modulation diversity for digital simulcast,” *[1991 Proceedings] 41st IEEE Veh. Technol. Conf.*, pp. 848–853, 1991.

[14] N. Seshadri, S. W, and Vij. WeerackodJ, “Advanced Techniques for Modulation , Error Correction , Channel Equalization , and Diversity,” *AT&T Tech. J.*, vol. 72,

no. 4, pp. 48–63, 1993.

[15] S. M. Alamouti, “A simple transmit diversity technique for wireless communications,” *IEEE J. Sel. Areas Commun.*, vol. 16, no. 8, pp. 1451–1458, 1998.

[16] G. J. Foschini, “Layered space-time architecture for wireless communication in a fading environment when using multi-element antennas,” *Bell Labs Tech. J.*, vol. 1, no. 2, pp. 41–59, 1996.

[17] G. J. Foschini, “V-BLAST An architecture for realizing very high data rates over the rich-scattering wireless channel.pdf,” *Signals, Syst. Electron.*, pp. 295–300, 1998.

[18] Ellen Jensen, “Iospan introduces broadband wireless technology,” *Wireless Network Online*, 2001. [Online]. Available: https://www.wirelessnetworksonline.com/doc/iospan-introduces-broadband-wireless-technolo-0001. [Accessed: 09-April-2017].

[19] T. L. Marzetta and B. M. Hochwald, “Capacity of a mobile multiple-antenna communication link in rayleigh flat fading,” *IEEE Trans. Inf. Theory*, vol. 45, no. 1, pp. 139–157, 1999.

[20] G. J. Foschini and M. J. Gans, “On limits of wireless communications in a fading environment when using multiple antennas,” *Wirel. Pers. Commun.*, vol. 6, no. 3, pp. 311–335, 1998.

[21] D. Gesbert, M. Kountouris, R. W. H. Jr, C.-B. Chae, and T. Sälzer, “From Single User to Multiuser Communications: Shifting the MIMO Paradigm,” *IEEE Signal Process. Mag.*, pp. 1–29, 2007.

[22] S. C. Swales, M. A. Beach, D. J. Edwards, and J. P. Mcgeehan, “The performance enhancement of multibeam adaptive base-station antennas for cellular land mobile radio systems,” vol. 39, no. I, 1990.

[23] J. H. Winters, “Optimum Combining in Digital Mobile Radio with Cochannel Interference,” *IEEE Trans. Veh. Technol.*, vol. 33, no. 3, pp. 144–155, 1984.

[24] B. Hassibi and M. Sharif, “Fundamental Limits in MIMO Broadcast Channels,” *IEEE J. Sel. Areas Commun.*, vol. 25, no. 7, pp. 1333–1344, 2007.

[25] P. By, “World ’ s largest Science , Technology & Medicine Open Access book publisher Multi User MIMO Communication : Basic Aspects , Multi User MIMO Communication : Basic Aspects , Benefits and Challenges Benefits and Challenges.”

[26] A. Adhikary, J. Nam, J. Y. Ahn, and G. Caire, “Joint spatial division and multiplexing-The large-scale array regime,” *IEEE Trans. Inf. Theory*, vol. 59, no. 10, pp. 6441–6463, 2013.

[27] T. S. Rappaport, S. Sun, R. Mayzus, H. Zhao, Y. Azar, and K. Wang, “Millimeter wave mobile communications for 5G cellular: It will work!,” *IEEE Access*, vol. 1, pp. 335–349, 2013.

[28] M. N. Tehrani, M. Uysal, and H. Yanikomeroglu, "Device-to-device communication in 5G cellular networks: Challenges solutions and future directions," *IEEE Commun. Mag.*, vol. 52, no. 5, pp. 86–92, 2014.

[29] W. Nam, D. Bai, J. Lee, and I. Kang, "Advanced interference management for 5G cellular networks," *IEEE Commun. Mag.*, vol. 52, no. 5, pp. 52–60, 2014.

[30] A. Osseiran, F. Boccardi, V. Braun, K. Kusume, and P. Marsch, "Scenarios for 5G mobile and wireless communications: The vision of the METIS project," *IEEE Commun. Mag.*, vol. 52, no. 5, pp. 26–35, 2014.

[31] C.-X. Wang, F. Haider, X. Gao, X.-H. You, and Y. Yang, "Cellular architecture and key technologies for 5G wireless communication networks," *IEEE Commun. Mag.*, vol. 52, no. 2, pp. 122–130, 2014.

[32] K. R. Santhi, V. K. Srivastava, G. SenthilKumaran, and A. Butare, "Goals of true broad band's wireless next wave (4G–5G)," *IEEE Veh. Technol. Conf.*, vol. 4, pp. 2317–2321, 2003.

[33] R. Baldemair, E. Dahlman, G. Fodor, G. Mildh, and S. Parkvall, "Evolving wireless communications: Addressing the challenges and expectations of the future," *IEEE Veh. Technol. Mag*, vol. 8, pp. 24–30, 2013.

[34] M. Peng, Y. Li, Z. Zhao, and C. Wang, "System architecture and key technologies for 5G heterogeneous cloud radio access networks," *IEEE Netw.*, vol. 29, no. 2, pp. 6–14, 2015.

[35] P. Rost, C. J. Bernardos, A. De Domenico, and M. Di Girolamo, “Cloud technologies for flexible 5G radio access networks,” *IEEE Commun. Mag*, vol. 52, no. 5, pp. 68–76, 2014.

[36] G. Wunder, M. Kasparick, S. ten Brink, F. Schaich, and T. Wild, “5GNOW: Challenging the LTE design paradigms of orthogonality and synchronicity,” *Proc. IEEE 77th Veh. Technol. Conf*, vol. 1–5, 2013.

[37] H. Tullberg, Z. Li, A. Hoglund, P. Fertl, and D. Gozalvez-Serrano, “Towards the METIS 5G concept: First view on horizontal topics concepts,” *Proc. Eur. Conf. Netw. Commun*, vol. 1–5, 2014.

[38] J. F. Monserrat, “Rethinking the mobile and wireless network architecture: The METIS research into 5G,” *Proc. Eur. Conf. Netw. Commun*, pp. 1–5, 2014.

[39] Tama´s Haidegger, J. Sa´ndor, and Z. Benyo, “Surgery in space: The future of robotic telesurgery,” *Surg. Endosc. Other Interv. Tech.*, vol. 25, no. 3, pp. 681–690, 2011.

[40] “How connectivity is driving the future of the cars ?,” *Wired*, 2017. [Online]. Available: https://www.wired.com/brandlab/2016/02/how-connectivity-is-driving-the-future-of-the-car/.[Accessed: 19-April-2017].

[41] Y. Zhang and M. Chen, *Cloud Based 5G Wireless Networks*. Springer International Publishing, 2016.

[42] "Understanding 5G: Perspectives on future technological advancements in mobile," *GSMA Intell.*, no. December, pp. 3–15, 2014.

[43] S. S. Sahoo, M. K. Hota, and K. K. Barik, "5G Network a New Look into the Future : Beyond all Generation Networks," vol. 2, no. 4, pp. 108–112, 2014.

[44] M. Dohler, R. W. Heath, A. Lozano, C. B. Papadias, and R. A. Valenzuela, "Is the PHY layer dead?," *IEEE Commun. Mag.*, vol. 49, no. 4, pp. 159–165, 2011.

[45] V. Chandrasekhar and J. G. Andrews, "Femtocell Networks: A Survey," *IEEE Commun. Mag.*, vol. Volume: 46, no. Issue: 9, p. Pages: 59-67, 2008.

[46] J. E. Flood, *Telecommunication networks*, 2nd ed. London : Institution of Electrical Engineers, 1997.

[47] J. G. Andrews, "Seven ways that hetnets are a cellular paradigm shift," *IEEE Commun. Mag.*, vol. 51, no. 3, pp. 136–144, 2013.

[48] J. G. Andrews, H. Claussen, M. Dohler, S. Rangan, and M. C. Reed, "Femtocells: Past, present, and future," *IEEE J. Sel. Areas Commun.*, vol. 30, no. 3, pp. 497–508, 2012.

[49] G. Kim, "Small Cell Backhaul: Fixed or Wireless?," *IP Carr.*, 2013.

[50] Z. Pi and F. Khan, "An introduction to millimeter-wave mobile broadband systems," *IEEE Commun. Mag.*, vol. 49, no. 6, pp. 101–107, 2011.

[51] S. Haykin, "Cognitive Radio : Brain-Empowered," vol. 23, no. 2, pp. 201–220,

2005.

[52] "RESOLUTION COM6/20 (WRC-15) Studies on frequency-related matters for International Mobile Telecommunications identification including possible additional allocations to the mobile services on a primary basis in portion(s) of the frequency range between 24," 2015.

[53] *Use of Spectrum Bands Above 24 GHz for Mobile Radio Services*, vol. 81, no. 219. 2016.

[54] "mmWave : The Battle of the Bands," 2016.

[55] D. Gesbert, M. Kountouris, R. W. Heath, C. B. Chae, and T. Sälzer, "Shifting the MIMO Paradigm," *IEEE Signal Process. Mag.*, vol. 24, no. 5, pp. 36–46, 2007.

[56] G. Caire, N. Jindal, M. Kobayashi, and N. Ravindran, "Multiuser MIMO achievable rates with downlink training and channel state feedback," *IEEE Trans. Inf. Theory*, vol. 56, no. 6, pp. 2845–2866, 2010.

[57] E. Björnson, M. Kountouris, and M. Bengtsson, "Receive combining vs . Multi-stream multiplexing in downlink systems with Multi-antenna users," vol. 61, no. 13, pp. 3431–3446, 2013.

[58] T. L. Marzetta, "How much training is required for multiuser MIMO?," *Conf. Rec. - Asilomar Conf. Signals, Syst. Comput.*, pp. 359–363, 2006.

[59] Z. Xiang, M. Tao, and X. Wang, "Massive MIMO multicasting in noncooperative

cellular networks," *IEEE JSAC Spec. Issue 5G Wirel. Commun. Syst.*, vol. 32, no. 6, pp. 1180–1193, 2014.

[60] Q. He, L. Xiao, X. Zhong, and S. Zhou, "Increasing the Sum-Throughput of Cells With a Sectorization Method for Massive MIMO," *IEEE Commun. Lett.*, vol. 18, no. 10, pp. 1827–1830, 2014.

[61] J. Choi, "Distributed Beamforming for Macro Diversity and Power Control With Large Arrays in Spatial Correlated Channels," *IEEE Trans. Wirel. Commun.*, vol. 14, no. 4, pp. 1871–1881, 2015.

[62] X. Lin, R. W. Heath, and J. G. Andrews, "The Interplay Between Massive MIMO and Underlaid D2D Networking," *IEEE Trans. Wirel. Commun.*, vol. 14, no. 6, 2015.

[63] C. Sun, X. Gao, S. Jin, and M. Matthaiou, "Beam Division Multiple Access Transmission for Massive MIMO Communications," *IEEE Trans. Commun.*, vol. 63, no. 6, pp. 2170–2184, 2015.

[64] Z. Zhang, X. Wang, K. Long, and A. V. Vasilakos, "No Title," *IEEE Commun. Soc.*, vol. 22, no. 5, pp. 58–66, 2015.

[65] L. Zhao, X. Wang, and K. Zhengu, "Hybrid Information and Energy Transfer with Massive MIMO," *IEEE Trans. Wirel. Commun.*, 2015.

[66] E. G. Larsson and H. V. Poor, "Joint Beamforming and Broadcasting in Massive

MIMO," *IEEE Trans. Wirel. Commun.*, 2016.

[67] T. Lv, F. Tan, H. Gao, and S. Yang, "A beamspace approach for 2-D localization of incoherently distributed sources in massive MIMO systems," *Signal Processing*, vol. 121, pp. 30–45, 2016.

[68] M. Hanif, H.-C. Yang, G. Boudreau, E. Sich, and H. Seyedmehdi, "Low complexity antenna subset selection for massive MIMO systems with multi-cell cooperation," *Proc. IEEE Globecom Work.*, 2015.

[69] E. Björnson, "Hardware impairments in Large-scale MISO systems : Energy efficiency , estimation , and capacity limits," *18th Int. Conf. Digit. Signal Process.*, pp. 1–6, 2013.

[70] M. Médard, "The effect upon channel capacity in wireless communications of perfect and imperfect knowledge of the channel," *IEEE Trans. Inf. Theory*, vol. 46, no. 3, pp. 933–946, 2000.

[71] "Circuits and Techniques for 5G Mobile Communications and Low Power Sensors," *UC San Diego*. [Online]. Available: http://cwc.ucsd.edu/research-projects. [Accessed: 01-March-2017].

[72] H. Q. Ngo, E. G. Larsson, and T. L. Marzetta, "Aspects of favorable propagation in Massive MIMO," *Eur. Signal Process. Conf.*, no. 1, pp. 76–80, 2014.

[73] H. Q. Ngo, H. A. Suraweera, M. Matthaiou, and E. G. Larsson, "Multipair full-

duplex relaying with massive arrays and linear processing," *IEEE J. Sel. Areas Commun.*, vol. 32, no. 9, pp. 1721–1737, 2014.

[74] J. Hoydis, C. Hoek, T. Wild, and S. ten Brink, "Channel measurements for large antenna arrays," *2012 Int. Symp. Wirel. Commun. Syst.*, pp. 811–815, 2012.

[75] D. Persson, B. K. Lau, and E. G. Larsson, "Scaling Up MIMO: Opportunities and challenges with very large arrays," *IEEE Signal Process. Mag.*, vol. 30, no. 1, pp. 40–60, 2012.

[76] Y. H. Thomas L. Marzetta, Erik G. Larsson, Hien Quoc Ngo, *Fundamentals of Massive MIMO*. Cambridge University Press, 2016, 2016.

[77] E. Bjornson, E. G. Larsson, and T. L. Marzetta, "Massive MIMO: ten myths and one critical question," *IEEE Commun. Mag.*, vol. 54, no. 2, pp. 114–123, 2016.

[78] H. Q. Ngo, E. G. Larsson, and T. L. Marzetta, "Energy and spectral efficiency of very large multiuser MIMO systems," *IEEE Trans. Commun.*, vol. 61, no. 4, pp. 1436–1449, 2013.

[79] A. Alshammari, S. Albdran, M. Ahad, and M. Matin, "Impact of Angular Spread on Massive MIMO Channel Estimation," in *The 19th IEEE International Conference on Computer and Information Technology*, 2016.

[80] E. Bjornson, J. Hoydis, M. Kountouris, and M. Debbah, "Massive MIMO systems with non-ideal hardware: Energy efficiency, estimation, and capacity limits," *IEEE*

Trans. Inf. Theory, vol. 60, no. 11, pp. 7112–7139, 2014.

[81] E. Larsson, O. Edfors, F. Tufvesson, and T. Marzetta, “Massive MIMO for next generation wireless systems,” *IEEE Commun. Mag.*, vol. 52, no. 2, pp. 186–195, 2014.

[82] A. Alshammari, “Impact of Spatial Correlation and Users Allocation on The Performance of Massive MIMO Systems,” *Int. J. Comput. Sci. Inf. Secur.*, 2017.

[83] “5G Massive MIMO Testbed: From Theory to Reality,” *National Instruments*, 2016. [Online]. Available: http://www.ni.com/white-paper/52382/en/.[Accessed: 09-Jan-2017].

[84] A. Nordrum, “5G Researchers Set New World Record For Spectrum Efficiency,” *IEEE Spectrum*, 2016.

[85] “MAMMOET: Massive MIMO for Efficient Transmission,” 2016. [Online]. Available: https://mammoet-project.eu/.[Accessed: 13-Feb-2017].

[86] “ELLIT,” 2015. [Online]. Available: http://old.liu.se/elliit/Communication?l=en. [Accessed: 03-May-2017].

[87] J. Vieira, S. Malkowsky, K. Nieman, Z. Miers, N. Kundargi, L. Liu, I. Wong, V. Owall, O. Edfors, and F. Tufvesson, “A flexible 100-antenna testbed for Massive MIMO,” *2014 IEEE Globecom Work. GC Wkshps 2014*, pp. 287–293, 2014.

[88] “Massive MIMO test bed (MATE),” 2017. [Online]. Available:

http://www.chalmers.se/en/projects/Pages/Massive-MIMO-test-bed.aspx. [Accessed: 02-April-2017].

[89] "EARS: Energy- and Cost-Efficient Spectrum Utilization with Full-Duplex mm-wave Massive MIMO," 2016. [Online]. Available: https://www.nsf.gov/awardsearch/showAward?AWD_ID=1642920. [Accessed: 18-Jan-2017].

[90] "Nokia and Sprint demonstrate massive MIMO at #MWC17," 2017. [Online]. Available: http://www.nokia.com/en_int/news/releases/2017/02/27/nokia-and-sprint-demonstrate-massive-mimo-at-mwc17. [Accessed: 09-Feb-2017].

[91] A. Alshammari, S. Albdran, and M. Matin, "Channel Capacity of Next Generation Large Scale MIMO Systems," in *SPIE 9970, Optics and Photonics for Information Processing*, 2016.

[92] S. L. Loyka, "Channel capacity of MIMO architecture using the exponential correlation matrix," *IEEE Commun. Lett.*, vol. 5, no. 9, pp. 369–371, 2001.

[93] C. C. Martin, J. H. Winters, N. R. Sollenberger, S. Drive, and R. Bank, "Multiple-Input Multiple-Output (MIMO) radio channel measurements," *IEEE Antennas Propag. Soc. Int. Symp.*, vol. 1, pp. 418–421, 2001.

[94] S. Albdran, A. Alshammari, and M. Matin, "Uplink channel estimation error for large scale MIMO system," in *SPIE 9970, Optics and Photonics for Information Processing*, 2016.

[95] S. Albdran, A. Alshammari, M. Ahad, and M. Matin, “Effect of Exponential Correlation Model on Channel Estimation for Massive MIMO,” in *The 19th International Conference on Computer and Information Technology*, 2016.

[96] J. P. Kermoal, L. Schumacher, K. I. Pedersen, P. E. Mogensen, and F. Frederiksen, “A Stochastic MIMO Radio Channel Model With Experimental Validation,” vol. 20, no. 6, pp. 1211–1226, 2002.

[97] E. Bj¨orson and B. Ottersten, “A framework for training-based estimation in arbitrarily correlated rician MIMO channels with rician disturbance,” *IEEE Trans. Signal Process*, vol. 58, no. 3, pp. 1807–1820, 2010.

[98] E. B. X. Li, S. Z. E. G. Larsson, and J. Wang, “A multicell MMSE detector for massive MIMO systems and new large system analysis,” *Proc. IEEE Globecom Work.*, 2015.

[99] S. Albdran, A. Alshammari, and M. Matin, “Spatial Correlation Influence on the Channel Estimation and Spectral Efficiency for Massive MIMO Systems,” *Int. J. Comput. Sci. Inf. Secur.*, 2017.

[100] A. Alshammari, S. Albdran, and M. Matin, “The Effect of Channel Spatial Correlation on Capacity and Energy Efficiency of Massive MIMO Systems,” in *The 7th IEEE annual Comuting and Communication Workshop and Confererrnce*, 2017.

Appendix

Effect of Exponential Correlation Model on Channel Estimation for Massive MIMO

Saleh Albdran[1], Ahmed Alshammari[1], Md. Atiqur Rahman Ahad[2] and Mohammad Matin[1], *Senior Member, IEEE*

[1]Department of Electrical Engineering, University of Denver

[2]Department of Electrical and Electronic Engineering, University of Dhaka

***Abstract*—In this paper the impact of exponential correlation model on massive multiple input multiple output (MIMO) channel estimation is analyzed using a large number of antennas in the base station (BS) and a user terminal. We consider pilot-based channel estimation in the UL channel. The Linear minimum mean square error (LMMSE) estimator is used to investigate the effect of correlation factor on the average mean square error (MSE). Different number of antennas and several signal to noise ratio (SNR) values are implemented to see the estimation accuracy in each case. The effect of pilot length on the LMMSE channel estimator and its relationship with the exponential correlation model is investigated. It is shown that for low SNR values, the exponential correlation model has high impact on channel estimation.**

Keywords—Massive MIMO; Channel State Information; Channel Estimation; Time Division Duplix; Correlation Factor; Pilot Length; Signal to Noise Ratio; Mean Square Error; Base Station

I. Introduction

Demand for higher data rate in wireless network will keep growing whereas the available electromagnetic spectrum is limited [1], [2]. Unlike fiber communications where it is applicable to meet the future demand, wireless communications are seeking for clever thoughts and new technologies [3]. One of the latest proposed technologies is massive multiple input multiple output (MIMO), also called large-scale MIMO, and it is known for its promising potentials [4], [5]. It is basically based on equipping the base station (BSs) with a much larger number of antennas compared to the number of users [3], [4]. The need to achieve accurate channel state information (CSI) has led to time division duplex (TDD) operation mode which gives the massive MIMO the ability to reach any desired number of antennas in the BS terminal since the number of training sequence is directly proportional to the number of users [6], [3]. At the BS terminal, CSI is essential to achieve the optimal performance and to reap the benefits of this technology [7], [8].

Massive MIMO system will consists of few hundreds of antennas instantaneously serving a big number of terminal users and sharing the same frequency [9]. This new technology has several benefits. one of them is improving spectral efficiency to meet increasing demand especially in dense metropolises and providing secure broadband network [1], [10]. Also, reduced transmitter/receiver complexity would cuts the cost of the components, improve the power efficiency and add more simplicity to the signal processing [3], [11].

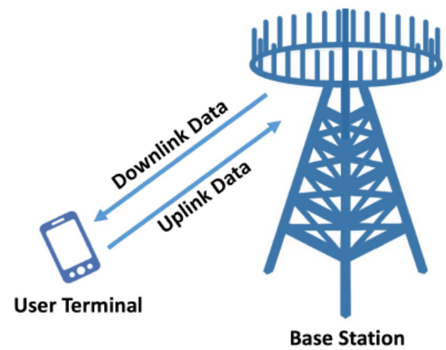

Fig. 1. The channel between the base station that has a big number of antennas and a user terminal.

Channel estimation accuracy is very important factor that could limit wireless spectral efficiency and it attracts the attention of several researchers [12], [13]. The linear minimum mean square error (LMMSE) estimator shows decent performance that goes with any value of SNR [12]. However, it has some challenges to obtain its optimal performance includes having perfect knowledge of the channel matrix [6], [14].

Notation: throughout this paper, notations that are written in bold lower case represents column vectors, such as $\mathbf{x}$. However bold upper case represents matrices, $\mathbf{X}$. The transpose of $\mathbf{X}$ is denoted by, $\mathbf{X}^{\mathbf{T}}$, its conjugate is expressed by, $\mathbf{X}^{*}$, and $\mathbf{X}^{\mathbf{H}}$ for conjugate transpose. $\mathbf{I}$ is the identity matrix with appropriate dimensions for the system. The expected value operation for $\mathbf{x}$ is represented by $\mathbb{E}\{\mathbf{x}\}$ and the conditional expected value for $\mathbf{x}$ with respect to $\mathbf{y}$ is denoted by $\mathbb{E}\{\mathbf{x}|\mathbf{y}\}$. $\mathbf{Q}$ is the covariance matrix and $\bar{\mathbf{x}}$ is the mean where the complex Gaussian vector $\mathbf{x}$ is expressed by $\mathbf{x} \sim \mathcal{CN}(\bar{\mathbf{x}}, \mathbf{Q})$.

The following parts of this paper are organized as follows: the system model is described in section II. In section III the exponential correlation model is introduced and its theoretical concept is explained. The uplink channel estimation and the LMMSE estimator conception described in section IV. Simulation results are obtained and analyzed in section V. Section VI is the last section of this paper where the viewpoints are wrapped up and concluded.

II. System Model

The main part of this work is to analyze the relative estimation error for the UL channel which is exposed to interference due to the nature of wireless channel. Our system model consists of a big number of N-antennas in the BS terminal and connected to a single antenna in the user terminal as shown in Fig.1. This system is a special case of massive MIMO and the protocol that is used in our system is TDD between the two sides of the link [15]. Since the estimation accuracy in TDD protocols is independent of N, we are able to increase the number BS antennas to a very large number [6], [16] .

By taking advantage of channel reciprocity, we are maintaining continues CSI to detect UL data information [17]. The block-fading channel between the two terminals is denoted by $\mathbf{h}$ and modeled as Rayleigh block fading $\mathbf{x} \sim \mathcal{CN}(\mathbf{0}, \mathbf{R})$, where $\mathbf{R}$ is represented as follows

$$\mathbf{R} = \mathbb{E}\{\mathbf{h}\mathbf{h}^{\mathrm{H}}\} \tag{1}$$

We are assuming that the statistical distribution is known by the base station terminal. The UL system model is based on pilot for the channel estimation where $\mathbf{y}$ represents the received signal at the BS

$$\mathbf{y} = \mathbf{h}d + \boldsymbol{n} \tag{2}$$

where $d \in \mathbb{C}$ is the received signal that could be the known pilot or the data signal, and its average power is

$$p = \mathbb{E}\{|d|^2\} \tag{3}$$

The noise is denoted by $\boldsymbol{n}$ and it consists of two combined terms as follows

$$\boldsymbol{n} = \boldsymbol{n}_{\text{noise}} + \boldsymbol{n}_{\text{if}} \tag{4}$$

where $\boldsymbol{n}_{\text{noise}}$ is the noise of the independent receiver that has zero mean and $(\sigma_{BS}^2\mathbf{I})$ covariance, while $\boldsymbol{n}_{\text{if}}$ is the interference noise from other transmissions.

We are assuming that $\boldsymbol{n}_{\text{if}}$ has zero mean and $\mathbb{E}\{\boldsymbol{n}_{\text{if}}\boldsymbol{n}_{\text{if}}^{\mathrm{H}}\}$ covariance and it is denoted by $\mathbf{S}$. The conditional covariance matrix is defined as $\boldsymbol{Q}_{\mathcal{H}} = \mathbb{E}\{\boldsymbol{n}_{\text{if}}\boldsymbol{n}_{\text{if}}^{\mathrm{H}}|\boldsymbol{\mathcal{H}}\}$, where $\boldsymbol{\mathcal{H}}$ is the channel realization. In our analysis, we are making an assumption: regardless of the number of antennas in the base station, the spectral norm of $\mathbf{R}$ is uniformly bounded [18].

III. Exponential Correlation Model

The exponential correlation is a model that is used to generate the channel covariance matrix and explained in more details in [19]. This model is assuming that $\mathbf{R}$ has two elements (i, j) as follows

$$[\mathbf{R}] = \begin{cases} \delta r^{j-i}, & i \leq j \\ \delta (r^{j-i})^*, & i > j \end{cases} \tag{5}$$

where r is the correlation factor between the neighboring branches and δ is a scaling factor.

The value of correlation factor r is bounded between 0 to 1 and its phase $\angle r$ is the arrival or departure angle. This model may not be the most accurate model for real-world situations. But, it is still simple model with small number of parameters which allow one to study the effect of the correlation factor on massive MIMO channel estimator [20]. The eigenvalue spread in $\mathbf{R}$ is represented by $|r|$ which is the correlation factor, while the corresponding eigenvectors are defined by $\angle r$. Since the angle of r has no impact on the mean square error, we assume that r is a real value.

IV. Uplink Channel Estimation

To estimate the channel $\mathbf{h}$, we take the received uplink signal $\mathbf{y}$ in (2) and compare it to the known uplink pilot signal d where the power of user equipment (p^{UE}) equals to $|d|^2$. The estimator in our work is the linear minimum mean square error estimator (LMMSE), where the estimation of the channel realization is represented as follows

$$\hat{\mathbf{h}} = d^*\mathbf{R}\overline{\mathbf{Y}}^{-1}\boldsymbol{y} \tag{6}$$

The covariance matrix of $\mathbf{y}$ is represented in (7) and it consists of combined terms that include the average power, $\mathbf{R}$ matrix, and the covariance of the received signal and the noise

$$\overline{\mathbf{Y}} = \mathbb{E}\{\mathbf{y}\mathbf{y}^{\mathrm{H}}\} = p^{UE}\mathbf{R} + \mathbf{S} + \sigma_{BS}^2\mathbf{I} \tag{7}$$

The error covariance matrix that is used to evaluate the total MSE is represented as follows

$$\mathbf{C} = \mathbb{E}\left\{\left(\hat{\mathbf{h}} - \mathbf{h}\right)\left(\hat{\mathbf{h}} - \mathbf{h}\right)^{H}\right\} = \mathbf{R} - p^{UE}\mathbf{R}\overline{\mathbf{Y}}^{-1}\mathbf{R} \tag{8}$$

by getting the value of $\mathbf{C}$ which is error covariance matrix in (8) we can get the total value of MSE

$$\mathbf{MSE} = \mathbb{E}\left\{\left\|\hat{\mathbf{h}} - \mathbf{h}\right\|_2^2\right\} = \mathbf{tr(C)} \tag{9}$$

Based on the previous observations in (9), the channel can be represented as a combination of two components

$$\mathbf{h} = \hat{\mathbf{h}} + \boldsymbol{\epsilon} \tag{10}$$

where the value of LMMSE estimate is denoted by $\hat{\mathbf{h}}$, while the unknown estimate error of the process is represented by the notation $\boldsymbol{\epsilon}$. The two components $\hat{\mathbf{h}}$ and $\boldsymbol{\epsilon}$ are uncorrelated and have zero mean for both of them. The covariance matrix for $\hat{\mathbf{h}}$ is represented as $\mathbb{E}\{\hat{\mathbf{h}}\hat{\mathbf{h}}^{\mathrm{H}}\} = \mathbf{R} - \mathbf{C}$ while the covariance matrix for $\boldsymbol{\epsilon}$ is formed as $\mathbb{E}\{\boldsymbol{\epsilon}\boldsymbol{\epsilon}^{H}\} = \mathbf{C}$, where the value of $\mathbf{C}$ was derived in (8).

In the previous LMMSE estimate statement there was a consideration of pilot signal d which is useful to reduce the total MSE. Assume that the pilot length is B and we want to compute the value of $\hat{\mathbf{h}}_i = \mathbf{h} + \boldsymbol{\epsilon}$ for $i = 1, .., B$, by taking the average we get

$$\widehat{\mathbf{h}} = \frac{1}{B}\sum_{i=1}^{B} \hat{\mathbf{h}}_i = \mathbf{h} - \frac{1}{B}\sum_{i=1}^{B} \boldsymbol{\epsilon} \qquad (11)$$

The total MSE of the estimate $\widehat{\mathbf{h}}$ for the case of having uncorrelated noise is obtained as follows

$$\mathbb{E}\left\{\left(\frac{1}{B}\sum_{i=1}^{B}\boldsymbol{\epsilon}_i\right)^H \left(\frac{1}{B}\sum_{j=1}^{B}\boldsymbol{\epsilon}_j\right)\right\} = \frac{\mathrm{tr}(\mathbf{C})}{B} \qquad (12)$$

from (12) we can see that by increasing the pilot length B, the total MSE of the estimate $\hat{\mathbf{h}}$ goes to zero for the ideal case scenario.

V. Simulation Results

The channel estimation accuracy using LMMSE estimator with N=100 antennas is demonstrated in Fig.2. The relative estimation error per antenna ($\mathrm{MSE}_{relative} = \frac{\mathrm{MSE}}{\mathrm{tr}(\mathbf{R})}$) is presented versus correlation factor. The channel covariance is created using exponential correlation model with coefficient values between 0 to 1 and an increment of 0.01. Fig.2 shows that the higher the SNR value the more accurate the estimation and we can see slight improvement in the estimation accuracy with higher correlation factor values.

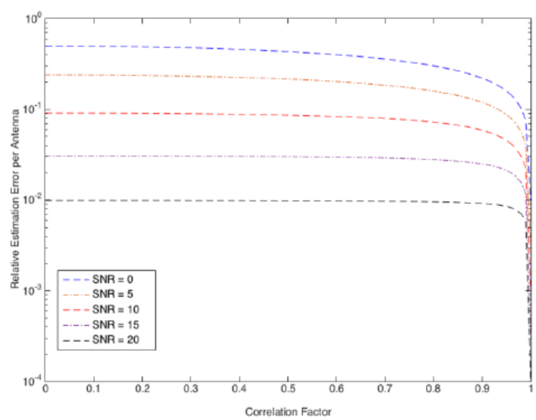

Fig. 2. Relative estimation error versus correlation factor for Linear MMSE estimator. The signal to noise ratio values are changed form 0 to 20 dB with an increment of 5 dB.

Fig.3 demonstrates the relative estimation error per antenna as a function of correlation factor with different number of antennas. We can see the enhancement of the estimator performance by increasing the value of correlation factor and getting closer to 1. Despite the minor improvement at the estimation accuracy at the beginning, increasing the number of antennas in the BS and reaching a large number does not change the estimation accuracy in the case of having the same system parameters.

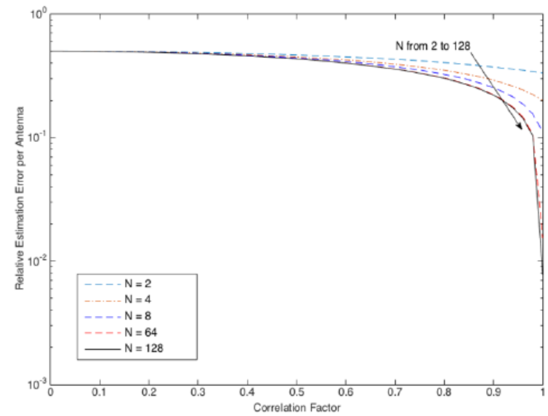

Fig. 3. Relative estimation error versus correlation factor for Linear MMSE estimator with different number of antennas N in the BS.

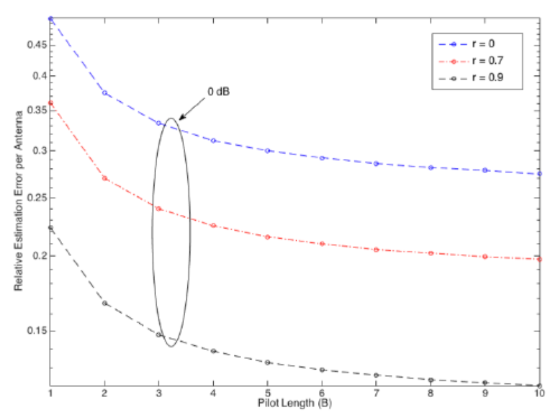

Fig. 4. Relative estimation error versus pilot length for Linear MMSE estimator. The SNR value is 0 dB and the correlation factor values are 0, 0.7, and 0.9.

The effect of pilot length on the estimation performance is shown in Fig.4. The relative estimation error is displayed versus pilot length with N=50 antennas. The obvious remark is that we can see the benefit of increasing the length of the pilot where the estimation is getting more accurate. The covariance channel matrix $\mathbf{R}$ is created using the exponential model. We start studying the impact of pilot length by choosing 0 dB SNR, the correlation factor is changed three times to see its effect. From Fig.4 we can see that the correlation factor has a large influence on the channel estimation accuracy where the higher the correlation factor the better the performance. Fig.5 is basically similar to Fig.4 but with 15 dB SNR where the relative estimation error per antenna is illustrated as a function of B with N=50 antennas. We can see that the impact of correlation factor choice is limited due to having higher SNR. Still the higher the correlation factor the better the estimation accuracy.

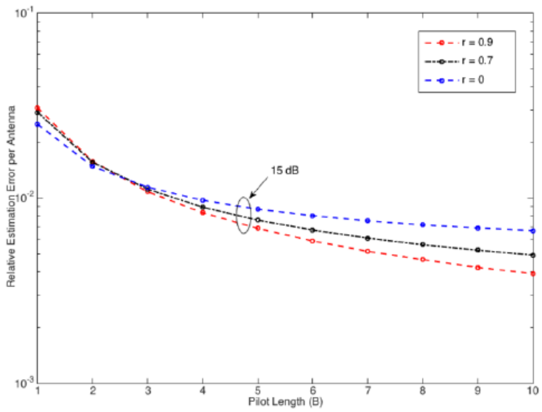

Fig. 5. Relative estimation error versus pilot length for Linear MMSE estimator. The SNR value is 15 dB and the correlation factor values are 0, 0.7, and 0.9.

VI. Conclusion

This paper investigated the estimation accuracy for massive MIMO system that has a large number of antennas in the BS and a single antenna in the user terminal. The impact of exponential correlation model on the relative estimation error per antenna is analyzed using pilot based LMMSE estimator for the UL channel. Simulation results have shown that at larger SNR values the channel estimation is more accurate. The increase in the number of antennas at the BS has a slight impact on the estimation error per antenna until we exceed 50 antennas then increasing N has no impact in the exponential correlation model. At higher SNR values, we observed that the impact of exponential correlation model is limited.

References

[1] J. Andrews, S. Buzzi, W. Choi, S. Hanly, A. Lozano, A. Soong, and J. C. Zhang, "What will 5G be?," *IEEE J. Sel. Areas Commun.*, vol. 32, no. 6, pp. 1065–1082, 2014.

[2] E. Bjornson, J. Hoydis, M. Kountouris, and M. Debbah, "Massive MIMO systems with non-ideal hardware: Energy efficiency, estimation, and capacity limits," *IEEE Trans. Inf. Theory*, vol. 60, no. 11, pp. 7112–7139, 2014.

[3] T. L. Marzetta, "Massive MIMO: An introduction," *Bell Labs Tech. J.*, vol. 20, pp. 11–22, 2015.

[4] J. Hoydis, S. Ten Brink, and M. Debbah, "Massive MIMO: How many antennas do we need?," *2011 49th Annu. Allert. Conf. Commun. Control. Comput. Allert. 2011*, pp. 545–550, 2011.

[5] F. Boccardi and T. L. Marzetta, "Five disruptive technology directions for 5G," *IEEE Commun. Mag.*, vol. 52, no. 2, pp. 74–80, 2014.

[6] D. Persson, B. K. Lau, and E. G. Larsson, "Scaling Up MIMO: Opportunities and challenges with very large arrays," *IEEE Signal Process. Mag.*, vol. 30, no. 1, pp. 40–60, 2012.

[7] B. Lv, Z. Yang, and Y. Feng, "Temporally and spatially correlated uplink channel estimation for massive MIMO systems," *2015 Int. Conf. Wirel. Commun. Signal Process. (WCSP)*, pp. 1–5, 2015.

[8] J. Hoydis, C. Hoek, T. Wild, and S. ten Brink, "Channel measurements for large antenna arrays," *2012 Int. Symp. Wirel. Commun. Syst.*, pp. 811–815, 2012.

[9] X. Gao, O. Edfors, F. Rusek, and F. Tufvesson, "Linear pre-coding performance in measured very-large MIMO channels," *IEEE Veh. Technol. Conf. (VTC Fall)*, pp. 1–5, 2011.

[10] E. Larsson, O. Edfors, F. Tufvesson, and T. Marzetta, "Massive MIMO for next generation wireless systems," *IEEE Commun. Mag.*, vol. 52, no. 2, pp. 186–195, 2014.

[11] H. Q. Ngo, E. G. Larsson, and T. L. Marzetta, "Energy and spectral efficiency of very large multiuser MIMO systems," *IEEE Trans. Commun.*, vol. 61, no. 4, pp. 1436–1449, 2013.

[12] A. Assalini, E. Dall'Anese, and S. Pupolin, "On the robustness of MIMO LMMSE channel estimation," *IEEE Trans. Wirel. Commun.*, vol. 9, no. 11, pp. 3313–3319, 2010.

[13] M. Médard, "The effect upon channel capacity in wireless communications of perfect and imperfect knowledge of the channel," *IEEE Trans. Inf. Theory*, vol. 46, no. 3, pp. 933–946, 2000.

[14] E. Bjornson, E. G. Larsson, and T. L. Marzetta, "Massive MIMO: ten myths and one critical question," *IEEE Commun. Mag.*, vol. 54, no. 2, pp. 114–123, 2016.

[15] E. Björnson, M. Kountouris, and M. Bengtsson, "Receive combining vs . Multi-stream multiplexing in downlink systems with Multi-antenna users," vol. 61, no. 13, pp. 3431–3446, 2013.

[16] E. Björnson, "Hardware impairments in Large-scale MISO systems : Energy efficiency , estimation , and capacity limits," *18th Int. Conf. Digit. Signal Process.*, pp. 1–6, 2013.

[17] T. L. Marzetta, "Noncooperative cellular wireless with unlimited numbers of base station antennas," *IEEE Trans. Wirel. Commun.*, vol. 9, no. 11, pp. 3590–3600, 2010.

[18] J. Hoydis, S. ten Brink, and M. Debbah, "Massive MIMO in the UL / DL of cellular networks : How many antennas do we need ?," *IEEE J. Sel. Areas Commun.*, vol. 31, no. 2, pp. 160–171, 2013.

[19] S. L. Loyka, "Channel capacity of MIMO architecture using the exponential\ncorrelation matrix," *IEEE Commun. Lett.*, vol. 5, no. 9, pp. 369–371, 2001.

[20] C. C. Martin, J. H. Winters, N. R. Sollenberger, S. Drive, and R. Bank, "Multiple-Input Multiple-Output (MIMO) radio channel measurements," *IEEE Antennas Propag. Soc. Int. Symp.*, vol. 1, pp. 418–421, 2001. [1] T. L. Marzetta, "Massive MIMO: An introduction," *Bell Labs Tech. J.*, vol. 20, pp. 11–22, 2015.

Spectral and Energy Efficiency for Massive MIMO Systems Using Exponential Correlation Model

Saleh Albdran, *Student Member, IEEE,* Ahmed Alshammari, *Student Member, IEEE,* and Mohammad A. Matin, *Senior Member, IEEE*
Department of Electrical and Computer Engineering, University of Denver
Denver, CO, USA

***Abstract*— The use of massive multiple input multiple output (MIMO) systems can improve the performance of energy efficiency and increase the capacity limits due to the improvement of the spatial correlation. The effect of the exponential correlation model on the massive MIMO energy and spectral efficiencies is investigated using a base station (BS) with a large number of antennas and a single antenna user terminal. To generate the lower capacity bounds, we used least minimum mean square error (LMMSE) as a pilot based channel estimator for the uplink channel. Different scenarios are implemented by using several numbers of BS antennas and changing the signal to noise ratio (SNR) values. The spectral efficiency was more sensitive to the change of the correlation factor when using higher SNR. It is shown that for the higher number of BS antennas we have, more energy efficient performance we get.**

Keywords—massive MIMO; channel state information; spatial correlation; signal to noise ratio; base station

I. INTRODUCTION

In the past few years, the request for wireless throughput was keep growing while the available range of electromagnatic spectrum is limited [1], [2]. Massive MIMO system is a new and promising technology that grabbed the attention of researcher due to its ability to improve the capacity limits and increase the energy efficiency [3], [4]. In the massive MIMO systems, the base station has a couple of hundreds of antennas and communicates with much smaller number of users where each terminal has single antenna [5], [6]. Commonly, the communication systems are operating in such a way where the BSs communicate with each terminal user separately both in time and frequency which is not the optimal case [7]. In massive MIMO systems, BS antennas are serving a number of user terminals at the same time and sharing the same frequency [8].

Massive MIMO systems have their own benefits which include improving spectral efficiency to meet the higher demand in the future especially in dense areas [9]. Also, this new technology will provide more secure networks and more efficient system in terms of energy [2]. The cost of the hardware components in the BSs will be reduced due to the simplicity of the signal processing [1], [3]. The enhancement of the spectral efficiency in this new technology can be achieved without needing to add more expensive and sophisticated BSs [10]. Due

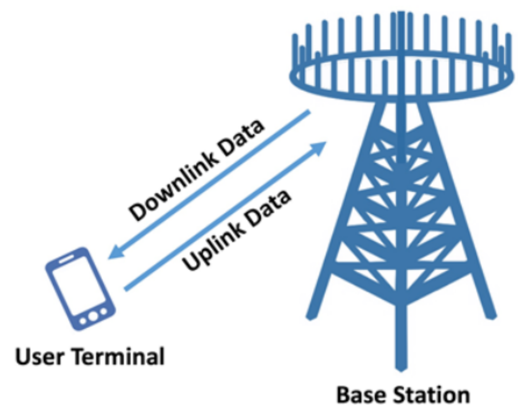

Fig. 1. The uplink and downlink channel between the base station terminal and the user terminal.

to the massive spatial diversity, the response of the wireless channel is much smoother [2]. The large number of antennas is the main reason behind energy efficiency improvement where the energy is sharply focused into small space [9], [11].

To get accurate channel state information (CSI), it is important to use time division duplexing (TDD) as operation mode to get the benefits of reciprocity [12], [13]. By using TDD mode we obtain several advantages, one of them is the knowledge of the uplink channel need to be obtained only by the BS to operate coherently [5]. One of the benefits of using TDD is having the ability of reaching any wanted number of BS antennas since the estimation accuracy in this protocol is independent of the base station antennas number N [10]. The channel estimation accuracy will not only be immune of getting larger number of antennas but it will be improved in case of having a perfect knowledge of the correlation structure [5].

The accuracy of channel estimation is critical factor that has great impact on the spectral efficiency [14], [15]. Based on the channel estimation procedure we can derive capacity limits for

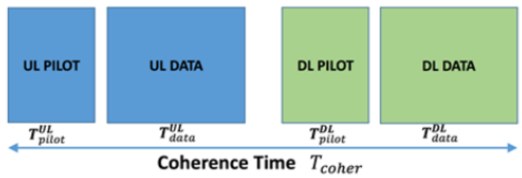

Fig. 2. TDD system with coherence time devided into different stages for uplink and downlink.

uplink and downlink transmission of data. The precision of CSI plays a significant role in the calculation of capacity bounds [16], [17]. The energy efficiency (EE) can be described as the ratio between spectral efficiency (SE) and emitted power [3].

The next segments of the paper are ordered as follows: system model is defined in section II where the uplink and downlink system models and channel estimation model are listed as subtitles. Section III is the exponential correlation model where the channel spatial correlation is described in details. Afterword, the uplink and downlink data transmission is explained in section IV and section V where the spectral and energy efficiency numerical illustrations are shown. Finally, the last section of this paper is the conclusion where our views are wrapped up.

II. System Model

In this paper we are mainly studying energy efficiency and spectral efficiency bounds for UL and DL data transmission. The model of our system consists of single base station with large number of antennas. Base station terminal sends and receives data from a user terminal as presented in Fig 1. The protocol that is used between the two terminals of our system is TDD as shown in Fig 2, where we are able to increase the number of BS antennas to any desired value because the accuracy of channel estimation is independent of the number of base station antennas [18].

A. Uplink System Model

Due to the channel reciprocity we are able to maintain continues CSI to detect uplink data information [19]. Between the two terminals there is Rayleigh block fading $\mathbf{x} \sim \mathcal{CN}\ (\mathbf{0}, \mathbf{R})$, where the channel represented as $\mathbf{h}$ and the channel covariance matrix $\mathbf{R}$ denoted as

$$\mathbf{R} = \mathbb{E}\{\mathbf{h}\mathbf{h}^{\mathrm{H}}\} \quad (1)$$

We assume that the statistical distribution of the channel is known by the BS where the channel estimation in the system model is pilot based. Equation (2) represents the received signal $\mathbf{y}$ at the BS as follows

$$\mathbf{y} = \mathbf{h}d + \boldsymbol{n} \quad (2)$$

$$p = \mathbb{E}\{|d|^2\} \quad (3)$$

In equation (2) the received signal $d \in \mathbb{C}$ and it could be either pilot signal or data signal and the average power is represented in (3). The following equation denotes the noise $\boldsymbol{n}$ that is a combination of two terms

$$\boldsymbol{n} = \boldsymbol{n}_{\mathrm{noise}} + \boldsymbol{n}_{\mathrm{if}} \quad (4)$$

where $\boldsymbol{n}_{\mathrm{if}}$ represents other transmissions interference noise and $\boldsymbol{n}_{\mathrm{noise}}$ denotes the independent receiver noise that has $(\sigma^2_{BS}\mathbf{I})$ covariance and zero mean. For the interference noise $\boldsymbol{n}_{\mathrm{if}}$, it is assumed that it has zero mean and its covariance represented as $\mathbb{E}\{\boldsymbol{n}_{\mathrm{if}}\boldsymbol{n}_{\mathrm{if}}^{\mathrm{H}}\}$. The conditional covariance matrix with a channel realization of $\boldsymbol{\mathcal{H}}$ is represented as follows

$$\boldsymbol{Q}_{\boldsymbol{\mathcal{H}}} = \mathbb{E}\{\boldsymbol{n}_{\mathrm{if}}\boldsymbol{n}_{\mathrm{if}}^{\mathrm{H}}|\boldsymbol{\mathcal{H}}\} \quad (5)$$

In our system analysis we are assuming that for $\mathbf{R}$ we have uniformly bounded spectral norm independently to the number of BS antennas.

B. Downlink System Model

For the channel estimators that are based on pilot we use downlink channel as shown in Fig. 1. The received downlink signal is flat fading channel that can be represented as follows

$$\mathbf{z} = \mathbf{h}^{\mathrm{T}}\mathbf{s} + \boldsymbol{v} \quad (6)$$

where $\mathbf{s} \in \mathbb{C}^{\mathrm{Nx1}}$ and it could be either pilot signal or data signal that is stochastic and has zero mean.

The covariance matrix of the signal $\mathbf{s}$ is $\mathbf{W} = \mathbb{E}\{\mathbf{s}\mathbf{s}^{\boldsymbol{H}}\}$ and the average power is the trace of $\mathbf{W}$. On the other hand, the additive term $\boldsymbol{v}$ is the noise and it is a combination of two terms

$$\boldsymbol{v} = \boldsymbol{v}_{\mathrm{noise}} + \boldsymbol{v}_{\mathrm{if}} \quad (7)$$

where $\boldsymbol{v}_{\mathrm{if}}$ is interference noise and $\boldsymbol{v}_{\mathrm{noise}}$ denotes the independent receiver noise.

C. LMMSE Uplink Channel Estimation

In our work we used linear minimum mean square error (LMMSE) where we compare the received signal with the identified uplink pilot signal. The following equation represents LMMSE estimator of the channel realization

$$\hat{\mathbf{h}} = d^{*}\mathbf{R}\overline{\mathbf{Y}}^{-1}\boldsymbol{y} \quad (8)$$

where d is the known pilot signal. The value of user equipment power (p^{UE}) equals to $|d|^2$. The covariance matrix of the received signal $\mathbf{y}$ consists of a combination of several terms including average power of user equipment, covariance channel matrix and the noise

$$\overline{\mathbf{Y}} = \mathbb{E}\{\,\mathbf{y}\mathbf{y}^{\mathrm{H}}\} = p^{UE}\mathbf{R} + \mathbf{S} + \sigma^2_{BS}\mathbf{I} \quad (9)$$

$$\mathbf{C} = \mathbb{E}\left\{\left(\,\hat{\mathbf{h}} - \mathbf{h}\right)\left(\,\hat{\mathbf{h}} - \mathbf{h}\right)^{\boldsymbol{H}}\right\} = \mathbf{R} - p^{UE}\mathbf{R}\overline{\mathbf{Y}}^{-1}\mathbf{R} \quad (10)$$

The total value of mean square error can be derived based on the value of **C** in (10) as follows

$$\mathbf{MSE} = \mathbb{E}\left\{ \left\|\hat{\mathbf{h}} - \mathbf{h}\right\|_2^2 \right\} = \mathbf{tr}(\mathbf{C}) \tag{11}$$

Based on (11) we can represent the channel as a combination of two terms includes $\hat{\mathbf{h}}$ which is the LMMSE estimate value and the unknown estimate error $\boldsymbol{\epsilon}$ where the channel can be represented as follows

$$\mathbf{h} = \hat{\mathbf{h}} + \boldsymbol{\epsilon} \tag{12}$$

III. Exponential Correlation Model

The exponential correlation is a channel covariance model which can be implemented to create channel covariance matrix [16]. It is assumed in this model that **R** consists of two elements (i, j) as represented in the following equation

$$[\mathbf{R}] = \begin{cases} \delta r^{j-i}, & i \leq j \\ \delta (r^{j-i})^*, & i > j \end{cases} \tag{13}$$

where δ is a factor that is used for scaling and r is the correlation factor for the adjoining subchannels.

The value of correlation factor r is limited between 0 and 1 while the angle of arrival and departure is $\angle r$. The exponential correlation model might not be the most accurate model to create the channel covariance matrix but it is still easy to be implemented [20]. The value of correlation factor $|r|$ represents **R** eigenvalue spread while $\angle r$ denotes the eigenvectors for **R**. We are assuming that r is a real value since its angle has no effect on the mean square error. The increase in correlation factor affects the spectral efficiency in a similar way of decreasing the signal to noise ratio.

IV. Downlink and Uplink Data Transmission

For our analysis we study the channel capacity using TDD protocol that is shown in Fig. 2. We derive the lower capacity of the uplink and downlink data transmission and see the impact of the exponential correlation model. The lower capacity bound is studied based on imperfect knowledge of **h** where we used pilot based estimator (LMMSE). The imperfect knowledge of CSI in BS and user equipment (UE) terminals are denoted as $\mathcal{H}^{\mathrm{BS}}$ and $\mathcal{H}^{\mathrm{UE}}$ respectively, while $\mathcal{H}$ is the actual state of the channel. The downlink capacity could be expressed as

$$\mathrm{C}^{\mathrm{DL}} = \frac{T_{\mathrm{data}}^{\mathrm{DL}}}{\mathrm{T}_{cohr}} \mathbb{E}\left\{ \max_{f\left(\mathbf{s}\middle|\mathcal{H}^{\mathrm{BS}}\right):\mathbb{E}\{\|\mathbf{s}\|_2^2\}\leq p^{BS}} \mathcal{I}\left(\mathbf{s};\mathbf{z}\middle|\mathcal{H},\mathcal{H}^{\mathrm{BS}},\mathcal{H}^{\mathrm{UE}}\right)\right\} \tag{14}$$

where the mutual information for the signal that is received **z** and the signal of data s for $\mathcal{H}, \mathcal{H}^{\mathrm{BS}}$ and $\mathcal{H}^{\mathrm{UE}}$ is denoted as $\mathcal{I}(\mathbf{s};\mathbf{z}|\mathcal{H},\mathcal{H}^{\mathrm{BS}},\mathcal{H}^{\mathrm{UE}})$. On the other hand, the capacity for uplink system can be derived as follows

$$\mathrm{C}^{\mathrm{UL}} = \frac{T_{\mathrm{data}}^{\mathrm{UL}}}{\mathrm{T}_{cohr}} \mathbb{E}\left\{ \max_{f\left(d\middle|\mathcal{H}^{\mathrm{UE}}\right):\mathbb{E}\{\|d\|_2^2\}\leq p^{UE}} \mathcal{I}\left(d;\mathbf{y}\middle|\mathcal{H},\mathcal{H}^{\mathrm{BS}},\mathcal{H}^{\mathrm{UE}}\right)\right\} \tag{15}$$

The main point in this section is to study the behavior of the capacity bounds when the correlation factor goes from 0 to 1 which gives us an idea of how the exponential correlation factor would affect the capacity bounds.

A. Lower Limits of Channel Capacity

For the lower bound capacity, we are assuming that we have Gaussian noise in the interference and for the downlink we assume that we use single stream. Furthermore, we use channel estimator based on pilot and due to maximizing Gaussian distribution we have uncertain channel state information for uplink and downlink.

Based on (14) and (15) and by using (18) and (19), DL and UL capacities are represented as

$$\mathrm{C}^{\mathrm{DL}} \geq \mathrm{C}_{lower}^{DL} = \frac{T_{\mathrm{data}}^{\mathrm{DL}}}{\mathrm{T}_{cohr}} \mathbb{E}\{\log_2(1 + \mathrm{SINR}_{lower}^{DL}(\mathbf{v}^{DL}))\} \tag{16}$$

$$\mathrm{C}^{\mathrm{UL}} \geq \mathrm{C}_{lower}^{UL} = \frac{T_{\mathrm{data}}^{\mathrm{UL}}}{\mathrm{T}_{cohr}} \mathbb{E}\{\log_2(1 + \mathrm{SINR}_{lower}^{UL}(\mathbf{v}^{UL}))\} \tag{17}$$

where the vectors $\mathbf{v}^{DL}$ and $\mathbf{v}^{UL}$ represent beamforming and receive combining respectively. Both vectors are having unit norm and they are a function of $\hat{\mathbf{h}}$.

$$\mathrm{SINR}_{low}^{\mathrm{DL}}(\mathrm{v}^{\mathrm{DL}}) = \frac{\left|\mathbb{E}\{\mathrm{h}^H \mathrm{v}^{\mathrm{DL}}|\widetilde{\mathcal{H}}^{\mathrm{UE}}\}\right|^2}{\left\{\left|\mathrm{h}^H \mathrm{v}^{\mathrm{DL}}\right|^2|\widetilde{\mathcal{H}}^{\mathrm{UE}}\right\} - \left|\mathbb{E}\{\mathrm{h}^H \mathrm{v}^{\mathrm{DL}}|\widetilde{\mathcal{H}}^{\mathrm{UE}}\}\right|^2 + \frac{\mathbb{E}\left\{I_{\mathcal{H}}^{UE}|\widetilde{\mathcal{H}}^{\mathrm{UE}}\right\} + \sigma_{\mathrm{UE}}^2}{p^{BS}}} \tag{18}$$

$$\mathrm{SINR}_{low}^{\mathrm{UL}}(\mathrm{v}^{\mathrm{UL}}) = \frac{\left|\mathbb{E}\{\mathrm{h}^H \mathrm{v}^{\mathrm{UL}}|\widetilde{\mathcal{H}}^{\mathrm{BS}}\}\right|^2}{\left\{\left|\mathrm{h}^H \mathrm{v}^{\mathrm{UL}}\right|^2|\widetilde{\mathcal{H}}^{\mathrm{BS}}\right\} - \left|\mathbb{E}\{\mathrm{h}^H \mathrm{v}^{\mathrm{UL}}|\widetilde{\mathcal{H}}^{\mathrm{BS}}\}\right|^2 + \frac{\mathbb{E}\{(\mathrm{v}^{\mathrm{UL}})^H(\mathrm{Q}_{\mathcal{H}} + \sigma_{\mathrm{BS}}^2 \mathrm{I})\mathrm{v}^{\mathrm{UL}}|\widetilde{\mathcal{H}}^{\mathrm{BS}}\}}{p^{UE}}} \tag{19}$$

B. Simulation Results

Our numerical illustrations are conducted to see the behavior of the capacity limits based on different values of correlation factor. The average SNR for uplink and downlink channel are $p^{\mathrm{UE}}\frac{\mathrm{tr}(\mathbf{R})}{N\sigma_{\mathrm{BS}}^2}$ and $p^{\mathrm{BS}}\frac{\mathrm{tr}(\mathbf{R})}{N\sigma_{\mathrm{UE}}^2}$, respectively. We take into consideration the value of SNR where we use two different values 0 dB and 30 dB. We assume that the values of uplink and downlink data percentage are equal to 0.45 and by making this assumption we get identical capacities for both cases. Fig. 3 considers a scenario with SNR equals to 0 dB and number of antennas N equals to 50 and 200 in the BS terminal. The figure shows spectral efficiency, with a unit of (bit/channel use), versus the exponential correlation factor. The maximum value of the spectral efficiency is reached when we have zero correlation, which means having completely independent subchannels.

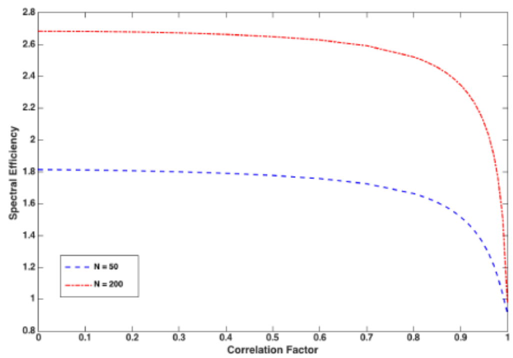

Fig. 3. Spectral efficiency versus exponential correlation factor with signal to noise ratio equals to 0 dB.

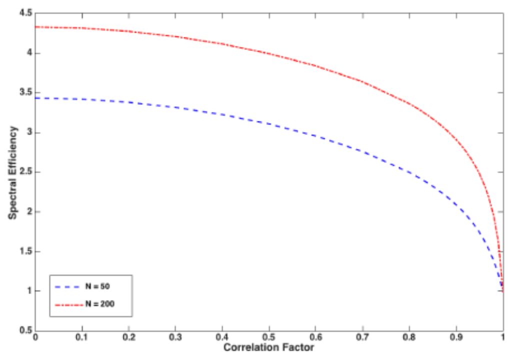

Fig. 4. Spectral efficiency versus exponential correlation factor with signal to noise ratio equals to 30 dB.

The bounds of spectral efficiency keep decreasing when we increase the correlation factor until we get to correlation factor of 1 where we have the worst channel capacity. Also, we can see that at larger number of BS antennas we have higher channel capacity.

Fig. 4 shows similar scenario as in Fig. 3 except that the SNR value equals to 30 dB. The capacity limits are much higher compared to the limits in Fig. 3 due to using larger SNR. We can also observe that the capacity behavior has better performance when we have larger number of antennas in the BS terminal. It is obvious that the spectral efficiency is more sensitive to the change of exponential correlation factor.

V. Energy Efficiency

Energy efficiency can be expressed as the ratio between spectral efficiency and emitted power and it is measured in (bit/Joule). The transmit power in (Joule/channel use) is represented as the energy consumed by the amplifier divided by the coherence time. The following equations (20) and (21) represent uplink and downlink transmit power respectively

$$\left(\frac{\mathrm{E}_{amp}}{\mathrm{T}_{cohr}}\right)_{UL} = \alpha_{UL}\left(\frac{T^{\mathrm{DL}}_{\mathrm{pilot}}}{\mathrm{T}_{cohr}}\frac{p^{BS}}{\omega^{BS}} + \frac{T^{\mathrm{UL}}_{\mathrm{pilot}}}{\mathrm{T}_{cohr}}\frac{p^{UE}}{\omega^{UE}}\right) + \frac{T^{\mathrm{UL}}_{\mathrm{pilot}}}{\mathrm{T}_{cohr}}\frac{p^{UE}}{\omega^{UE}} \quad (20)$$

$$\left(\frac{\mathrm{E}_{amp}}{\mathrm{T}_{cohr}}\right)_{DL} = \alpha_{DL}\left(\frac{T^{\mathrm{DL}}_{\mathrm{pilot}}}{\mathrm{T}_{cohr}}\frac{p^{BS}}{\omega^{BS}} + \frac{T^{\mathrm{UL}}_{\mathrm{pilot}}}{\mathrm{T}_{cohr}}\frac{p^{UE}}{\omega^{UE}}\right) + \frac{T^{\mathrm{DL}}_{\mathrm{pilot}}}{\mathrm{T}_{cohr}}\frac{p^{BS}}{\omega^{BS}} \quad (21)$$

where ω^{BS} and ω^{UE} are the power efficiency of the amplifiers at the two terminals where they are bounded from 0 to 1. The uplink and downlink ratios that are used in the previous equations can be interpreted as follows

$$\alpha_{UL} = \frac{T^{\mathrm{UL}}_{\mathrm{data}}}{T^{\mathrm{DL}}_{\mathrm{data}} + T^{\mathrm{UL}}_{\mathrm{data}}} \quad (22)$$

$$\alpha_{DL} = \frac{T^{\mathrm{DL}}_{\mathrm{data}}}{T^{\mathrm{DL}}_{\mathrm{data}} + T^{\mathrm{UL}}_{\mathrm{data}}} \quad (23)$$

The energy efficiency can be represented as a ratio between capacity and consumed power as the following equations show

$$EE^{UL} = \frac{\mathrm{C}^{UL}}{\left(\frac{T^{\mathrm{DL}}_{\mathrm{pilot}}\, p^{BS}}{\mathrm{T}_{cohr}\,\omega^{BS}} + \frac{T^{\mathrm{UL}}_{\mathrm{pilot}}\, p^{UE}}{\mathrm{T}_{cohr}\,\omega^{UE}} + N\rho + \zeta\right) + \frac{T^{\mathrm{UL}}_{\mathrm{pilot}}\, p^{UE}}{\mathrm{T}_{cohr}\,\omega^{UE}}} \quad (24)$$

$$EE^{DL} = \frac{\mathrm{C}^{DL}}{\left(\frac{T^{\mathrm{DL}}_{\mathrm{pilot}}\, p^{BS}}{\mathrm{T}_{cohr}\,\omega^{BS}} + \frac{T^{\mathrm{UL}}_{\mathrm{pilot}}\, p^{UE}}{\mathrm{T}_{cohr}\,\omega^{UE}} + N\rho + \zeta\right) + \frac{T^{\mathrm{DL}}_{\mathrm{pilot}}\, p^{BS}}{\mathrm{T}_{cohr}\,\omega^{BS}}} \quad (25)$$

The previous equations represent the uplink and downlink energy efficiency respectively where ρ is the circuit power and ζ is the static circuit power.

A. *Simulation Results*

Our numerical illustrations show how the energy efficiency behavior would be affected by the exponential correlation factor. We choose to have 0 splitting between ρ and ζ, also we consider 0.02×10^{-6} (Joule/channel use) for $\rho+\zeta$. In our simulation, to have identical uplink and downlink energy efficiency we let $\alpha_{UL} = \alpha_{DL} = 0.5$.

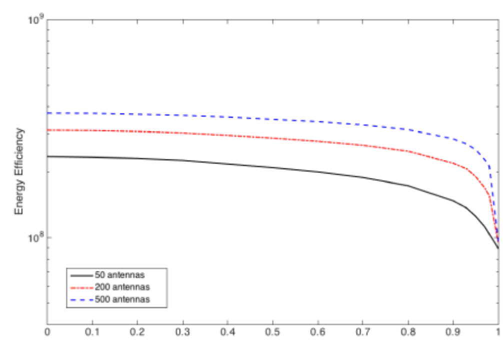

Fig. 5. Energy efficiency as a function of exponential correlation factor with signal to noise ratio equals to 20 dB

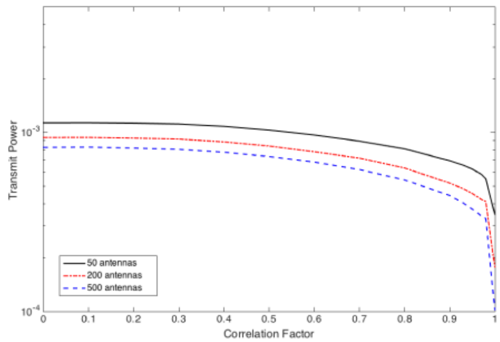

Fig. 6. Transmit power as a function of exponential correlation factor with signal to noise ratio equals to 20 dB

Fig. 5 demonstrates energy efficiency (in bit/Joule) with SNR equals to 20 dB. We can see three curves each one indicates different base station antenna numbers where the scenario of having 500 antennas gives us the highest energy efficiency while we have the lowest energy efficiency by using 50 antennas. Also, it is noticeable that the highest energy efficiency occurred when the correlation factor is 0 and it decreases gradually until we get the lowest energy efficiency at 1 correlation factor. Fig. 6 shows transmit power (in *u* Joule/channel use) with SNR equals to 20 dB. We can see three curves each one represents different number of BS antennas. We can realize that the highest transmit power is happening when the number of BS antennas is 50 while the lowest transmit power is occurring when we have 500 antennas in the base station. Also, it is clear that the highest transmit power occurred when the correlation factor is 0 and it decreases regularly until we get the lowest transmit power at 1 correlation factor.

VI. Conclusion

Massive MIMO as a promising technology can develop the spectral efficiency and energy efficiency due to the enhanced spatial correlation. In our paper we investigated the effect of exponential correlation model on the performance of the energy efficiency and spectral efficiency where we used a massive MIMO system with a large number of BS antennas and single antenna in the user equipment terminal. By using pilot-based channel estimator we generated the lower bounds of the channel capacity where we noticed that the capacity is more sensitive to the correlation factor variation when using higher SNR. In terms of transmit power, when we are using higher number of base station antennas we have lower transmit power and vise versa. Also, it is observed that we have higher energy efficiency when we use higher number of BS antennas.

References

[1] T. L. Marzetta, "Massive MIMO: An introduction," *Bell Labs Tech. J.*, vol. 20, pp. 11–22, 2015.

[2] J. Andrews, S. Buzzi, W. Choi, S. Hanly, A. Lozano, A. Soong, and J. C. Zhang, "What will 5G be?," *IEEE J. Sel. Areas Commun.*, vol. 32, no. 6, pp. 1065–1082, 2014.

[3] H. Q. Ngo, E. G. Larsson, and T. L. Marzetta, "Energy and spectral efficiency of very large multiuser MIMO systems," *IEEE Trans. Commun.*, vol. 61, no. 4, pp. 1436–1449, 2013.

[4] E. Bjornson, J. Hoydis, M. Kountouris, and M. Debbah, "Massive MIMO systems with non-ideal hardware: Energy efficiency, estimation, and capacity limits," *IEEE Trans. Inf. Theory*, vol. 60, no. 11, pp. 7112–7139, 2014.

[5] E. Bjornson, E. G. Larsson, and T. L. Marzetta, "Massive MIMO: ten myths and one critical question," *IEEE Commun. Mag.*, vol. 54, no. 2, pp. 114–123, 2016.

[6] F. Boccardi and T. L. Marzetta, "Five disruptive technology directions for 5G," *IEEE Commun. Mag.*, vol. 52, no. 2, pp. 74–80, 2014.

[7] G. Caire, N. Jindal, M. Kobayashi, and N. Ravindran, "Multiuser MIMO achievable rates with downlink training and channel state feedback," *IEEE Trans. Inf. Theory*, vol. 56, no. 6, pp. 2845–2866, 2010.

[8] X. Gao, O. Edfors, F. Rusek, and F. Tufvesson, "Linear pre-coding performance in measured very-large MIMO channels," *IEEE Veh. Technol. Conf. (VTC Fall)*, pp. 1–5, 2011.

[9] E. Larsson, O. Edfors, F. Tufvesson, and T. Marzetta, "Massive MIMO for next generation wireless systems," *IEEE Commun. Mag.*, vol. 52, no. 2, pp. 186–195, 2014.

[10] D. Persson, B. K. Lau, and E. G. Larsson, "Scaling Up MIMO: Opportunities and challenges with very large arrays," *IEEE Signal Process. Mag.*, vol. 30, no. 1, pp. 40–60, 2012.

[11] A. Alshammari, S. Albdran, M. Ahad, and M. Matin, "Impact of Angular Spread on Massive MIMO Channel Estimation," in *The 19th International Conference on Computer and Information Technology*, in press, 2016.

[12] J. Hoydis, C. Hoek, T. Wild, and S. ten Brink, "Channel measurements for large antenna arrays," *2012 Int. Symp. Wirel. Commun. Syst.*, pp. 811–815, 2012.

[13] S. Albdran, A. Alshammari, M. Ahad, and M. Matin, "Effect of Exponential Correlation Model on Channel Estimation for Massive MIMO," in *The 19th International Conference on Computer and Information Technology*, in press, 2016.

[14] A. Assalini, E. Dall'Anese, and S. Pupolin, "On the robustness of MIMO LMMSE channel estimation," *IEEE Trans. Wirel. Commun.*, vol. 9, no. 11, pp. 3313–3319, 2010.

[15] M. Médard, "The effect upon channel capacity in wireless communications of perfect and imperfect knowledge of the channel," *IEEE Trans. Inf. Theory*, vol. 46, no. 3, pp. 933–946, 2000.

[16] S. L. Loyka, "Channel capacity of MIMO architecture using the exponential correlation matrix," *IEEE Commun. Lett.*, vol. 5, no. 9, pp. 369–371, 2001.

[17] D. Bethanabhotla, O. Y. Bursalioglu, H. C. Papadopoulos, and G. Caire, "Optimal User-Cell Association for Massive MIMO Wireless Networks," *IEEE Trans. Wirel. Commun.*, vol. 15, no. 3, pp. 1835–1850, 2016.

[18] E. Björnson, "Hardware impairments in Large-scale MISO systems : Energy efficiency , estimation , and capacity limits," *18th Int. Conf. Digit. Signal Process.*, pp. 1–6, 2013.

[19] T. L. Marzetta, "Noncooperative cellular wireless with unlimited numbers of base station antennas," *IEEE Trans. Wirel. Commun.*, vol. 9, no. 11, pp. 3590–3600, 2010.

[20] C. C. Martin, J. H. Winters, N. R. Sollenberger, S. Drive, and R. Bank, "Multiple-Input Multiple-Output (MIMO) radio channel measurements," *IEEE Antennas Propag. Soc. Int. Symp.*, vol. 1, pp. 418–421, 2001.

International Journal of Computer Science and Information Security (IJCSIS),
Vol. 15, No. 6, June 2017

Spatial Correlation Influence on The Channel Estimation and Spectral Efficiency for Massive MIMO Systems

Saleh Albdran, Ahmed Alshammari, and Mohammad Matin

***Abstract*— The need for more wireless communication will keep increasing while there is limited electromagnetic spectrum. To meet this demand, new clever and efficient technologies need to be implemented. Massive MIMO as a new technology would improve the data throughput due to the enhanced spatial correlation. By deploying exponential correlation model, the impact of the channel spatial correlation on the energy and spectral efficiencies of massive MIMO is studied. This paper investigates a system model that has a base station (BS) with a large number of antennas and one user equipment with multiple antennas. The linear minimum mean square error (LMMSE) is used as pilot based estimator to create the lower capacity limits. Also, the influence of the channel spatial correlation on the estimation accuracy is investigated. Several scenarios are applied by adding different base station antenna numbers and several values of user terminal antennas. The spectral efficiency tends to be sensitive to the variation of correlation factor in the case of using higher signal to noise ratio (SNR). It is observed that the system is more energy efficient with higher number of antennas in the base station. Moreover, the spectral efficiency is getting higher with greater number of antennas in the user equipment.**

***Index Terms*— base station; massive MIMO; user equipment; channel state information; spatial correlation**

I. Introduction

DURING the previous decade, the demand for wireless data traffic has been increasing rapidly while the available electromagnetic spectrum is limited [1]. This high demand will keep growing due to the large growth in the number of smart phones and tablet devices [2]. By 2020, it is forecasted that the mobile data traffic will surpass 30 Exabyte a month while it was 6.2 Exabyte a month in 2016 [3]. The number of connections and mobile devices are expected to increase also from 7.9 billion in 2016 to more than 11.6 billion by 2020.

It is necessary to increase the wireless throughput by applying efficient new technologies that can be implemented in reality [4], [5]. The wireless spectral efficiency depends on several factors such as channel estimation accuracy, spatial correlation, SNR and resources of signal processing [6]. The implementation of multiple antennas in the BS is significantly affective approach to enhance the wireless system and improve its spectral efficiency [7]. The multiple input multiple output (MIMO) is engaged into several wireless standers such as LTE-Advanced [8], [9]. One of the improved shape of this technology is Multiuser MIMO where the base station is equipped with multiple antennas and serves multiple users simultaneously where each user has single antenna [8]. This method has its own problems such as multiusers interference and channel state information (CSI) acquisition.

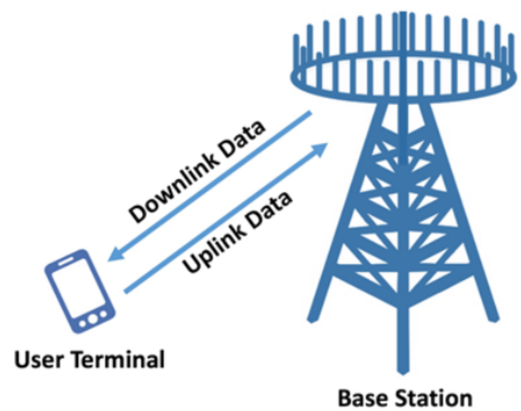

Fig. 1. Wireless channel between the BS and the user terminal for uplink and downlink.

The ultimate form of multiple antennas technology is called Massive MIMO [10]. The proposed concept of massive MIMO is based on equipping the base station (BS) by hundreds of antenna arrays which is much larger than the number of user terminals. Theoretically, massive MIMO can provide higher capacity that can be increased by simply having more antennas at the BS [1]. Also, the large number of antennas in the BS can reduce the transmit power for uplink and downlink transmissions. Moreover, because of the channel reciprocity, the overhead pilot sequences are linearly related to the number of user terminals and have nothing to do with the number of antennas in the BS. Since the number of BS antennas is higher than the users, the channel estimation will be more accurate and the signal processing will be simpler [11]. The great number of BS antennas would increase the energy efficiency since the antenna beam is focused sharply into limited area. Thus, each user would only receive the intended signal with the lowest amount of interference from other nearby channels [12].

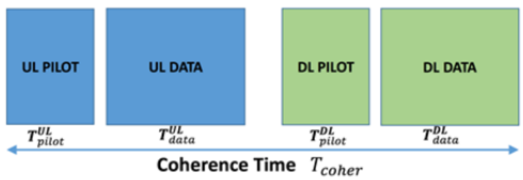

Fig. 2. Time division duplixing system that has coherence time divided into several stages for UL and DL.

Massive MIMO depends on measuring the channel frequency response where either the BS terminal or the user terminal sends known training signals and the receiver can estimate frequency response [13], [14]. The environment of the channels spatial correlation can affect the accuracy of the estimated channel [7]. To have accurate CSI, the system should operates in time division duplexing mode (TDD) [7], [15]. As shown in Fig. 2, the TDD system divides the coherence time into several periods for uplink and downlink signals. There are several benefits by applying TDD mode, one of them is having more accurate channel estimation if there is a good knowledge of the channel correlation structure [16]. Also in the TDD systems, it is possible to escalate the number of BS antennas to any wanted value since it has no impact on the accuracy of channel estimator.

The spectral efficiency can be affected by different factors, one of them is the accuracy of channel estimation [17], [18]. Depending on the technique of channel estimation, it is possible to get the channel capacity for uplink and downlink data transmission. Channel state information precision is a significant factor that would affect the calculation of the channel capacity [19], [20]. After getting the spectral efficiency, it is possible to derive the energy efficiency which is the ratio between the emitted power and the spectral efficiency [21]. The transmit power can be interpreted as the ratio between the consumed energy by the amplifier and the coherence time.

Notation: in this paper. The column vectors are represented in lower case bold like $\mathbf{x}$. On the other hand, the bold upper case is a representation of matrices such as $\mathbf{X}$. For matrix $\mathbf{X}$, the transpose is represented as $\mathbf{X}^{\mathbf{T}}$, the conjugate is $\mathbf{X}^{*}$ and the transpose of the conjugate is represented as $\mathbf{X}^{\mathbf{H}}$. $\mathbb{E}\{\mathbf{x}\}$ is a representation of the expected value of $\mathbf{x}$, while $\mathbb{E}\{\mathbf{x}|\mathbf{y}\}$ represents the expected conditional value of $\mathbf{x}$ with respect to $\mathbf{y}$.

The upcoming sections of this paper are arranged as follows: the system architecture is explained in section II, in which the system models of UL and DL and exponential correlation model are included as subsections. Section III includes the LMMSE channel estimator which is explained in details. Furthermore, the spectral efficiency for uplink and downlink is described in section IV in which part of the simulation results is shown. Section V is the energy efficiency and the transmit power where the numerical illustrations are displayed. Finally, section VI is the conclusion of this paper.

II. System Architecture

In this paper, it is taking into consideration a single cell system model that is based on TDD. Since the accuracy of the channel estimation is not depending on the number of BS antennas N, it is possible to reach any desired number of N. The base station has N antennas and sends signals to single user terminal as shown in Fig. 1. It is assumed that the channel for uplink and downlink is spatially correlated using exponential correlation model. Channel estimation accuracy is studied using pilot based LMMSE. Also, the spectral and energy efficiencies are investigated for UL and DL data transmission.

A. Uplink and Downlink System Models

To detect the uplink data transmission, the channel reciprocity is playing a significant role that provide the system with continues CSI [10]. Between the BS terminal and the UE terminal we have Rayleigh block fading $\mathbf{x} \sim \mathcal{CN}\,(\mathbf{0}, \mathbf{R})$, where $\mathbf{R}$ as a channel covariance matrix can be represented as

$$\mathbf{R} = \mathbb{E}\{\mathbf{h}\mathbf{h}^{\mathbf{H}}\} \tag{1}$$

where $\mathbf{h}$ represents the block-fading stochastic channel between the BS and the user equipment. It is assumed that the base station knows the channel statistical distribution where the system model has a pilot based channel estimator. The signal $\mathbf{y}$ that is received by the BS is denoted as

$$\mathbf{y} = \mathbf{h}d + \boldsymbol{n} \tag{2}$$

$$p = \mathbb{E}\{|d|^2\} \tag{3}$$

In the above equations, the received element is denoted as $d \in \mathbb{C}$ where it can be data or pilot signal. In equation (3), The uplink average power is shown. The received noise can be denoted as

$$\boldsymbol{n} = \boldsymbol{n}_{\text{noise}} + \boldsymbol{n}_{\text{if}} \tag{4}$$

where $\boldsymbol{n}$ is a combination of two terms, the first term is $\boldsymbol{n}_{\text{noise}}$ which represents the independent received noise with zero mean and covariance of $(\sigma_{BS}^2 \mathbf{I})$. The second term is $\boldsymbol{n}_{\text{if}}$ which is the interference noise from adjacent transmissions and it has mean equals to zero and covariance equals to $\mathbb{E}\{\boldsymbol{n}_{\text{if}}\boldsymbol{n}_{\text{if}}^{\text{H}}\}$. With a channel realization $\boldsymbol{\mathcal{H}}$, the conditional covariance matrix can be shown as follows

$$\boldsymbol{Q}_{\mathcal{H}} = \mathbb{E}\{\boldsymbol{n}_{\text{if}}\boldsymbol{n}_{\text{if}}^{\text{H}}|\boldsymbol{\mathcal{H}}\} \tag{5}$$

We assumed in this investigation that for the channel covariance matrix $\mathbf{R}$, independent to the number of BS antennas, there is spectral norm that is uniformly bounded. For the downlink system model there is a flat fading for the received channel that can be represented as

$$\mathbf{z} = \mathbf{h}^{\mathrm{T}}\mathbf{s} + \boldsymbol{v} \tag{6}$$

$$\boldsymbol{v} = \boldsymbol{v}_{\text{noise}} + \boldsymbol{v}_{\text{if}} \tag{7}$$

where $\boldsymbol{v}$ is the noise and $\mathbf{s} \in \mathbb{C}^{\text{Nx1}}$ is the received signal that has zero mean and a covariance matrix $\mathbb{E}\{\boldsymbol{s}\boldsymbol{s}^{\boldsymbol{H}}\}$ where the average power of $\boldsymbol{v}$ is the trace of the covariance matrix of $\mathbf{s}$. The noise $\boldsymbol{v}$ is a combination of two components, the first one is the independent received noise and the second one is the interference noise.

B. *Exponential Correlation Model*

To create the channel covariance matrix, the exponential correlation model is utilized [22]. It is supposed that there are two elements *(i, j)* for the channel covariance $\mathbf{R}$ and can be peresented as follows

$$[\mathbf{R}] = \begin{cases} \delta r^{j-i}, & i \leq j \\ \delta (r^{j-i})^{*}, & i > j \end{cases} \tag{8}$$

where r represents the adjacent channel correlation factor while the scaling factor is denoted by δ. The component r is bounded between 0 to 1 and the component $\angle r$ denotes the angle of arraival or departure. The exponential correlation model that is used to create the covariance matrix may not be the most exact model for real-world implemontations, yet it is simple to be implemented [23]. The spread of eigenvalue of $\mathbf{R}$ is represented as $|r|$ while the eigenvectors of $\mathbf{R}$ is denoted as $\angle r$. In our system it is assumed that the value of r is real since mean square error is not affected by the angle of r.

III. LMMSE Channel Estimator

The least minimum mean square error (LMMSE) estimator is applied for the UL channel etimation in which received signal is compared to the defined uplink pilot signal [24]. For the channel relization, the LMMSE estimator is defined as

$$\hat{\mathbf{h}} = d^{*}\mathbf{R}\overline{\mathbf{Y}}^{-1}\boldsymbol{y} \tag{9}$$

where the identified pilot signal is denoted by d. The power in the user terminal (p^{UE}) can be represented as $|d|^{2}$. For the received signal $\mathbf{y}$, its covariance matrix consists of few terms such as covariance channel matrix, user equipment average power, and the noise

$$\overline{\mathbf{Y}} = \mathbb{E}\{\,\mathbf{y}\mathbf{y}^{\mathrm{H}}\} = p^{UE}\mathbf{R} + \mathbf{S} + \sigma_{BS}^{2}\mathbf{I} \tag{10}$$

$$\mathbf{C} = \mathbb{E}\left\{\left(\hat{\mathbf{h}} - \mathbf{h}\right)\left(\hat{\mathbf{h}} - \mathbf{h}\right)^{H}\right\} = \mathbf{R} - p^{UE}\mathbf{R}\overline{\mathbf{Y}}^{-1}\mathbf{R} \tag{11}$$

based on (11) where the value of $\mathbf{C}$ is shown, the mean square error total value can be represented as

$$\mathbf{MSE} = \mathbb{E}\left\{\left\|\hat{\mathbf{h}} - \mathbf{h}\right\|_{2}^{2}\right\} = \mathbf{tr(C)} \tag{12}$$

$$\mathbf{h} = \hat{\mathbf{h}} + \boldsymbol{\epsilon} \tag{13}$$

where the channel $\mathbf{h}$ is represented in terms of the LMMSE estimate $\hat{\mathbf{h}}$ and the unknown estimate error $\boldsymbol{\epsilon}$.

A. *Simulation Results*

The numerical illustrations for the channel estimation are conducted to analyze the accuracy of the LMMSE estimator. The relationship between the mean square error and the trace of the channel covariance matrix $\mathbf{R}$ is called relative estimation error and can be represented as

$$\text{MSE}_{relative} = \frac{\text{MSE}}{\text{tr}(\mathbf{R})} \tag{14}$$

The estimation error per antenna versus exponential correlation factor is show in Fig. 3. The exponential correlation model is applied to create the channel covariance matrix with 100 antennas in the BS. It is shown that the estimator is more accurate with higher values of signal to noise ratio. Also, it is noticeable that the estimation accuracy is affected by correlation factor especially when correlation factor increases and goes to 1.

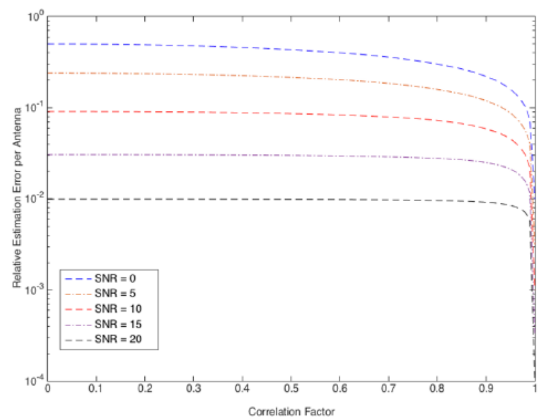

Fig. 3. Estimation error per antenna versus exponential correlation factor for LMMSE. The SNR values increased from 0 to 20 dB.

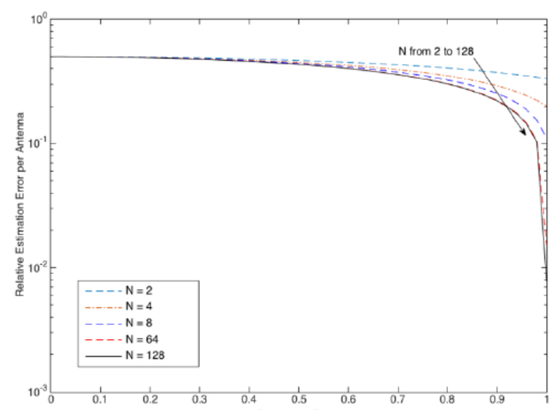

Fig. 4. Estimation error per antenna versus exponential correlation factor for LMMSE with different values of *N*.

The channel estimation error versus exponential correlation factor is show in Fig. 4. The covariance matrix of the channel is produced using exponential correlation model and the SNR equals to 30 dB. It is indicated that the channel estimation accuracy has slight improvement when the correlation factor is increasing and getting closer to 1. When the number of BS antennas is increased, there is a clear improvement at the beginning then there is no more improvement in the estimation accuracy by reaching large number of antennas.

IV. Spectral Efficiency for Uplink and Downlink

The channel capacity is examined by utilizing TDD mode which is displayed in Fig. 2. Mainly, lower spectral efficiency is going under investigation for uplink and downlink data transmission to understand the influence of using exponential correlation factor. The pilot based estimator (LMMSE) is used while the study of the lower capacity is depending on imperfect channel knowledge. The real channel state is denoted as $\mathcal{H}$ while $\mathcal{H}^{\mathrm{UE}}$ and $\mathcal{H}^{\mathrm{BS}}$ are the imperfect knowledge of channel state information for the user equipment and the base station respectively. The capacity for the downlink transmission can be demonstrated as follows

$$\mathrm{C}^{\mathrm{DL}} = \frac{T_{\mathrm{data}}^{\mathrm{DL}}}{\mathrm{T}_{cohr}} \mathbb{E}\left\{ \max_{f(\mathbf{s}|\mathcal{H}^{\mathrm{BS}}):\mathbb{E}\{\|\mathbf{s}\|_2^2\}\le p^{BS}} \mathcal{I}(\mathbf{s};\mathbf{z}|\mathcal{H},\mathcal{H}^{\mathrm{BS}},\mathcal{H}^{\mathrm{UE}}) \right\} \quad (15)$$

where $\mathcal{I}(\mathbf{s};\mathbf{z}|\mathcal{H},\mathcal{H}^{\mathrm{BS}},\mathcal{H}^{\mathrm{UE}})$ represents mutual information of the received and data signals for the actual state of the channel and the imperfect knowledge of the channel. Similarly, the uplink data transmission capacity can be expressed as

$$\mathrm{C}^{\mathrm{UL}} = \frac{T_{\mathrm{data}}^{\mathrm{UL}}}{\mathrm{T}_{cohr}} \mathbb{E}\left\{ \max_{f(d|\mathcal{H}^{\mathrm{UE}}):\mathbb{E}\{\|d\|_2^2\}\le p^{UE}} \mathcal{I}(d;\mathbf{y}|\mathcal{H},\mathcal{H}^{\mathrm{BS}},\mathcal{H}^{\mathrm{UE}}) \right\} \quad (16)$$

where $\mathcal{I}(d;\ \mathbf{y}|\mathcal{H},\mathcal{H}^{\mathrm{BS}},\mathcal{H}^{\mathrm{UE}})$ represents mutual information of the data signal and received signal for the actual state of the channel and the imperfect knowledge of the channel. The most important point of this section is to investigate the behavior of the spectral efficiency which may give an idea on the influence of using the exponential correlation model when it goes from 0 to 1.

A. Channel Capacity

It is assumed that the interference noise is Gaussian for the lower bound and assumed also the single stream is used for the downlink. The estimator is pilot based and the CSI for the UL and DL data are not certain because the Gaussian distribution is maximized. The SINR values for uplink and downlink are presented as follows

$$\mathrm{SINR}_{low}^{\mathrm{DL}}(\mathrm{v}^{\mathrm{DL}}) = \frac{\left|\mathbb{E}\{\mathrm{h}^{H}\mathrm{v}^{\mathrm{DL}}|\widehat{\mathcal{H}}^{\mathrm{UE}}\}\right|^2}{\left\{|\mathrm{h}^{H}\mathrm{v}^{\mathrm{DL}}|^2|\widehat{\mathcal{H}}^{\mathrm{UE}}\right\} - \left|\mathbb{E}\{\mathrm{h}^{H}\mathrm{v}^{\mathrm{DL}}|\widehat{\mathcal{H}}^{\mathrm{UE}}\}\right|^2 + \frac{\mathbb{E}\{I_{\mathcal{H}}^{UE}|\widehat{\mathcal{H}}^{\mathrm{UE}}\}+\sigma_{\mathrm{UE}}^2}{p^{BS}}} \quad (17)$$

$$\mathrm{SINR}_{low}^{\mathrm{UL}}(\mathrm{v}^{\mathrm{UL}}) = \frac{\left|\mathbb{E}\{\mathrm{h}^{H}\mathrm{v}^{\mathrm{UL}}|\widehat{\mathcal{H}}^{\mathrm{BS}}\}\right|^2}{\left\{|\mathrm{h}^{H}\mathrm{v}^{\mathrm{UL}}|^2|\widehat{\mathcal{H}}^{\mathrm{BS}}\right\} - \left|\mathbb{E}\{\mathrm{h}^{H}\mathrm{v}^{\mathrm{UL}}|\widehat{\mathcal{H}}^{\mathrm{BS}}\}\right|^2 + \frac{\mathbb{E}\{(\mathrm{v}^{\mathrm{UL}})^{H}(\mathrm{Q}_{\mathcal{H}}+\sigma_{\mathrm{BS}}^2\mathrm{I})\mathrm{v}^{\mathrm{UL}}|\widehat{\mathcal{H}}^{\mathrm{BS}}\}}{p^{UE}}} \quad (18)$$

By using (15) and (16) and based on (17) and (18), downlink and uplink capacity limits are denoted as

$$\mathrm{C}^{\mathrm{DL}} \ge \mathrm{C}_{lower}^{DL} = \frac{T_{\mathrm{data}}^{\mathrm{DL}}}{\mathrm{T}_{cohr}} \mathbb{E}\{\log_2(1+\mathrm{SINR}_{lower}^{DL}(\mathbf{v}^{DL}))\} \quad (19)$$

$$\mathrm{C}^{\mathrm{UL}} \ge \mathrm{C}_{lower}^{UL} = \frac{T_{\mathrm{data}}^{\mathrm{UL}}}{\mathrm{T}_{cohr}} \mathbb{E}\{\log_2(1+\mathrm{SINR}_{lower}^{UL}(\mathbf{v}^{UL}))\} \quad (20)$$

where the beamforming vector is denoted as $\mathbf{v}^{DL}$ and the receive combining vector is denoted as $\mathbf{v}^{UL}$. The vectors $\mathbf{v}^{DL}$ and $\mathbf{v}^{UL}$ are a function of $\hat{\mathbf{h}}$ and they have a unit norm.

B. Simulation Results

In this paper, the numerical results are conducted to study the behavior of the spectral efficiency. The exponential correlation model is applied to generate the channel covariance matrix. The average uplink and downlink signal to noise ratios are $p^{\mathrm{UE}}\frac{\mathrm{tr}(\mathbf{R})}{N\sigma_{\mathrm{BS}}^2}$ and $p^{\mathrm{BS}}\frac{\mathrm{tr}(\mathbf{R})}{N\sigma_{\mathrm{UE}}^2}$, respectively. To get identical capacities for uplink and downlink, It is assumed that the data percentage for UL and DL are identical (equal to 0.45).

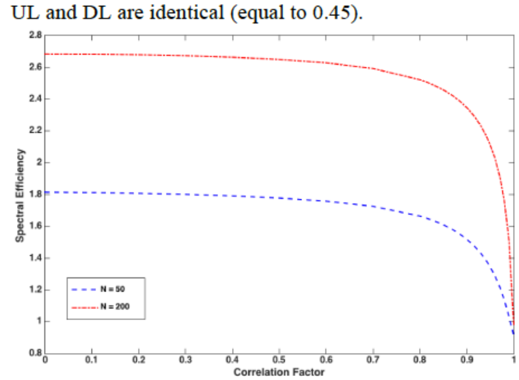

Fig. 5. Spectral efficiency for data transmission versus correlation factor with 0 dB SNR.

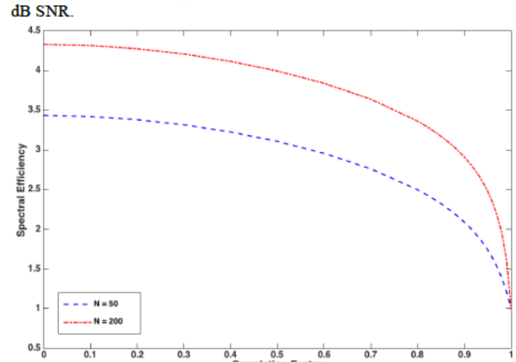

Fig. 6. Spectral efficiency for data transmission versus correlation factor with 30 dB SNR.

Fig. 5 considers a case with 0 dB SNR and 50 antennas at the base station for the blue curve and 200 antennas for the red curve. The result shows the spectral efficiency in (bit/channel use) versus correlation factor. By having correlation factor of 0 (no correlation between the antennas) the spectral efficiency at its highest values. The spectral efficiency will be decreasing when the exponential correlation factor increases till reaching correlation factor of 1 where the spectral efficiency reaches its worst values. It is clear that the larger number of antennas at the BS we have the higher spectral efficiency we get.

Fig. 6 demonstrates spectral efficiency versus correlation factor which is similar scenario compared to Fig. 5 with different SNR value. By using SNR of 30 dB, the spectral efficiency is getting higher. In Fig. 6, channel spectral efficiency tends to be sensitive to exponential correlation factor due to using larger SNR. By having 200 antennas in the base station, the spectral efficiency is having much better performance.

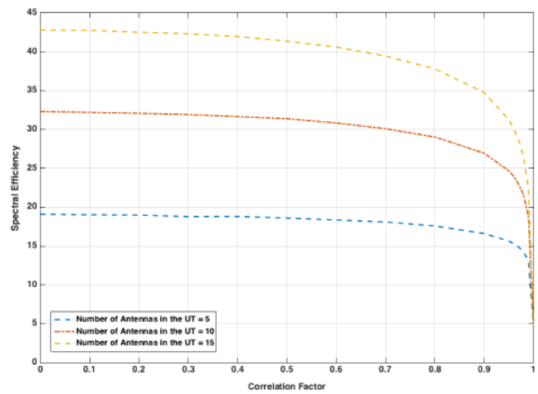

Fig. 7. Spectral efficiency for data transmission versus correlation factor with 30 dB SNR and N equals to 50.

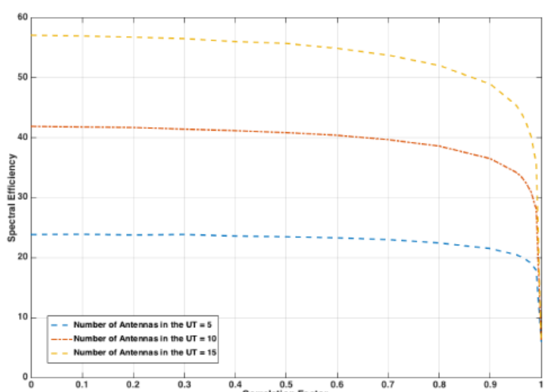

Fig. 8. Spectral efficiency for data transmission versus correlation factor with 30 dB SNR and N equals to 200.

Fig. 7. considers a different scenario with 30 dB SNR and 50 antennas in the BS. In this figure the number of user terminal antennas is changed several times to examine the impact of increasing the number of antennas in the user terminal. Fig. 7 shows that the highest value of the spectral efficiency is achieved when there is uncorrelated subchannels at correlation factor equals to 0. By increase the correlation factor, the limits of spectral efficiency go down until reaching correlation factor of 1. Also it is observed that at higher number of user terminal antennas, there is higher channel spectral efficiency.

Fig. 8. displays similar situation to Fig. 8 with signal to noise ratio equals to 30 dB and antennas equal to 200 at the base station terminal. In this figure the number of antennas in the user terminal is changed several times to investigate the effect of increasing it. Fig. 8 displays that the higher spectral efficiency is achieved when there is no correlation, which means the subchannel are completely independent. Also, it is observed that at higher number of antennas in the user terminal we have higher spectral efficiency.

V. Energy Efficiency and Transmit Power

The transmit power can be expressed as the ratio between the amplifier consumed energy and the coherence time and it is measured in (Joule/channel use) [25], [26]. The following equations demonstrate the transmit power for uplink and downlink channels

$$\left(\frac{E_{amp}}{T_{cohr}}\right)_{UL} = \alpha_{UL}\left(\frac{T^{DL}_{pilot}}{T_{cohr}}\frac{p^{BS}}{\omega^{BS}} + \frac{T^{UL}_{pilot}}{T_{cohr}}\frac{p^{UE}}{\omega^{UE}}\right) + \frac{T^{UL}_{pilot}}{T_{cohr}}\frac{p^{UE}}{\omega^{UE}} \qquad (21)$$

$$\left(\frac{E_{amp}}{T_{cohr}}\right)_{DL} = \alpha_{DL}\left(\frac{T^{DL}_{pilot}}{T_{cohr}}\frac{p^{BS}}{\omega^{BS}} + \frac{T^{UL}_{pilot}}{T_{cohr}}\frac{p^{UE}}{\omega^{UE}}\right) + \frac{T^{DL}_{pilot}}{T_{cohr}}\frac{p^{BS}}{\omega^{BS}} \qquad (22)$$

where the power amplifier efficiency at the base station is denoted as ω^{BS} and the power amplifier efficiency at the user terminal is denoted as ω^{UE}, where they have values from 0 to 1. The ratios for uplink and downlink that are used in (21) and (22) can be expressed as

$$\alpha_{UL} = \frac{T^{UL}_{data}}{T^{DL}_{data}+T^{UL}_{data}}$$

$$\alpha_{DL} = \frac{T^{DL}_{data}}{T^{DL}_{data}+T^{UL}_{data}}$$

The energy efficiency that has a unit of (bit/J) is represented as spectral efficiency and transmit power. By using the circuit power ρ and the static circuit power ζ, the uplink and downlink energy efficiencies can be represented as

$$EE^{UL} = \frac{c^{UL}}{\left(\frac{T^{DL}_{pilot}}{T_{cohr}}\frac{p^{BS}}{\omega^{BS}} + \frac{T^{UL}_{pilot}}{T_{cohr}}\frac{p^{UE}}{\omega^{UE}} + N\rho + \zeta\right) + \frac{T^{UL}_{pilot}}{T_{cohr}}\frac{p^{UE}}{\omega^{UE}}} \qquad (23)$$

$$EE^{DL} = \frac{C^{DL}}{\left(\frac{T^{\mathrm{DL}}_{\mathrm{pilot}}}{\mathrm{T}_{cohr}}\frac{p^{BS}}{\omega^{BS}} + \frac{T^{\mathrm{UL}}_{\mathrm{pilot}}}{\mathrm{T}_{cohr}}\frac{p^{UE}}{\omega^{UE}} + N\rho + \zeta\right) + \frac{T^{\mathrm{DL}}_{\mathrm{pilot}}}{\mathrm{T}_{cohr}}\frac{p^{BS}}{\omega^{BS}}} \quad (24)$$

A. Simulation Results

The simulation results have been conducted to investigate the energy efficiency and the transmit power and to see the impact of using the correlation model on them. It is assumed that the splitting ratio between the static circuit power and the circuit power is 0. Also, it is chosen that the value of $\rho+\zeta$ equals to 0.02×10^{-6} (J/channel use). It is assumed that $\alpha_{UL} = \alpha_{DL} = 0.5$ to get identical energy effeciencies for uplink and downlink channels.

Fig. 9 shows the values of energy efficiency in (bit/joule) with signal to noise ratio of 20 dB. The figure demonstrates three curves where each curve denotes different number of antennas in the BS. It is noticeable that the larger the antennas number in the base station we have the higher energy efficiency we get. Also, the correlation factor effect is clear, where the energy efficiency at its highest values when there are completely independent antennas at 0 correlation factor. The energy efficacy performance is gradually going down by increasing the correlation factor until reaching 1.

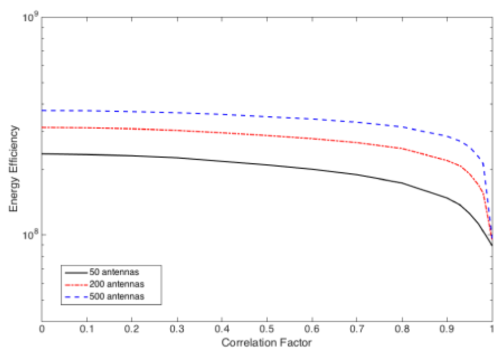

Fig. 9. Energy efficiency versus correlation factor with 20 dB SNR.

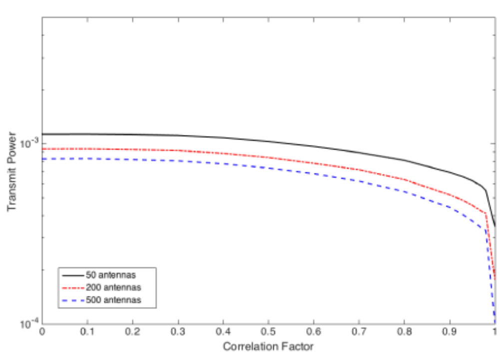

Fig. 10. Transmit power versus exponential correlation factor 20 dB SNR.

Fig. 10 demonstrates the transmit power with 20 dB signal to noise ratio where the transmit power is measured in (μJoule/channel use). Each one of the three curves represents different number of antennas in the BS. The maximum transmit power is occurring when the base station antennas N is 50. The scalability of this massive MIMO is clear since at 500 base station antennas we get the lowest transmit power and the maximum energy efficiency. Moreover, if exponential correlation factor is increasing the transmit power is decreasing.

VI. Conclusion

This paper studied the channel estimation accuracy by applying exponential correlation model and using a BS with large antennas number and a single user terminal with multiple antennas It is observed that at higher signal to noise ratio, the estimator is more precise. Massive MIMO which is a new technology can enhance the energy and spectral efficiency because of the improved spatial correlation. In this work the impact of using exponential correlation model on the spectral and energy efficiencies is investigated. Based on LMMSE channel estimator, the spectral efficiency is generated where it was noticeable that the spectral efficiency is affected by the correlation factor more sensitively at higher SNR. The scalability of massive MIMO system is clear by using 500 antennas in the BS where we have higher energy efficiency and lower transmit power.

References

[1] J. Hoydis, S. ten Brink, and M. Debbah, "Massive MIMO in the UL / DL of cellular networks : How many antennas do we need ?," *IEEE J. Sel. Areas Commun.*, vol. 31, no. 2, pp. 160–171, 2013.

[2] T. L. Marzetta, "Massive MIMO: An introduction," *Bell Labs Tech. J.*, vol. 20, pp. 11–22, 2015.

[3] T. J. Barnett, A. Sumits, S. Jain, and U. Andra, "Cisco Visual Networking Index (VNI) Update Global Mobile Data Traffic Forecast," 2016.

[4] F. Boccardi and T. L. Marzetta, "Five disruptive technology directions for 5G," *IEEE Commun. Mag.*, vol. 52, no. 2, pp. 74–80, 2014.

[5] J. Andrews, S. Buzzi, W. Choi, S. Hanly, A. Lozano, A. Soong, and J. C. Zhang, "What will 5G be?," *IEEE J. Sel. Areas Commun.*, vol. 32, no. 6, pp. 1065–1082, 2014.

[6] E. Bjornson, J. Hoydis, M. Kountouris, and M. Debbah, "Massive MIMO systems with non-ideal hardware: Energy efficiency, estimation, and capacity limits," *IEEE Trans. Inf. Theory*, vol. 60, no. 11, pp. 7112–7139, 2014.

[7] J. Hoydis, C. Hoek, T. Wild, and S. ten Brink, "Channel measurements for large antenna arrays," *2012 Int. Symp. Wirel. Commun. Syst.*, pp. 811–815, 2012.

[8] D. Gesbert, M. Kountouris, R. W. Heath, C. B. Chae, and T. Sälzer, "Shifting the MIMO Paradigm," *IEEE Signal Process. Mag.*, vol. 24, no. 5, pp. 36–46, 2007.

[9] G. Caire, N. Jindal, M. Kobayashi, and N. Ravindran, "Multiuser MIMO achievable rates with downlink training and channel state feedback," *IEEE Trans. Inf. Theory*, vol. 56, no. 6, pp. 2845–2866, 2010.

[10] T. L. Marzetta, "Noncooperative cellular wireless with unlimited numbers of base station antennas," *IEEE Trans. Wirel. Commun.*, vol. 9, no. 11, pp. 3590–3600, 2010.

[11] E. Larsson, O. Edfors, F. Tufvesson, and T. Marzetta, "Massive MIMO for next generation wireless systems," *IEEE Commun. Mag.*, vol. 52, no. 2, pp. 186–195, 2014.

[12] D. Persson, B. K. Lau, and E. G. Larsson, "Scaling Up MIMO: Opportunities and challenges with very large arrays," *IEEE Signal Process. Mag.*, vol. 30, no. 1, pp. 40–60, 2012.

[13] H. Q. Ngo, E. G. Larsson, and T. L. Marzetta, "Aspects of favorable propagation in Massive MIMO," *Eur. Signal Process. Conf.*, no. 1, pp. 76–80, 2014.

[14] H. Q. Ngo, H. A. Suraweera, M. Matthaiou, and E. G. Larsson, "Multipair full-duplex relaying with massive arrays and linear processing," *IEEE J. Sel. Areas Commun.*, vol. 32, no. 9, pp. 1721–1737, 2014.

[15] S. Albdran, A. Alshammari, M. Ahad, and M. Matin, "Effect of Exponential Correlation Model on Channel Estimation for Massive MIMO," in *The 19th International Conference on Computer and Information Technology*, 2016.

[16] E. Bjornson, E. G. Larsson, and T. L. Marzetta, "Massive MIMO: ten myths and one critical question," *IEEE Commun. Mag.*, vol. 54, no. 2, pp. 114–123, 2016.

[17] A. Assalini, E. Dall'Anese, and S. Pupolin, "On the robustness of MIMO LMMSE channel estimation," *IEEE Trans. Wirel. Commun.*, vol. 9, no. 11, pp. 3313–3319, 2010.

[18] M. Médard, "The effect upon channel capacity in wireless communications of perfect and imperfect knowledge of the channel," *IEEE Trans. Inf. Theory*, vol. 46, no. 3, pp. 933–946, 2000.

[19] D. Bethanabhotla, O. Y. Bursalioglu, H. C. Papadopoulos, and G. Caire, "Optimal User-Cell Association for Massive MIMO Wireless Networks," *IEEE Trans. Wirel. Commun.*, vol. 15, no. 3, pp. 1835–1850, 2016.

[20] E. Björnson, "Hardware impairments in Large-scale MISO systems : Energy efficiency , estimation , and capacity limits," *18th Int. Conf. Digit. Signal Process.*, pp. 1–6, 2013.

[21] H. Q. Ngo, E. G. Larsson, and T. L. Marzetta, "Energy and spectral efficiency of very large multiuser MIMO systems," *IEEE Trans. Commun.*, vol. 61, no. 4, pp. 1436–1449, 2013.

[22] S. L. Loyka, "Channel capacity of MIMO architecture using the exponential correlation matrix," *IEEE Commun. Lett.*, vol. 5, no. 9, pp. 369–371, 2001.

[23] C. C. Martin, J. H. Winters, N. R. Sollenberger, S. Drive, and R. Bank, "Multiple-Input Multiple-Output (MIMO) radio channel measurements," *IEEE Antennas Propag. Soc. Int. Symp.*, vol. 1, pp. 418–421, 2001.

[24] A. Alshammari, S. Albdran, M. Ahad, and M. Matin, "Impact of Angular Spread on Massive MIMO Channel Estimation," in *The 19th IEEE International Conference on Computer and Information Technology*, 2016.

[25] A. Alshammari, S. Albdran, and M. Matin, "The Effect of Channel Spatial Correlation on Capacity and Energy Efficiency of Massive MIMO Systems," in *The 7th IEEE annual Comuting and Communication Workshop and Conferernce*, 2017.

[26] S. Albdran, A. Alshammari, and M. Matin, "Spectral and Energy Efficiency for Massive MIMO Systems Using Exponential Correlation Model," in *The 7th IEEE annual Comuting and Communication Workshop and Conferernce*, 2017.